

**NOVEL ISOTOPE EFFECTS AND ORGANIC REACTION
MECHANISMS**

A Dissertation

by

KELMARA K. KELLY

Submitted to the Office of Graduate Studies of
Texas A&M University
in partial fulfillment of the requirements for the degree of

DOCTOR OF PHILOSOPHY

May 2009

Major Subject: Chemistry

**NOVEL ISOTOPE EFFECTS AND ORGANIC REACTION
MECHANISMS**

A Dissertation

by

KELMARA K. KELLY

Submitted to the Office of Graduate Studies of
Texas A&M University
in partial fulfillment of the requirements for the degree of

DOCTOR OF PHILOSOPHY

Approved by:

Chair of Committee,
Committee Members,

Head of Department,

Daniel A. Singleton
Frank M. Raushel
Simon W. North
Jim C. Hu
David H. Russell

May 2009

Major Subject: Chemistry

ABSTRACT

Novel Isotope Effects and Organic Reaction Mechanisms. (May 2009)

Kelmara K. Kelly, B.S., St. Francis College

Chair of Advisory Committee: Dr. Daniel A. Singleton

A variety of organic reactions provide experimental observations that are not explained by current models of reactivity and selectivity. This dissertation describes a combination of experimental and theoretical studies of such reactions. In the ene reaction of singlet oxygen with tetramethylene, it is found that standard statistical rate theories fail to account for the observed kinetic isotope effects, particularly with regard to their broad temperature independence. Dynamics trajectories are found to account for the observed isotope effects. In the dimerization of cyclopentadiene, novel “dynamic” isotope effects are observed on the ^{13}C distribution in the product, and a method for the prediction of these isotope effects is developed here. In the cycloaddition of diazomethane with dimethylfulvene, it is found that the current model of the mechanism as a [6 + 4] cycloaddition is incorrect, and a new mechanism is proposed. Isotope effects have been measured for the recently reported unusual “on water” quadricyclane cycloadditions, and the implications of these observations toward the mechanism are discussed.

DEDICATION

To My Family

ACKNOWLEDGMENTS

I would like to thank my advisor, Dr. Singleton, for his guidance, patience, and support throughout my tenure as a graduate student under his tutelage.

I would like to thank my committee members, Dr. Raushel, Dr. North, and Dr. Hu for their time and direction.

A special thanks to the past and current Singleton group members that have provided me a fruitful arena for learning and discussion I am indebted to their friendship and encouragement. I am thankful for the many friends, acquaintances, and experiences that I have had so far in my career.

Lastly and most importantly, I have to thank my family who have always supported and encouraged me.

TABLE OF CONTENTS

	Page
ABSTRACT	iii
DEDICATION	iv
ACKNOWLEDGMENTS.....	v
TABLE OF CONTENTS	vi
LIST OF FIGURES.....	ix
LIST OF TABLES	xi
CHAPTER	
I INTRODUCTION	1
Purpose	1
Origin of Kinetic Isotope Effects	2
Types of Kinetic Isotope Effects.....	8
Methodology for Determining Kinetic Isotope Effects.....	11
Dynamic Effects.....	15
Summary	19
II TEMPERATURE INDEPENDENCE OF DYNAMIC ISOTOPE EFFECTS.....	21
Introduction	21
Results	24
Experimental Kinetic Isotope Effects	24
Theoretical Models.....	26
Variational Transition State Theory Calculations	26
RRKM (Rice, Ramsperger, Kassel, Marcus) Calculations	27
Dynamics Calculations: PROGDYN	28
Predicted Kinetic Isotope Effects.....	28
Discussion	33
Conclusion.....	34

CHAPTER	Page
III OBSERVATION AND PREDICTION OF HEAVY-ATOM DYNAMIC ISOTOPE EFFECTS	36
Introduction	36
Result.....	38
Experimental ¹³ C Kinetic Isotope Effects	38
Theoretical Calculations.....	40
Trajectory Analysis	41
Predicted Isotope Effects.....	41
Discussion	43
Conclusion.....	44
IV DYNAMIC EFFECTS ON PERISELECTIVITY	45
Introduction	45
Results	48
Low Temperature NMR Studies	49
Experimental ¹³ C Kinetic Isotope Effects.	50
Theoretical Calculations.....	51
Dynamics.....	52
Discussion	52
Conclusion.....	53
V KINETIC ISOTOPE EFFECT STUDY ON THE RATE ACCELERATION OBSERVED “ON WATER” REACTIONS	54
Introduction	54
Results	56
Reaction of Quadricyclane with Diethyl Azodicarboxylate	58
Reaction of Quadricyclane with Dimethyl Acetylenedicarboxylate and 1,4-Benzoquinone.....	59
Theoretical Models.....	61
Discussion	63
Conclusion.....	65

CHAPTER	Page
VI EXPERIMENTAL SECTION	67
General Procedures	67
Singlet Oxygen Ene Reaction of 1	68
Synthesis of 1-d ₆	68
Example Procedure	69
NMR Measurements	70
Energy Distributions	70
RRKM Calculations	70
Equilibration of Dicyclopentadiene.....	76
Example Procedure	76
NMR Measurements	77
¹³ C Results.....	77
Reaction of Dimethylfulvene with Diazomethane	79
Example Procedure for the Reaction of Dimethylfulvene with Diazomethane	79
On Water Reactions of Quadricyclane.....	81
Synthesis of Quadricyclane.....	81
Preparation of Neat Diethyl Azodicarboxylate	81
Example 'On Water' Procedure	82
Example Procedure in Acetonitrile	82
Example Procedure for Preparation of Standard.....	83
VII CONCLUSIONS.....	88
REFERENCES	90
APPENDIX	98
VITA	228

LIST OF FIGURES

FIGURE	Page
1-1 The origin of a kinetic isotope effect arises from a difference in the ZPE of the reacting isotopomers as a reaction proceeds from starting material to the transition state	4
1-2 The origin of normal secondary isotope effects.....	10
1-3 The origin of inverse secondary isotope effects.....	10
1-4 The relationship between the isotopic ratio, R/R_0 , and the fractional conversion, F , and their effect on the KIE	14
1-5 Three dimensional potential energy surface illustrating how two products can be formed from one transition state	17
1-6 Bifurcating potential energy surfaces on which selectivity would be controlled by dynamic effects	19
2-1 A qualitative bifurcating potential energy surface, as proposed to be involved in ene reactions of $^1\text{O}_2$ (see ref 47).....	22
2-2 Illustration of the $^1\text{O}_2$ ene reaction of d_6 -tetramethylethylene	24
2-3 Plot of the experimental intramolecular KIE (k_H/k_D , defined by the 2 : 3 ratio) versus temperature for the ene reaction of $^1\text{O}_2$ with 1 , along with predicted isotope effects from various theoretical models.....	25
2-4 Ene product in a bath of 34 methanol molecules showing little product stabilization by solvent.....	32
3-1 Illustration showing different products resulting from C_2 – bispericyclic transition state on a symmetrical potential energy surface.....	37
3-2 Intramolecular ^{13}C KIEs in the dimerization of cyclopentadiene	39
4-1 Unsymmetrically bifurcating surface	46

FIGURE	Page
4-2 HOMO-LUMO interactions leading to [6 + 4] product	47
4-3 Low temperature NMR spectra of diazomethane reaction with dimethylfulvene a) t = 15 m b) t = 1 h	49
4-4 Observed kinetic isotope effects for the cycloaddition of diazomethane with dimethylfulvene a) relative ^{13}C integration b) KIEs	50
4-5 Scheme showing possible pathways from the [2 + 4] transition state to product both a [2 + 4] product and a [6 + 4] product	51
5-1 $2\sigma+2\sigma+2\pi$ transition structures proposed by Marcus for the cycloaddition of quadricyclane with dimethyl azodicarboxylate a) in organic solvent b) 'on water'	61

LIST OF TABLES

TABLE	Page
3-1 Results of trajectories employing superheavy carbons	42
5-1 Summary of the rate of the cycloaddition of quadricyclane with a) dimethylazodicarboxylate and b) diethyl azodicarboxylate	57
5-2 Rate of reaction of quadricyclane with dimethyl acetylenedicarboxylate in different solvents determined by ^1H NMR.....	60
5-3 Rate of reaction of quadricyclane with 1,4-benzoquinone in different solvents determined by ^1H NMR	60
5-4 Predicted KIEs for the generally accepted $2\sigma+2\sigma+2\pi$ theoretical model proposed by Marcus	62
5-5 Predicted KIEs for a theoretical model involving the formation of a quadricyclane cation radical as the rate limiting step.....	63
6-1 Rates of reaction for hydrogen abstraction in germinal d_6 -tetramethylethylene	71
6-2 Rates of reaction for deuterium abstraction in germinal d_6 -tetramethylethylene.	72
6-3 Rates of reaction for hydrogen abstraction in trans d_6 -tetramethylethylene	73
6-4 Rates of reaction for deuterium abstraction in germinal d_6 -tetramethylethylene	74
6-5 Calculated RRKM isotope effects for the $^1\text{O}_2$ ene reaction with geminal d_6 -tetramethylethylene	75
6-6 Calculated RRKM isotope effects for the $^1\text{O}_2$ ene reaction with trans d_6 -tetramethylethylene.....	76
6-7 Relative ^{13}C integrations for dicyclopentadiene, with standard deviations ..	78
6-8 Intramolecular ^{13}C KIEs in the dimerization of cyclopentadiene	78

TABLE	Page
6-9 Average ^{13}C integrations (n = 6) for recovered dimethylfulvene.....	80
6-10 Relative ^{13}C integrations for the cycloaddition of diazomethane with dimethylfulvene.....	80
6-11 ^{13}C KIES for the cycloaddition of diazomethane with dimethylfulvene.....	81
6-12 Rate of cycloaddition of quadricyclane with dimethyl acetylenedicarboxylate	84
6-13 Rate of cycloaddition of quadricyclane with 1,4-benzoquinone.....	84
6-14 Average ^{13}C integrations (n = 6) for DEAD on water product.....	85
6-15 ^{13}C KIEs for DEAD on water, with standard deviations.....	86
6-16 Average ^{13}C integrations (n = 6) for 1,4-benzoquinone on water product....	87
6-17 ^{13}C KIEs for 1,4-benzoquinone on water, with standard deviations.....	87

CHAPTER I

INTRODUCTION

Purpose

The mechanism of chemical reactions is integral to their understanding and control, so the study of reaction mechanisms is a cornerstone of physical organic chemistry. In this regard, it is natural that there is particular interest in the mechanism of reactions that appear to defy generally accepted principles. Such reactions are the central focus of this dissertation.

Conventionally, a reaction mechanism comprises the complete series of transition states and reactive intermediates in between a reaction's starting materials and products. Determining this series is no simple task, as reactive intermediates usually have lifetimes too short to be observed, while transition states are but fleeting moments even on atomic timescales, lasting but only a few femtoseconds. In recent years, however, it has been recognized that the problem of defining a mechanism is often even more complex. In reactions involving dynamic effects, the understanding of experimental observations requires not only a knowledge of transition states and

This dissertation follows the style and format of *The Journal of the American Chemical Society*.

intermediates but also the shape of energy surfaces and the rate at which they are traversed.

In most reactions, the first glimpse into the black box that is the reaction mechanism is the elucidation of the rate-limiting transition state. The transition state is a theoretical construct viewed as controlling the rates and selectivity observed in reactions. Because transition states can almost never be observed directly, their characterization relies on their association with the rates of reactions. Diverse kinetic probes exist for defining the structural features of transition states, including the study of rate laws, activation parameters, substituent effects, and solvent effects. A probe of particular utility in the Singleton group is the determination of the small rate changes that occur in reactions when a molecule is replaced by an isotopologue. These rate changes are referred to as kinetic isotope effects (KIEs).

Origin of Kinetic Isotope Effects

Isotopic substitution does not significantly affect the molecular structure, as the weight of an atom has no effect on the potential energy surface. Isotopic substitution also generally has no effect on the mechanism of a reaction or the pathway by which it proceeds from starting materials to products. However, isotopic substitution can effect the rate. The change in rate, the KIE, is defined based on the rate constants for isotopologues as in eq 1-1 through 1-3.¹



$$\text{KIE} = \frac{k_{\text{H}}}{k_{\text{D}}} \quad (1-3)$$

A starting point for the understanding of KIEs is the theory of equilibrium isotope effects (EIEs). EIEs are changes in equilibrium constants when a molecule is replaced by an isotopologue, as defined in eq 1-4 through 1-6. Equilibrium isotope effects arise from the effect of isotopic substitution on the vibrational, rotational, and translational partition functions of molecules. The largest of these effects is usually on the vibrational partition function, arising from changes in the zero-point energy on isotopic substitution. The theory of equilibrium isotope effects is considered to be well understood and theoretical calculations can, when accurate and done with sufficient care, predict equilibrium isotope effects with high accuracy.



$$\text{EIE} = \frac{K_{\text{H}}}{K_{\text{D}}} \quad (1-6)$$

KIEs, then, are generally understood in a way that parallels the understanding of EIEs. The effect of changes in the zero-point energy between isotopomers as a reaction proceeds from the ground state to the transition state may be understood with reference to Figure 1-1.

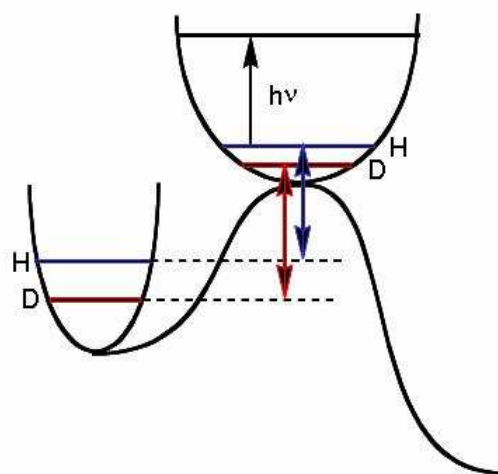


Figure 1-1. The origin of a kinetic isotope effect arises from a difference in the ZPE of the reacting isotopomers as a reaction proceeds from starting material to the transition state.

The zero-point energy in both the ground state and the transition state is a function of the frequencies of the normal modes eq 1-7, as defined by the quantum mechanics of harmonic oscillators. These frequencies are in turn a function of the isotopic masses. For a harmonic oscillator, the frequency is related to the mass by eq 1-8.

In a molecule, the relationship of the frequency to the mass is somewhat more complicated, involving *reduced masses*, but the approximate relationship that the frequency and therefore the zero-point energy is inversely proportional to the square root of the mass remains. As a result, the zero-point energy always decreases when the mass is increased. As also implied by eqs 1-7 and 1-8, the zero-point energy is a function of the force constants for the normal modes. Bond-stretching force constants are high when bonds are strong and bond-bending force constants are high when the central atom for the bend is highly substituted. In going from the ground state to the transition state, these force constants will change so the total zero-point energy in the molecule will change, and the amount of the change will depend on the masses of the isotopes involved. Because of this, as Figure 1-1 illustrates, the barrier of activation for isotopologues will differ.

$$\text{ZPE} = 1/2 h\nu \quad (1-7)$$

$$\nu = \frac{1}{2\pi} \sqrt{\frac{k}{m}} \quad (1-8)$$

In more detail, the statistical mechanical theory of isotope effects is based on the work of Bigeleisen and Mayer.² This theory goes beyond the approximation of considering only zero-point energies by allowing for the full harmonic vibrational, rotational, and translational partition functions. Using the Teller-Redlich product rule to simplify the combination of partition functions, Bigeleisen and Mayer defined a

“reduced isotopic partition function,” $(s_2/s_1)f$, for isotopologues that importantly depends only on the frequencies of the normal modes, as shown in eq 1-9. In this equation, the subscripts 1 and 2 refer to isotopologues and i is an index number for the normal mode, going up to $3N-6$ for ground state molecules where N is the number of atoms. Knowing the frequencies of the molecules involved, equilibrium isotope effects can be calculated from the ratio of the $(s_2/s_1)f$ s for the starting materials versus the products.

$$(s_2/s_1)f_{GS} = \prod_i^{3N-6} \frac{\nu_{2i}}{\nu_{1i}} \frac{1 - e^{-u_{1i}}}{1 - e^{-u_{2i}}} \frac{e^{u_{1i}/2}}{e^{u_{2i}/2}} \quad (1-9)$$

$$u_i = h\nu_i/kT$$

The theory behind kinetic isotope effects is slightly more complicated. Bigeleisen factored out the imaginary frequency associated with the transition vector to get the revised formula for the reduced isotopic partition function for transition states shown in eq 1-10.² In this formula, the ν 's at the front of the equation refer to the imaginary frequencies. The KIE from conventional transition state theory is then calculated by eq 1-11.

$$(s_2/s_1)f_{TS} = \prod_i^{3N-7} \frac{\nu_{2i}}{\nu_{1i}} \frac{1 - e^{-u_{1i}}}{1 - e^{-u_{2i}}} \frac{e^{u_{1i}/2}}{e^{u_{2i}/2}} \quad (1-10)$$

$$\text{KIE}_{\text{TST}} = \frac{v_1^\ddagger (s_2 / s_1) f_{\text{GS}}}{v_2^\ddagger (s_2 / s_1) f_{\text{TS}}} \quad (1-11)$$

At this point, however, there is one more complication to consider, tunneling. Tunneling is the quantum mechanical process by which barriers can be traversed without sufficient energy to go over the barrier. A full allowance for tunneling in reactions is complicated because there are a great many ways in which tunneling may occur in 3N-6 dimensions to get a molecular geometry from one side of the barrier to the other. In the work to be described, we employ a simplified model for tunneling that only considers motion along the transition vector, and treats the barrier as an infinite parabola with the curvature of the parabola defined by theoretical frequency calculations.³ The resulting one-dimensional tunneling correction is defined in eq 1-12 and the overall calculated KIE is defined as in eq 1-13.

$$\text{KIE}_{\text{1D-tunneling-IP}} = \frac{u_1^\ddagger / 2 \sin(u_1^\ddagger / 2)}{u_2^\ddagger / 2 \sin(u_2^\ddagger / 2)} \quad (1-12)$$

$$\text{KIE}_{\text{calc}} = \text{KIE}_{\text{TST}} \times \text{KIE}_{\text{1D-tunneling-IP}} \quad (1-13)$$

While the zero-point-energy view of isotope effects is useful for their qualitative understanding, the utility of the full statistical mechanical treatment is that it allows a quantitative calculation of the isotope effects from theoretical calculations. Such

predictions have proven highly accurate in reactions not involving hydrogen transfer, as long as the calculation accurately depicts the mechanism and the transition state geometries. In this way, the isotope effects may be used to check the validity of theoretically calculated transition states.

Types of Kinetic Isotope Effects

Isotope effects are generally categorized within two broad headings, primary isotope effects and secondary isotope effects. Primary isotope effects are observed when there is an isotopic substitution at an atom which undergoes σ -bond making or breaking during the kinetic step of interest. If the bond to atom is broken, a stretching frequency is lost as it becomes a translation on the potential energy surface, and the zero-point energy associated with this stretching frequency is either lost or greatly changed. As a result, the isotope effect is large. For reasons understandable from consideration of Figure 1-1, lighter atoms tend to react faster, and primary KIEs have values ranging from 2 to 7 for k_H/k_D and 1.01 to 1.05 for $k_{^{12}C}/k_{^{13}C}$.

Secondary isotope effects are those observed at other atoms in a molecule and result from more subtle changes in the frequencies of the normal modes associated with these atoms. These isotope effects are smaller and may either have the lighter atom react faster, a normal isotope effect, or have the heavier atom react faster, an inverse isotope effect.

Some examples here will illustrate the factors influencing the direction of secondary KIEs and the structural interpretation. A normal secondary KIE is generally observed for isotopically substitution at atoms attached to a reactive center undergoing a change in hybridization from sp^3 to sp^2 with values ranging from 0.7 to 1.0 for k_H/k_D and 0.99 to 1.00 for k_{12C}/k_{13C} ; inverse secondary KIEs are observed for hybridization changes in the opposite direction i.e. from sp^2 to sp^3 with values of 1.0-1.4 and 1.00-1.01 for k_H/k_D and k_{12C}/k_{13C} respectively illustrated in Figures 1-2 and 1-3. A general rule is that normal secondary KIEs are observed at atoms undergoing a weakening of their bonds in the transition state, while inverse secondary KIEs result from crowding of an atom at the transition state.

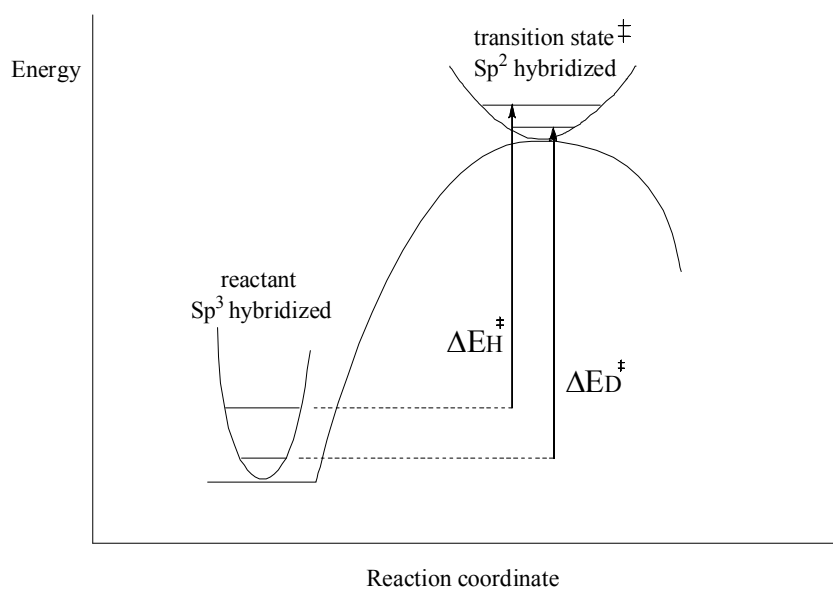


Figure 1-2. The origin of normal secondary isotope effects.

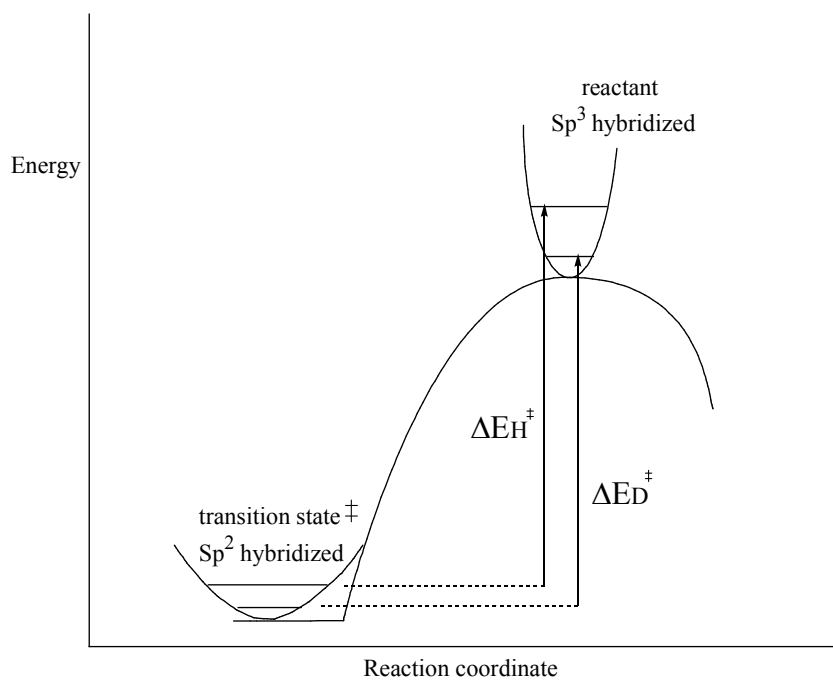


Figure 1-3. The origin of inverse secondary isotope effects.

Methodology for Determining Kinetic Isotope Effects

The definition in eq 1-3 of KIEs in terms of the ratio of rate constants suggests that KIEs are measured by direct kinetic measurements on separate reactions of isotopologues. Such a measurement is referred to as a non-competitive. There are substantial shortcomings in this approach. One issue is the arduous task of synthesizing isotopically labeled material. A second issue is the problem of obtaining sufficiently precise and accurate absolute kinetic measurement of the rate constants. Because of these issues, non-competitive methods are rarely used for small isotope effects such as carbon KIEs. A final, subtle issue is that the step of interest may not be the rate-limiting step in a reaction, so that the observed kinetics for the overall reaction may not reflect the step about which information is desired.

Alternatively, KIEs can be determined competitively. Methods utilizing this approach avoid most of the major limitations associated with non-competitive measurements. A particular advantage that both isotopic substrates are in the same reaction flask and are thus subjected to identical reaction conditions. The measurement of KIEs competitively relies on the fact that the products of a reaction are enriched in the faster reacting isotopomers while the reactants are enriched in the slower reacting isotopomers as the reaction proceeds. One can then calculate the KIE based on the change in the isotopic composition in recovered starting material versus original starting material or product at low conversion versus product at 100% conversion, given an accurate measurement of the percent conversion in the reaction.

There are three major ways to determine the requisite changes in isotopic composition, by scintillation counting (utilized for radioactive isotopomers), mass spectrometry and nuclear magnetic resonance spectroscopy. Scintillation counting has been historically valuable but it is limited by necessity for synthetically labeled isotopomers, the synthesis of which can be quite labor intensive. For each new isotope effect desired, a new substrate must be synthesized. Mass spectrometry, particularly isotope ratio mass spectrometry, can be applied at natural abundance and has the advantage of great precision in its measurements. A disadvantage of mass spectrometry, however, is that it is usually only directly applicable to small molecules such as CO₂. To determine KIEs for positions in larger molecules, the position of interest must be synthetically cleaved from the rest of the molecule.

NMR, in contrast, can be applied to the determination of KIEs at natural abundance without the use of synthetic labels.⁴ Further, NMR can be used to determine KIEs “combinatorially.” These abilities rely on the fact that NMR spectra exhibit separate peaks for each non-equivalent position in a molecule and the size of the peaks is proportional to the amount of the particular isotope being examined at each position. Because NMR is nucleus-specific, it can be used to look at trace nuclei in the presence of large amounts of alternative isotopes. For almost two decades, it has been recognized that these properties of NMR allow its use to determine deuterium kinetic isotopic effects at natural abundance, at least in special cases.⁵ A particular advance came in 1995, when the Singleton group reported a general methodology for the simultaneous determination of KIEs at natural abundance.⁴ A key trick in this work was a process that

allowed for high-precision results. As a result, the Singleton methodology allows for the combinatorial determination of ^2H and ^{13}C KIEs at every atomic position within a molecule both efficiently and precisely.

The advantage to the Singleton methodology is that reactions are taken to high conversion, usually $>80\%$, and the recovered starting material is analyzed. High precision NMR spectra of identically prepared samples are obtained for the enriched starting material and compared to a standard sample containing starting material of the same lot that has not been exposed to the reaction conditions. An atom whose isotopic composition is assumed not to be changing over the course of the reaction, and is distant from the reaction center is typically chosen as the internal standard. The changes in isotopic composition of the other atoms are obtained from comparing changes in the integration to that of the internal standard. By NMR methods, the relative isotopic composition at positions in the recovered material versus the original material (R/R_0) is determined by calculating the ratio of the average integrations for the peak of interest versus the internal standard peak. The KIE can then be calculated from R/R_0 and the fractional conversion F using eq 1-14.⁴

$$\text{KIE}_{\text{calcd}} = \frac{\ln(1 - F)}{\ln[(1 - F)R/R_0]} \quad (1-14)$$

The improved precision obtained by the Singleton methodology may be understood by rearranging eq 1-14 to eq 1-15 and making a plot of R/R_0 versus F for a

series of values of the KIE, Figure 1-4. In the process of going to high conversion, the natural abundance isotopic mixture is fractionated, leading to larger changes in the isotopic composition relative to the size of the isotope effect involved.

$$R/R_0 = (1-F)^{(1/KIE-1)} \quad (1-15)$$

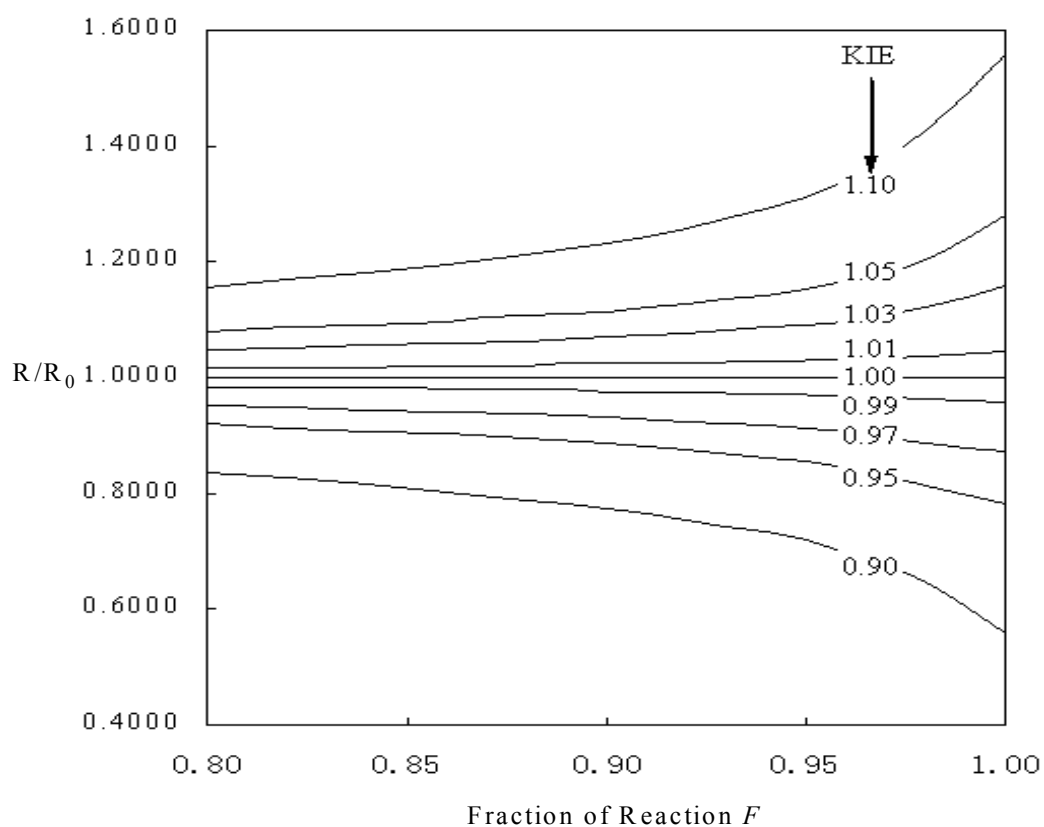


Figure 1-4. The relationship between the isotopic ratio, R/R_0 , and the fractional conversion, F , and their effect on the KIE.

Dynamic Effects

The general understanding of rates and selectivity in chemical reactions is based on transition state theory. However, a growing number of reactions exhibit observations that cannot be explained by current versions of transition state theory.⁶⁻¹² We will refer to such observations as dynamic effects, because when transition state theory fails, analyses must fall back on the usually ignored combination of positions and momenta of atoms.

The consideration of dynamic trajectories can explain or even predict the outcome of reactions in cases where transition state theory gives incorrect predictions or cannot be applied. One well-studied example in the literature is the rearrangement of vinylcyclopropane to cyclopentene. The unusual stereochemistry of this reaction fueled a debate that lasted nearly two decades—until Doubleday found that dynamic effects in the rearrangement can account for the experimental observations.^{8,9,13-16} Beginning in 1985 Carpenter published a number of reactions in which the product distributions cannot be explained within the framework of statistical theories of unimolecular kinetics such as RRKM theory, transition state theory and variational transition state theory.^{6,7}

In the Carpenter cases, the dynamic effects arise from a phenomenon referred to as “dynamic matching.” An assumption in the application of transition state theory to reactions is that intramolecular vibrational energy redistribution (IVR) is fast on the time scale of reaction coordinate motion.¹⁷ However, IVR is not instantaneous, and this has consequences.

One result of relatively slow IVR is that the selection of trajectories passing through an initial transition state can influence selectivity among subsequent transition states. This is dynamic matching, and an understanding of the selectivity among products requires consideration of dynamic trajectories.¹⁸ Related effects can impact reactions in which trajectories pass through a flat, typically diradicaloid, area of a potential energy surface.¹⁹⁻²¹ Alternatively, trajectories can effectively bypass minima on the reaction coordinate.^{22,23}

A second form of dynamic effect that can result from slow IVR is "non-statistical recrossing." Recrossing is when trajectories pass a delineated transition state then return to starting materials. Most recrossing is thought to be predicted reasonably well by modern statistical versions of TST and related theory, such as microcanonical variational TST.²⁴ However, transition state theorists understand well that some recrossing occurs that is not statistically predictable. This recrossing is usually ignored, but theoretical studies have suggested that this non-statistical recrossing is sometimes substantial. Hase in particular has studied this effect theoretically in gas-phase S_N2 reactions.^{24,25} An important advance came when Singleton and Ussing reported evidence for non-statistical recrossing in an experimental reaction, the cycloaddition of diphenylketene with cyclopentadiene.¹²

A third form of dynamic effect is central to this dissertation. A pervasive implicit assumption in understanding selectivity is that *separate products arise from separate transition states*. The intertwined idea that a transition state may only connect a reactant set with a single product set was once considered a rule, usable to exclude certain symmetries in transition states.²⁶ For over 30 years, it has been recognized theoretically that this assumption is not reliable.²⁷⁻²⁹ On a bifurcating energy surface, such as those shown in Figure 1-5, reactants that pass through a rate-limiting transition state can proceed to two product wells without barrier.

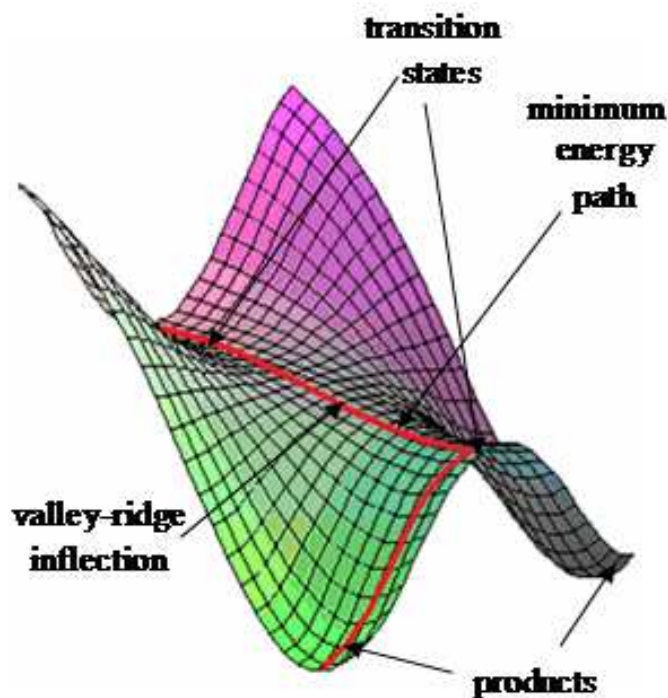


Figure 1-5. Three dimensional potential energy surface illustrating how two products can be formed from one transition state.

In these circumstances, there is no way to apply transition state theory and its derivatives to predict the selectivity among the two products. Instead, the momenta of atoms at the rate-limiting transition state and their course on the downhill slope of the energy surface must be considered to predict the reaction outcome. The orientation of the molecule and forces thereon as it traverses the region of the transition state will determine the path taken. The shape of the potential energy surface also has an effect on the path taken. This is evident when one considers the intrinsic shape of a potential energy surface with two transition states connected by a minimum energy path. The initial rate-limiting transition state is in a valley which descends onto a ridge as it approaches the second transition state. This point is nominally the valley-ridge inflection and is defined by the point on the minimum-energy path when curvature of a transverse mode passes from positive to 0, eq 1-18, on its way to negative. Past the valley-ridge inflection, trajectories will tend to diverge toward opposite products.

$$d^2E/dx^2=0 \quad (1-18)$$

The nature of a bifurcating potential energy surface can be of two types illustrated in Figure 1-6. The first of these is a symmetrical bifurcation in which both exit channels result in identical products (equal energy). The second type of potential energy surface is an unsymmetrical bifurcation which may lead to two different products with very different energies. Reactions involving an unsymmetrical bifurcating surface

are a much more complicated case as there is no simple way to predict the product ratio and it may be difficult to realize that the second possible product can be formed from the initial transition state.

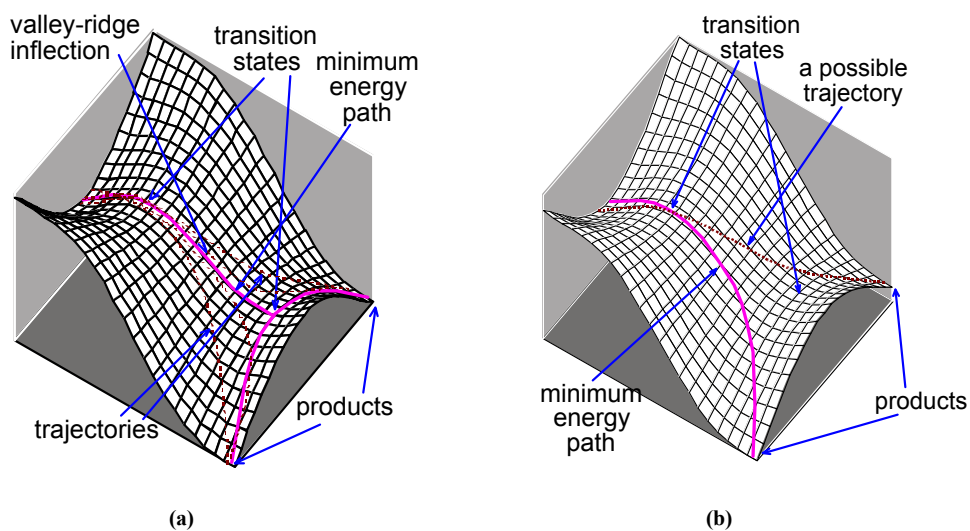


Figure 1-6. Bifurcating potential energy surfaces on which selectivity would be controlled by dynamic effects. (a) Symmetrical surface on which the MEP bifurcates at the second transition state. Trajectories tend to diverge from the MEP in the area of the VRI. (b) An unsymmetrical potential energy surface on which the MEP does not bifurcate. However, some possible trajectories afford a product not on the MEP.

Summary

The control of rates and selectivity of reactions is generally understood in terms of energetic barriers (i.e. the relative energy of the transition states in a reaction determines the ratio of products formed). Reactions whose outcomes cannot be explained by transition state theory will be the focus of this dissertation. KIEs have been treated as a close parallel to transition state theory which, for the most part is adequate for the majority of reactions. Here I will expand the general understanding of KIEs using diverse experimental examples to show new forms of KIEs which are dynamical in origin.

For all reaction mechanisms studied herein, the focus will be to apply the above described theories and methodology to obtain a qualitative and quantitative picture of the rate-limiting transition state to gain valuable clues in discerning a reaction's path.

CHAPTER II

TEMPERATURE INDEPENDENCE OF DYNAMIC ISOTOPE EFFECTS

Introduction

Transition state theory in its various forms has been the most broadly applicable model for understanding the rates of chemical reactions. Within transition state theory, the selectivity k/k' between two competitive reactions may be interpreted in terms of a difference between free energies of activation ($\Delta\Delta G_{act}^0$), which in turn may be subdivided into differences in phenomenological enthalpies and entropies of activation ($\Delta\Delta H_{act}^0$ and $\Delta\Delta S_{act}^0$, eq 1-1). These quantities provide a formalistic interpretation of the origin of selectivity in a reaction. Normally, selectivity should grow without bound (or shrink to 0) as T approaches 0. The rare exception is when $\Delta\Delta H_{act}^0$ is identically zero, as expected at sufficiently low temperatures in reactions dominated by tunneling.³⁰⁻³⁷

$$k/k' = e^{-\Delta\Delta G_{act}^0/RT} = e^{-\Delta\Delta H_{act}^0/RT} e^{\Delta\Delta S_{act}^0/R} \quad (2-1)$$

This application of transition state theory to selectivity subtly assumes that separate products arise from *separate* transition states. The theoretical unreliability of

this assumption has long been recognized, particularly for reactions in which symmetry is broken after a symmetrical transition state.³⁸⁻⁴⁶ On such bifurcating energy surfaces, as in Figure 2-1, it is downhill from the initial transition state to two products, and trajectories tend to diverge in the area of the valley-ridge inflection point (VRI). The reaction's product or mechanistic selectivity is then decided on the slope of the energy surface. Recent work has brought to light several ordinary experimental reactions of this type, but little is understood about the nature of their selectivity.⁴⁷⁻⁵⁰

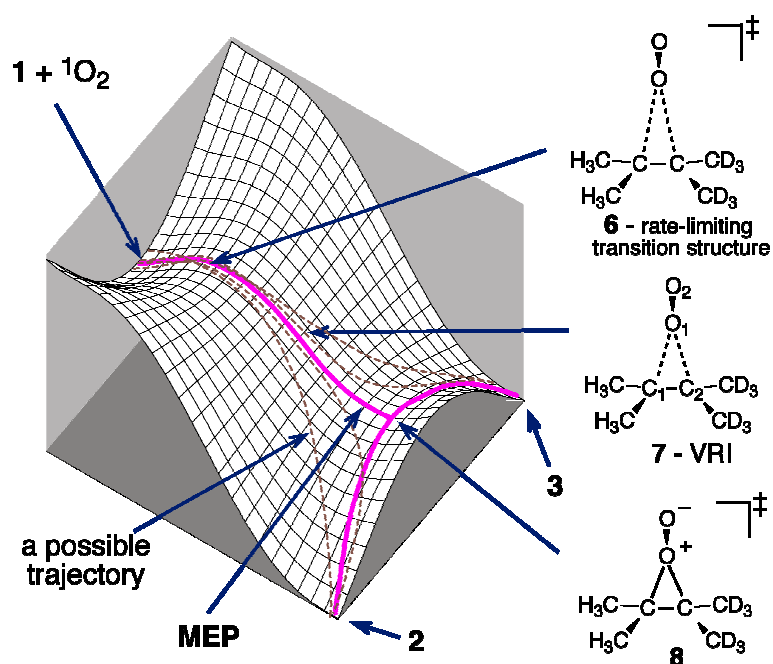


Figure 2-1. A qualitative bifurcating potential energy surface, as proposed to be involved in ene reactions of $^1\text{O}_2$ (see ref 47). In the reaction of **1**, the intramolecular KIE is the selectivity between **2** and **3**.

The example studied here is the ene reaction of singlet ($^1\Delta_g$) oxygen (1O_2) with alkenes. Experimental and computational studies have suggested that the rate-limiting transition state in these reactions arises from a bisecting approach of the 1O_2 to the olefinic π bond.⁴⁷ Two regioisomeric products may then be formed after the rate-limiting transition state. When the products differ only in isotopic substitution, the selectivity represents an intramolecular kinetic isotope effect (KIE). Ene reactions of 1O_2 have played a prominent role in the development of intramolecular KIEs as a mechanistic probe.^{51,52} We have proposed that the observed isotopic selectivity constitutes a new form of KIE that can be understood only by consideration of dynamic trajectories.⁵⁰ This proposal has been questioned, as Lluch and coworkers have claimed that such KIEs can be predicted using variational transition state theory (VTST).⁵³

Reactions of 1O_2 are difficult theoretical problems, in part due to the limitations of standard theoretical approaches in describing the electronic structure of 1O_2 as it interacts with other molecules. As a result, varying calculational methods make drastically differing predictions of the ene energy surface and mechanism.⁴⁷ Practically, the decisive assignment of the detailed mechanism compels careful consideration of experimental observations. We describe here a unique experimental observation in the 1O_2 ene reaction of d_6 -tetramethylethylene (**1**), figure 2-2, show a near temperature-independence of the KIE over a 250° temperature range. This result is predictable from trajectory studies on a bifurcating energy surface, but it is not satisfactorily predictable from statistical rate theories.

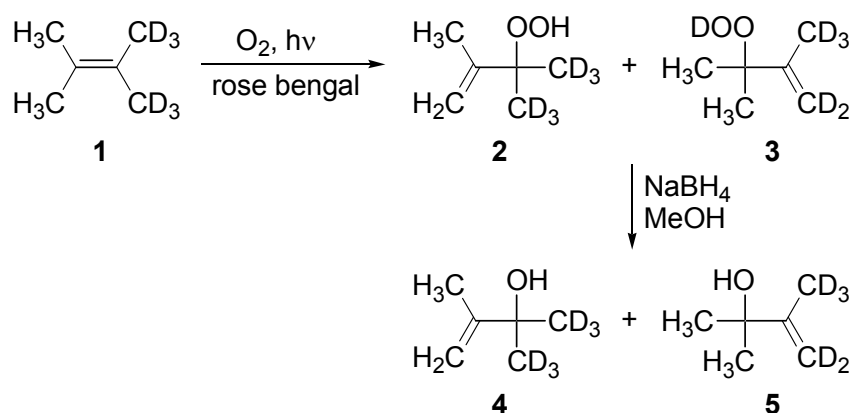


Figure 2-2. Illustration of the ¹O₂ ene reaction of d₆-tetramethylethylene.

Results

Experimental Kinetic Isotope Effects

The experimental intramolecular KIE for the ¹O₂ ene reaction of **1** was studied at temperatures ranging from 77 K to 328 K. The KIE was determined by ¹H NMR from the ratio of isotopomeric alcohols **4** and **5** formed after deoxygenation of the initial hydroperoxides **2** and **3** with NaBH₄ in methanol. The accuracy of these measurements was improved by referencing the observed integrations to those from unlabeled materials (see Chapter VI), in analogy with the process we have used to determine ¹³C KIEs.⁵⁴ The results are shown in Fig. 2-3. There were necessarily some differences in the reaction conditions across the temperature span – the reactions at 193 K and higher were conducted in methanol, while reactions at 118 K to 163 K were conducted in Freons (CHClF₂ or 2:1 CHClF₂:CHF₃) containing 5% methanol, and the reaction at 77 K used liquid nitrogen with **1** and 5% methanol suspended heterogeneously. The variation in

the reaction conditions may contribute to some apparent scatter in the observed KIEs, along with a limited precision of the measurements (estimated uncertainty of ± 0.03). Nonetheless, all of the KIEs are between 1.44 and 1.58, and such little change across a broad temperature range is remarkable.

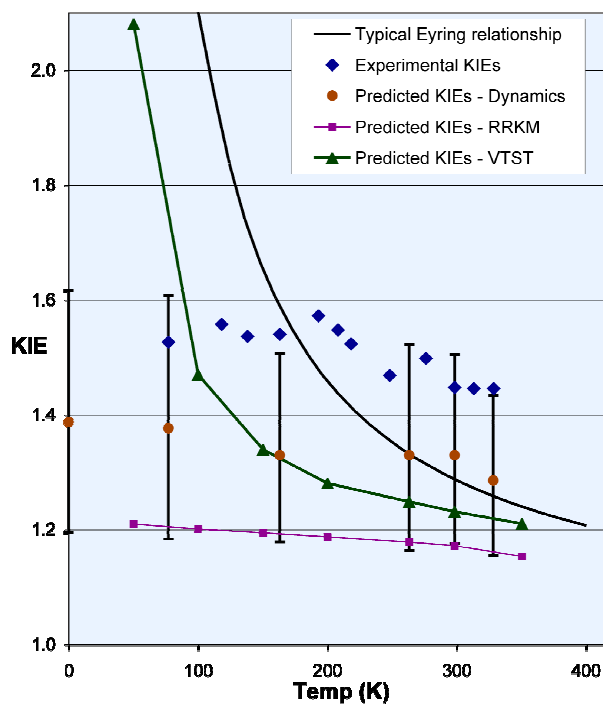
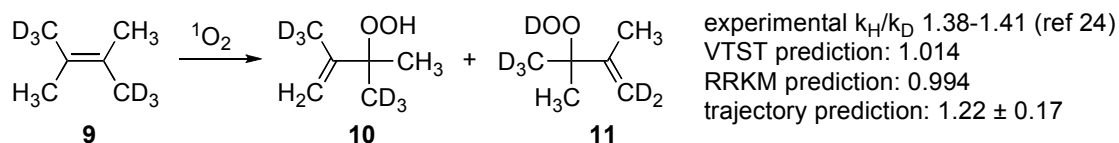


Figure 2-3. Plot of the experimental intramolecular KIE (k_H/k_D , defined by the 2 : 3 ratio) versus temperature for the ene reaction of $^1\text{O}_2$ with **1**, along with predicted isotope effects from various theoretical models. Error bars on the KIEs predicted from trajectories represent 95% confidence limits.

For transition state theory to explain this observation, $\Delta\Delta H_{act}^0$ would have to be approximately zero (<20 cal/mol). In enzymatic reactions, KIEs that are nearly temperature independent over much more limited ranges have been of substantial interest in recent years,⁵⁵⁻⁵⁸ and the explanations for these observations have invoked tunneling effects. Tunneling-based models can readily account for a phenomenological $\Delta\Delta H_{act}^0$ being approximately zero over a limited temperature regime, but such models cannot account for the broad temperature independence here. Outside of tunneling complications, KIEs in conventional transition state theory arise mainly from zero-point energy effects and $\Delta\Delta H_{act}^0$ should not be zero when the KIE is not unity (it is generally >200 cal/mol for a KIE of 1.45 at 298°). The failure of transition state theory here is qualitative and unique.

Theoretical Models

Variational Transition State Theory Calculations

Following the process used by Lluch in ref. 53, steepest-descent paths in mass-weighted coordinates were followed from geometries near the valley-ridge inflection point on the B3LYP/6-31G* energy surface. This was done for geometries of both the geminal and cis d₆-tetramethylethylene leading to abstraction of either a proton or deuterium by ¹O₂. The steepest-descent paths were obtained using a modified version of PROGDYN in which no momentum is given to nuclei and very small steps (< 0.00025 Å) are used, varying the size of the steps continually to avoid oscillations. This approach has the problem of being extremely slow compared to other approaches, but it

has the virtue of being extremely reliable.

At regular intervals along the steepest-descent paths, frequency calculations were carried out and free energies were calculated using the harmonic approximation without scaling. Isotope effects were then based on the free-energy maxima at the various temperatures along the H-abstraction and D-abstraction paths.

RRKM (Rice, Ramsperger, Kassel, Marcus) Calculations

RRKM theory predicts the rate of chemical reactions at a given energy.^{59,60} Its application in the current case is complicated by the fact that reactants passing through initial transition state **6** will have a thermal distribution of energy that is assumed to be maintained further along the reaction coordinate, in addition to that picked up from proceeding down the surface. To allow for this, the rate constant was calculated for a distribution of energies based on a thermal distribution in **6** + 6.554 kcal/mol. This 6.554 kcal/mol is the amount of extra energy within the molecule as it falls off the initial rate limiting transition structure, **6**, on the potential energy surface. This latter energy was calculated as the energy difference (CCSD(T)/aug-cc-pdz//B3LYP/6-31G* + zpe) between **6** and a point further along the path used as the “starting material” for the RRKM calculations. The particular choice of starting material structure makes no difference in the isotope effect calculation, since its number of states cancels out in the calculation. Isotope effects were then based on an energy-distribution weighted average of the minimum RRKM rate constants along each of the steepest-descent paths obtained above. The RRKM calculations were carried out using an available program⁶¹ and employing the Beyer-Swinehart direct count algorithm.⁶²

Dynamics Calculations: PROGDYN

Trajectories were started in an area shortly before the VRI on the B3LYP surface, centered on the minimum-energy path (MEP) with O₁-C₁ and O₁-C₂ distances of 1.95 Å. The starting atomic positions were randomized using a sampling of possible displacements for each normal mode, in effect randomizing the phase of each mode. The trajectories were initialized at various temperatures, giving each mode its zero point energy (zpe) plus a Boltzmann sampling of vibrational levels, with a random sign for its initial velocity. The mode associated with the approach of the O₂ toward the olefinic carbons was given a Boltzmann sampling of translational energy. Employing a Verlet algorithm with all atomic motions freely variable, 1-fs steps were taken until either **2** or **3** was formed. The program suite PROGDYN used for dynamics is listed in the Appendix as a series of component programs as either Unix shell scripts or awk programs. Gaussian03⁶³ was used to calculate the forces at each point in trajectories. The original version of this program was published in the Supporting Information for ref. 50.

Predicted Kinetic Isotope Effects

Figure 2-3 includes predictions using VTST by the method of Lluch and coworkers.^{53,64} Lluch had previously noted that VTST substantially underestimated the KIE at 263 K, as 1.126 but it was argued that this was simply a quantitative error resulting from inaccuracy in the potential energy surface employed. The results here suggest that the failure of VTST is qualitative, as VTST, like conventional transition state theory, incorrectly predicts the shape of the temperature versus selectivity curve.⁶⁵

VTST errs notably in another respect, predicting a much smaller intramolecular KIE for isotopomer **9** than **1**. Experimentally, the KIE with **9** at 263 K is 1.38-1.41,⁵¹ only slightly smaller than the KIE for **1**, while the VTST prediction is only 1.014 (based on CCSD(T)/aug-cc-pvdz energies on the B3LYP/6-31G* paths). Inaccuracy in the energy surface can perhaps account for the error in any single VTST prediction but is unlikely to account for the qualitative error in the comparison of **9** versus **1**.

An alternative statistical rate theory that could in principle be applicable to these reactions is microcanonical variational RRKM theory.^{66, 67} The rationale for applying RRKM theory is that 6.9 kcal/mol (CCSD(T)/aug-cc-pdz//B3LYP/6-31G*) of potential energy is lost between the rate-limiting transition structure **6** and the second saddle point on the surface, **8** (a “peroxide”). This excess energy is normally ignored in condensed-phase reactions, but it will be retained as molecular enthalpy for several picoseconds while product formation occurs within a few hundred femtoseconds. Crim has demonstrated that it is possible for a molecule with excess energy to form product before this excess energy is redistributed to all the modes in the molecule even in condensed phase reactions.⁶⁸ In the low-temperature realm, this energy is much greater than the average thermal energy in **6** or **8**, so the predicted isotope effect varies little with temperature. In the high-temperature realm, the average thermal energy is comparable to the excess energy and the isotope effect changes slowly with temperature. Overall, the microcanonical variational RRKM predictions are highly successful in predicting the general trend observed experimentally. However, they underpredict the experimental w KIE substantially. In addition, the RRKM prediction for isotopomer **9** is

only 0.994, departing drastically from experiment and demonstrating the same qualitative error seen in the VTST calculations.

We had previously reported that quasiclassical trajectories on the gas-phase B3LYP/6-31G* surface could satisfactorily account for the KIE at 263 K,⁵⁰ and we have undertaken here a much more extensive study of the trajectories to see if they can account for the temperature-insensitivity of the selectivity. Over 5000 trajectories were started in an area shortly before the VRI on the B3LYP surface, centered on the minimum-energy path (MEP) with O₁-C₁ and O₁-C₂ distances of 1.95 Å. The starting atomic positions were randomized using a sampling of possible displacements for each normal mode, in effect randomizing the phase of each mode. The trajectories were initialized at various temperatures, giving each mode its zero point energy (zpe) plus a Boltzmann sampling of vibrational levels, with a random sign for its initial velocity. The mode associated with the approach of the O₂ toward the olefinic carbons was given a Boltzmann sampling of translational energy. Employing a Verlet algorithm with all atomic motions freely variable, 1-fs steps were taken until either **2** or **3** was formed. The results are plotted in Figure 1-3 as the ratio of **2:3** (the KIE) at each temperature, along with the uncertainty (95% confidence) in the derived ratios due to the necessarily limited number of trajectories.

The results from the trajectories strikingly parallel those from experiment. As the temperature is lowered, the KIE appears to approach a limiting constant value of approximately 1.4. Due to the uncertainty in the ratios at each temperature, subtle trends in the predicted isotope effect versus temperature would not be discernable, but the trajectory results are clearly not predicting the kind of asymptotic rise in the selectivity at low temperatures that was predicted by VTST. Overall, the trajectory-predicted isotope effects are qualitatively consistent with experiment. They quantitatively underestimate the isotope effects, but to a much smaller extent than RRKM theory.

Importantly, the quasiclassical trajectory calculations perform qualitatively better in predicting the KIE for **9**. In 805 trajectories at 263 K for the isotopomeric system, 442 afforded **10** and 363 afforded **11**, for a ratio of 1.22 ± 0.17 . This mirrors the experimental observation of a modestly lower KIE in **9** versus **1**. In both systems the prediction is lower than observed, though the observed KIE is at the edge of the 95% confidence range in each case.

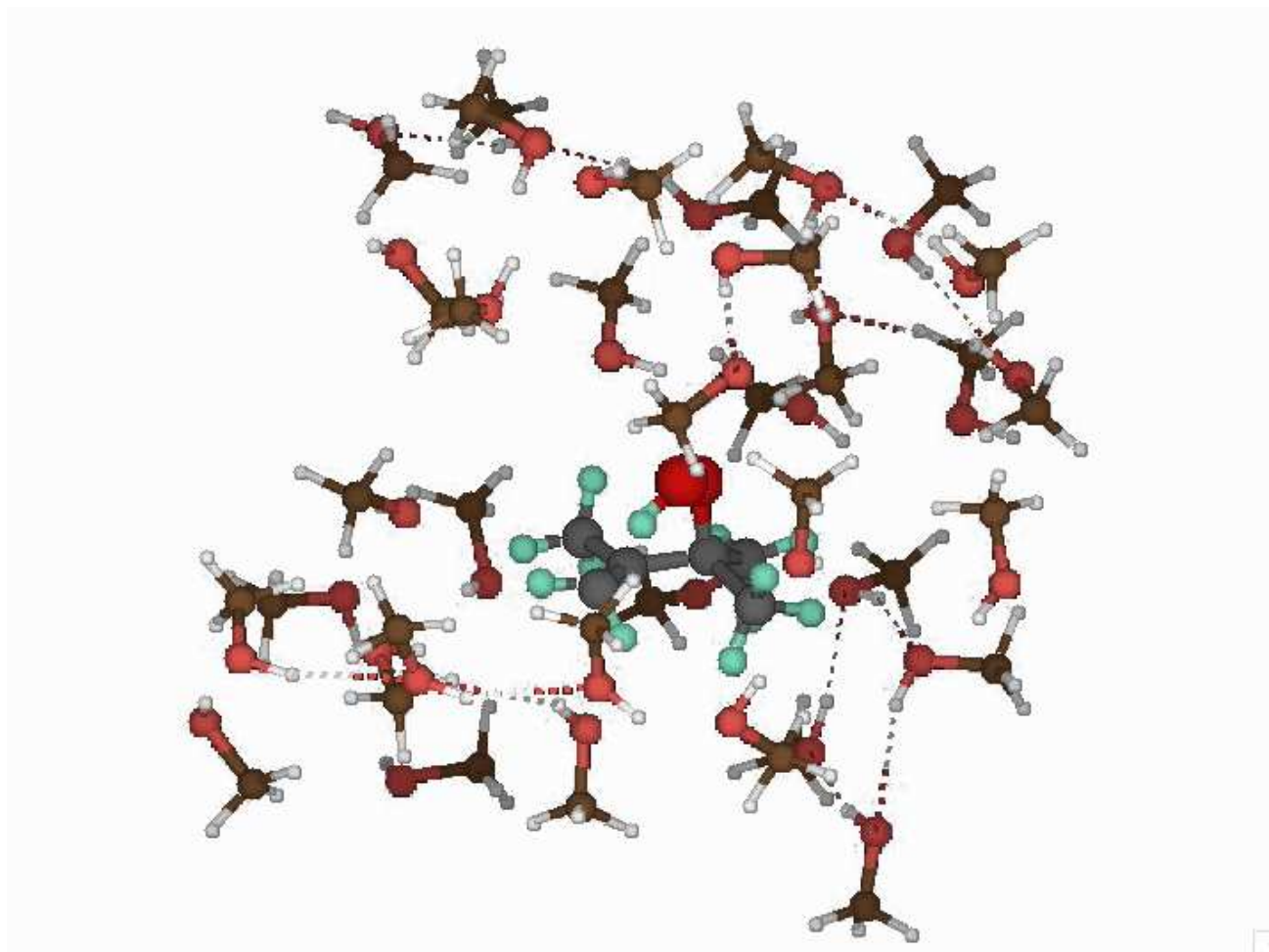


Figure 2-4. Ene product in a bath of 34 methanol molecules showing little product stabilization by solvent.

The ability of the gas-phase trajectories to account for the experimental observations in solution is perhaps surprising, but trajectory studies in the presence of solvent molecules suggest an intriguing explanation for a limited effect of solvent. A series of ONIOM (B3LYP/6-31G*:AM1) classical trajectories were started from **6** in a bath of 34 methanol molecules at 25 °C confined to a 15 Å cubic box, Figure 2-4. After equilibration periods spaced at 500 fs intervals up to 10,000 fs, fixed O₁-C₁ and O₁-C₂ distances of 2.38 Å were released and the reactions followed until product formation or a time limit of 1000 fs was reached. Of 39 trajectories started in this way, 32 (82%) afforded product within 1000 fs, with a median time of 328 fs. These results differ little from gas-phase classical trajectory results (see below) and suggest that solvent does not usually engender a long-lived intermediate. However, most trajectories (13 out of 20) started identically from **8** (with O₁-C distances of 1.68 Å), nominally farther along the reaction coordinate, do not react within 1000 fs. The difference in the latter case is that solvation equilibrated for the polar **8** stabilizes a polar intermediate.⁶⁹ In contrast, the starting ¹O₂ and **1** are nonpolar, as is the early transition state **6**, and in the trajectories started from **6** the solvent does not have enough time to organize to stabilize an intermediate before product formation. These results suggest that great care should be taken when inferring the presence of polar intermediates from standard theoretical methods that assume equilibrium solvation.

Discussion

What is the nature of the isotope effect observed in this system? The potential energy surface for the reaction of ¹O₂ with **1** is symmetrical in Cartesian coordinates, but

the energy surface loses symmetry in both a classical and a quantum-mechanical way. Classically, the potential energy surface is asymmetric in mass-weighted coordinates. There are two reasons to discount this form of asymmetry as a source of the isotope effect. The first is that the steepest-descent path in mass-weighted coordinates starting from **6** leads to minor product **3**. In other words, the mass-asymmetry of the surface favors the wrong product. A second reason is that fully classical trajectories fail to predict an isotope effect; of 501 classical trajectories started as above except using a classical 298 K Boltzmann distribution of energies in the modes, 249 afforded **2** and 252 afforded **3**.

Quantum-mechanically, the energy surface loses symmetry after the inclusion of zero-point energy. In fact, the steepest-descent paths to **2** and **3** encounter bottlenecks on the zpe surface, as found by Lluch,⁵³ and the area before these bottlenecks may be formally described as an intermediate. However, the barrier on this surface is only 0.2 kcal/mol (CCSD(T)/6-31+G**//B3LYP/6-31G* + zpe). The asymmetry of the zpe surface is a real effect that should contribute to the observed isotope effects, but as reflected by the RRKM KIE predictions, the surface asymmetry itself is not sufficient to account for the magnitude of the KIEs with **1** and **9**.

Conclusion

The bulk of the isotope effect observed in these reactions seems most likely due to a second effect of the inclusion of zero-point energy, the much greater energy put into the vibrations associated with C-H bonds than those associated with C-D bonds. In ordinary reactions where the rate is dominated by barriers, this energy difference affects

barrier heights. In the absence of a significant barrier here, it seems reasonable that this energy difference and the much greater motion of the lighter atom may have direct *dynamical* consequences. It is this dynamical effect that we are proposing as a new form of kinetic isotope effect. Within the terminology of transition state theory, this temperature-insensitive difference in the chance of two isotopes reacting would be associated with a difference in activation entropy.

The physical ideas underlying this isotopic selectivity and related product selectivities on bifurcating surfaces will require much further elaboration, but it is interesting to examine in general perspective the requirements for a quantitative theory. Transition state and RRKM theories predict rates from the properties of a dividing surface separating reactants from products. As a theorem, an optimized hypersurface in *phase space* can always lead to correct rate predictions, but current theories define dividing surfaces in *coordinate space*, with a temperature or energy-dependent placement of the dividing surface as the only extension beyond coordinate space. The failure of the statistical rate theories as compared to the success of quasiclassical trajectories in predicting the experimental observations here suggests that any quantitative theory of selectivity in these reactions will require a more complete consideration of phase space.

CHAPTER III

OBSERVATION AND PREDICTION OF HEAVY-ATOM DYNAMIC ISOTOPE EFFECTS

Introduction

Many simple reactions pass through symmetrical transition states to afford without barrier products of lower symmetry.^{70,71} Often this is inconsequential because the two or more formal products afforded may be identical or rapidly equilibrated by conformational interconversion. Even when the products are enantiomers, so as to be in principle distinguishable, the obligatory 1:1 selectivity is uninteresting. The situation changes with isotopic substitution, as a product selectivity, i.e. an intramolecular kinetic isotope effect (KIE), may now be observed and it is a challenge for current chemistry to quantitatively or qualitatively account for this selectivity. We describe here the observation of heavy-atom isotope effects of this type in a familiar reaction, along with an approach to the difficult problem of predicting these isotope effects.

Diverse calculational methods predict that the Diels-Alder dimerization of cyclopentadiene involves a C_2 -symmetric ‘bispericyclic’ transition structure.^{72,73} As the symmetric transition structure **1** morphs into the asymmetric product, the reaction pathway bifurcates into two, Figure 3-1. An isotopically labeled atom may be present in five positions (*a-e*) of **1**, and each possibility may give rise to a pair of distinguishable

isotopomeric products. For example, **1** containing a ^{13}C at the starred carbon *d* may afford either **2** or **3**. The ratios of the paired isotopomers constitute intramolecular KIEs that are decided on the downhill slope of a bifurcating energy surface.

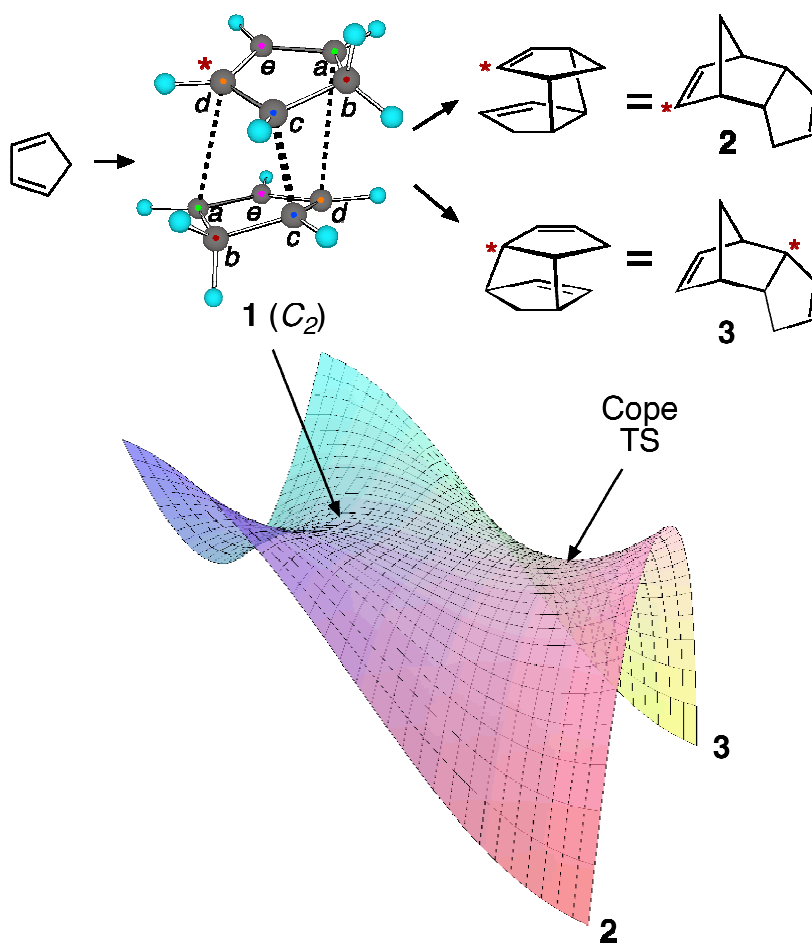


Figure 3-1. Illustration showing different products resulting from C_2 – bispericyclic transition state on a symmetrical potential energy surface.

Results

In principle the intramolecular ^{13}C KIEs in the cyclopentadiene dimerization could be determined by a direct measurement at natural abundance of the relative ^{13}C content in the various positions in the dimer.⁷⁴ However, the fact that 3 of the 4 olefinic peaks lie within a few Hz of each other with overlapping of the complex C-C couplings, makes this method impractical for this particular system. An indirect procedure employing intermolecular KIEs provided more precise results since, any errors from C-C couplings cancel between spectra. Dicyclopentadiene undergoes a degenerate [3,3]-sigmatropic (Cope) rearrangement at temperatures below its normal cracking temperature⁷⁵ and this rearrangement equilibrates the isotopomeric pairs formed in the dimerization process.

Experimental ^{13}C Kinetic Isotope Effects

The difference in the isotopic composition of equilibrated (140 °C, 6 h) dicyclopentadiene versus dicyclopentadiene prepared from cyclopentadiene at 25 °C (“kinetic dimer”) reflects the departure of the kinetic dimer from its equilibrium composition, and this difference is readily determined by NMR methodology.⁷⁶ The intramolecular KIEs were then obtained by correcting the raw results to allow for small calculated (B3LYP/6-311+G**) equilibrium isotope effects. The average results from seven independent determinations, each based on six spectra for each equilibrated and kinetic dimer sample, are summarized in Figure 3-2.

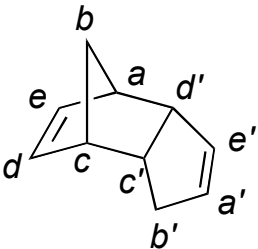
	Relative Amount ¹³ C	Intramolecular KIE
	<i>a/a'</i> 0.981(6)	<i>a/a'</i> 1.020(6)
	<i>b/b'</i> 0.998(2)	<i>b/b'</i> 1.002(2)
	<i>c/c'</i> 1.008(3)	<i>c/c'</i> 0.992(3)
	<i>d/d'</i> 1.017(4)	<i>d/d'</i> 0.983(4)
	<i>e/e'</i> 0.999(3)	<i>e/e'</i> 1.001(3)

Figure 3-2. Intramolecular ¹³C KIEs in the dimerization of cyclopentadiene. The intramolecular KIEs are defined as $k_{12C}/k_{13C}(a)/k_{12C}/k_{13C}(a')$, $k_{12C}/k_{13C}(b)/k_{12C}/k_{13C}(b')$, etc.

Strikingly, the intramolecular ¹³C KIEs observed are substantial, comparable in magnitude to ordinary ¹³C KIEs, despite the absence of a barrier between 1 and the five pairs of isotopomeric products. The largest KIEs are observed in the *a/a'* and *d/d'* positions, with a preference in both cases for ¹²C to be incorporated into the newly formed σ bond. The direction of these KIEs is interestingly what would be qualitatively expected if the transition state was highly unsymmetrical, though calculations weigh strongly against this explanation.⁷³

The prediction of an intramolecular isotope effect would conventionally require a comparison of the rates expected from transition state theory for two isotopomeric transition states. In the case here the pairs of products are each produced from a *single* cycloaddition transition state, so the conventional approach cannot be applied. Luch

has proposed that variational transition state theory can be applied in such cases.⁷⁷ A limitation of the Lluch approach, however, is that it requires the existence of dynamical bottlenecks along steepest-descent paths leading to the products. The variational transition state theory approach places the bottleneck at the dividing surface between reactants and products which maximizes the generalized activation free energy. Lluch emphasizes that by using variational transition state theory distinct dynamical bottlenecks leading to each particular product can be located in a reaction including those involving a VRI with no additional dynamic calculations being required to successfully predict the experimental product distributions.

Theoretical Calculations

In order to demonstrate the Lluch method, the VRI and any subsequent dynamical bottlenecks need to be located. To find the VRI the frequencies perpendicular to the potential energy surface were analyzed on the minimum energy path. The minimum energy path was determined from the rate limiting TS by taking 0.05 steps in the direction of the gradient toward product using a variation of the PROGDYN program. The VRI is defined as the geometry where the lowest harmonic mode perpendicular to the minimum energy path goes to nearly zero. Unlike the case observed with $^1\text{O}_2$ where there was a small saddlepoint after the VRI, no such saddlepoint and consequently, no bottleneck was located on the potential energy surface for the dimerization of cyclopentadiene. With the absence of bottlenecks on the potential energy surface leading to the product for the dimerization of cyclopentadiene, it is impossible to apply the Lluch method for prediction of the kinetic isotope effects.

Trajectory Analysis

The prediction of deuterium isotope effects in similar circumstances has been successfully accomplished using repetitive randomized quasiclassical trajectory calculations to establish a branching ratio for formation of the competitive products.⁷⁸ This approach requires a sufficient number of trajectories to make the uncertainty in the derived branching ratio smaller than the magnitude of the observed isotope effect. To obtain an uncertainty in the branching ratio of only $\pm 1\%$, as would be required here for a quantitative estimate of the KIEs, approximately 160,000 trajectories would be required. This is two orders of magnitude beyond what is practical in DFT calculations.

We reasoned that this problem may be circumvented by using, *in silico*, much heavier isotopes of carbon. Toward that end, quasiclassical trajectories were initiated from isotopologues of **1** containing a single carbon of mass 140 amu (¹⁴⁰C) at positions *a* or *d*. Each normal mode in **1** was given its zero-point energy plus a Boltzmann sampling of additional energy appropriate for 25 °C, with a random sign for its initial velocity. The transition vector was given a Boltzmann sampling of translational energy ‘forward’ from the col. Employing a Verlet algorithm, 1-fs steps were taken until the product was formed. In repetitive runs, trajectories affording product with the superheavy carbon in the *a* versus *a'* or *d* versus *d'* positions were counted. The results are summarized in Table 3-1.

Predicted Isotope Effects

Of 508 trajectories started with ¹⁴⁰C in position *a* of **1**, 306 afforded product with the ¹⁴⁰C in position *a'* and 202 afforded product with the ¹⁴⁰C in position *a*. Of 336

trajectories started with ^{140}C in position *d* of **1**, 156 afforded product with the ^{140}C in position *d'* and 252 afforded product with the ^{140}C in position *d*. Both of these observations differ from unity with a statistical significance of greater than 99.9% confidence. In both cases, the direction of the effect is the same as that observed experimentally for ^{13}C .

Table 3-1. Results of trajectories employing superheavy carbons.

label position in 1	weight	results	ratio
<i>a</i>	140	202 <i>a</i> , 306 <i>a'</i>	0.66 ± 0.12
	76	66 <i>a</i> , 95 <i>a'</i>	0.69 ± 0.23
<i>b</i>	140	398 <i>b</i> , 376 <i>b'</i>	1.06 ± 0.14
	76	240 <i>b</i> , 229 <i>b'</i>	1.05 ± 0.20
<i>c</i>	140	323 <i>c</i> , 242 <i>c'</i>	1.33 ± 0.23
	76	417 <i>c</i> , 319 <i>c'</i>	1.31 ± 0.18
<i>d</i>	140	252 <i>d</i> , 156 <i>d'</i>	1.52 ± 0.27
	76	228 <i>d</i> , 186 <i>d'</i>	1.11 ± 0.19
<i>e</i>	140	360 <i>e</i> , 337 <i>e'</i>	1.07 ± 0.15
	76	107 <i>e</i> , 96 <i>e'</i>	1.11 ± 0.32

Discussion

The most striking observation is the fact that there are significant isotope effects observed for the dimerization of cyclopentadiene. As chemists we instinctively look to transition state theory to determine product ratios for reactions in which multiple products are formed. The underlying concept in transition state theory is that one transition state leads to one product and thus, selectivity in reactions can be determined from the relative barriers of the transition states leading to different products, Figure 1-5. When transition state theory fails, we must look to a more elemental theory based on the fundamentals of motion. Dynamic theory is governed by the second law of Newtonian mechanics, in its most basic form, $F=ma$. Dynamic theory implies that the product outcome is a direct result of atomic motions at the transition state and it is the momentum (a vector which involves both magnitude and direction) of the atoms at this point that determines their position in the product.

The dimerization of cyclopentadiene shares some similarity with the $^1\text{O}_2$ ene reaction with tetramethylethylene as they both have a rate limiting symmetric transition state connected to a second, degenerate transition state on the minimum energy path. This second degenerate Cope transition state connects both products of the reaction which are identical with the exception for isotopically labeled material. The significant isotope effects observed at the a/a' and d/d' positions are clear indicators of selectivity

in a reaction where there should be no selectivity in accord with TST. These KIE's qualitatively suggest that the asymmetry produced in mass-weighted coordinates on the potential energy surface is enough to produce selectivity. The results suggest that the selectivity of the reaction can be explained by a new form of dynamic isotope effects, "heavy atom dynamic effects."

Conclusion

The dimerization of cyclopentadiene appears unique in having heavy-atom isotope selectivity for a reaction that goes through a symmetric rate limiting transition state. The preference of ^{13}C to be in the π bond of the product is an example of a new phenomenon, "heavy-atom dynamic isotope effect." This heavy-atom dynamic effect arises from the fact that the position of the heavy isotope, ^{13}C , in the product is determined after the rate-limiting transition state on the potential energy surface.

CHAPTER IV

DYNAMIC EFFECTS ON PERISELECTIVITY

Introduction

Frontier molecular orbital (FMO) theory is a conceptual support, developed by Fukui, used as a tool for understanding selectivity and reactivity in cycloaddition reactions.⁷⁹ FMO theory employs perturbation theory, emphasizing the interactions of the highest occupied molecular orbital (HOMO) with the lowest unoccupied molecular orbital (LUMO), otherwise referred to as the frontier orbitals. This analysis of orbital interaction ensures that selectivity prefers the product resulting from the transition state in which the frontier orbitals are closest in energy i.e. the transition state with the lowest activation energy. This of course should be familiar as it reflects a basic principle of transition state theory, the selectivity of a reaction is determined by the relative heights of the barriers to form product where preference is given to the product with the lower barrier for formation. A subtle but important assumption in transition state theory is the fact that a single transition state leads to a single product. This fundamental idea is so ingrained in our understanding of reaction mechanisms that it has long been accepted as an infallible rule. However, there have been a number of reactions whose mechanisms evoke exceptions to this rule.

In situations where there is a non-statistical distribution of products, other factors related to selectivity must be considered on a more fundamental level. To understand this non-statistical product distribution one needs to consider both the shape of the potential energy surface in addition to atomic motions at the transition state in terms of Newtonian mechanics, $F=ma$. Bifurcations arise on potential energy surfaces when two successive transition states are connected on the minimum energy path in which the first is rate limiting and the second is an intermediary between potential products. A bifurcating energy surface can be either of two forms, a symmetrical or unsymmetrical Figure 1-6. We have encountered a symmetrically bifurcating surface when dealing with the dimerization of cyclopentadiene, Figure 3-1, where the reaction produces two chemically equivalent products.

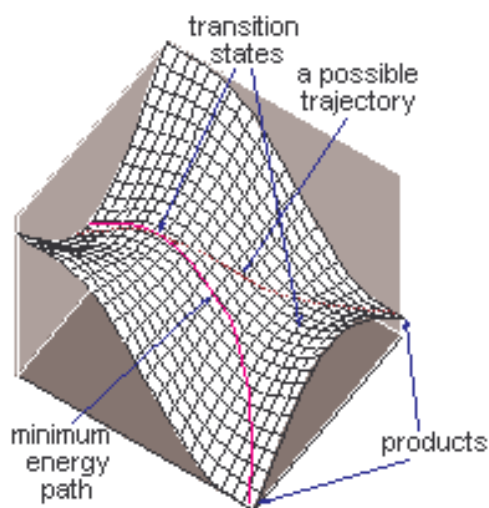


Figure 4-1. Unsymmetrically bifurcating surface.

On the other hand, an unsymmetrical bifurcating surface as is illustrated in Figure 4-1 is much less understood with far less documented cases.¹² In the case of unsymmetrical bifurcating surfaces, the minimum energy path does not bifurcate however; trajectories from the rate limiting transition state can lead to either of two chemically distinct products. For reactions which proceed via an unsymmetrical bifurcating surface, the product distribution cannot be explained in terms of transition state theory. On the other hand, selectivity in these reactions can be qualitatively predicted from trajectory studies.

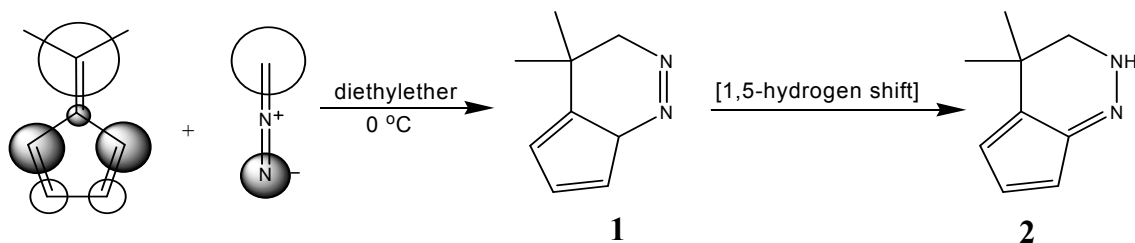


Figure 4-2. HOMO-LUMO interactions leading to [6 + 4] product.

To gain further understanding of selectivity on an unsymmetrical bifurcating energy surface, the cycloaddition of diazomethane with dimethylfulvene will be studied. The reaction is quite attractive because Houk indicated that the major product from the reaction was a [6 + 4] cycloaddition product, Figure 4-2, rather than the initial products reported by Alder.⁸⁰ He instead identified the major cycloadduct produced as **2**, the resultant tautomer of **1**, an initial [6 + 4] cycloaddition of dimethylfulvene with diazomethane. This of course, was quite fascinating, as it was the first reported case of a

6 electron + 4 electron cycloaddition. Upon reviewing Houk's report, a rather interesting alternative was envisioned, a second uncharacterized product was also observed which upon heating was converted to the major product. What if Houk was wrong? One way to determine this is to figure out the mechanism of the reaction. Standard theoretical calculations to locate the transition state for the [6 + 4] cycloaddition would be an adequate starting point.

Initial calculations resulted in the location of a transition state leading to a [2 + 4] cycloaddition adduct which may have some dynamic significance. This [2 + 4] product, if formed during the reaction, would be contra the FMO argument set forth as the accepted explanation for the mode of reaction. The FMO argument suggests that the LUMO of dimethylfulvene interacts with the HOMO of diazomethane—which is closer in energy, leading to a [6 + 4] reaction of dimethylfulvene and diazomethane, since the coefficients are largest on C-2 and C-6 of the dimethylfulvene.^{81,82}

A closer look at the reaction of dimethylfulvene with diazomethane is necessary to gain a definitive understanding of the reaction mechanism. Described here is an experimental and theoretical study of the mechanism for the reaction.

Results

The reaction of dimethylfulvene with diazomethane was carried out over the course of a week at 0 °C in a dilute ether solution by Houk. This procedure was modified using deuterated chloroform or d₆-benzene as the reaction solvent and the diazomethane was generated using a modified procedure to eliminate the ether and ethanol peaks which overlapped with product peaks in the ¹H NMR spectrum.

Low Temperature NMR Studies

Initial reactions were carried out by generating neat diazomethane directly into a 1:1 solution of dimethylfulvene in deuterated chloroform at $-78\text{ }^{\circ}\text{C}$ in a 5 mm NMR tube. The NMR tube was kept at $-78\text{ }^{\circ}\text{C}$ until placed inside the spectrometer. The reaction was monitored at 400 MHz by low temperature ^1H NMR to determine the initial products of the reaction. At $-1\text{ }^{\circ}\text{C}$, one can observe the formation of two different products by ^1H NMR spectra. Fifteen minutes into the reaction it is clear that one product is being formed faster than the other, figure 4-3. As time progressed, it became clear that the formation of one product became dominant while the relative concentration of the other product remained constant. It became apparent that this major product was being formed directly from the reaction of dimethylfulvene with diazomethane as well as from the initial product Figure 4-2.

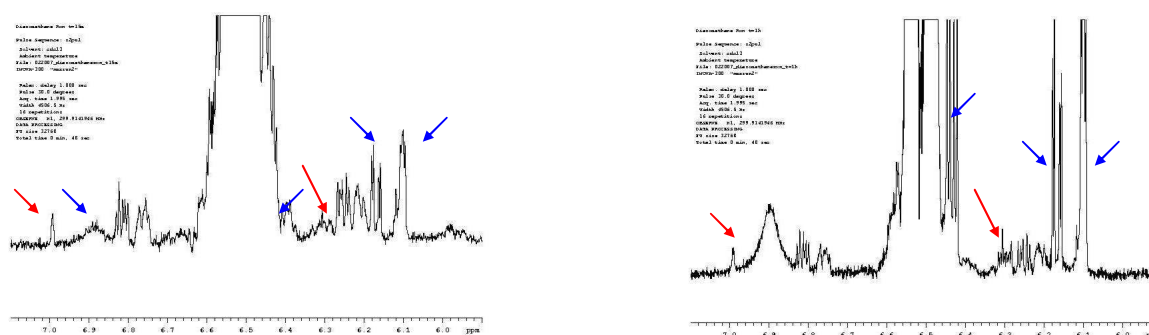


Figure 4-3. Low temperature NMR spectra of diazomethane reaction with dimethylfulvene a) $t = 15\text{ m}$ b) $t = 1\text{ h}$.

Experimental ^{13}C Kinetic Isotope Effects

From the observations at low temperature, we deduced that starting material KIEs would be able to confirm our observations of two products being formed initially. The magnitude of the isotope effects will give an idea of what is occurring at the rate limiting transition state. ^{13}C starting material KIEs for the reaction of dimethylfulvene with diazomethane were determined by NMR methodology at natural abundance. Two independent reactions of diazomethane with 1:1 dimethylfulvene in d_6 -benzene were taken to 80% conversion of dimethylfulvene. The unreacted dimethylfulvene was recovered by flash chromatography and compared to a standard sample of dimethylfulvene which was not subjected to the reaction conditions. The change in isotopic composition and the KIEs were determined relative to the methyl carbons of dimethylfulvene with the assumption that the isotopic fractionation at these positions is negligible, Figure 4-4.

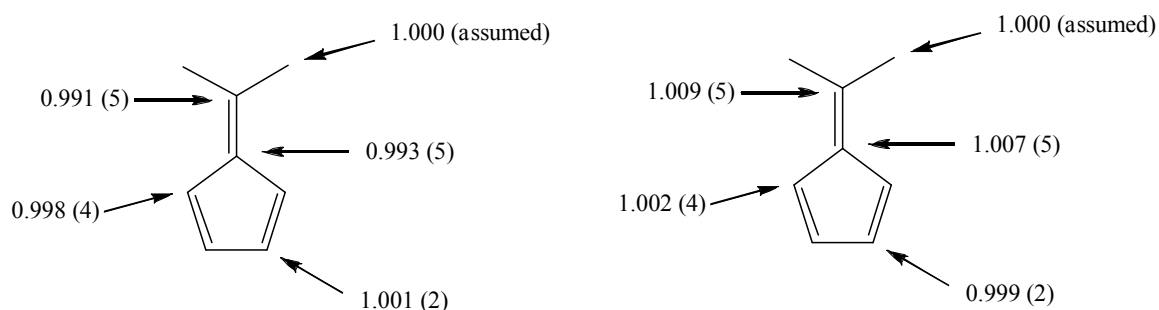


Figure 4-4. Observed kinetic isotope effects for the cycloaddition of diazomethane with dimethylfulvene a) relative ^{13}C integration b) KIEs.

Theoretical Calculations

To gain insight into the mechanism of the reaction effort was made to determine the transition state for the reaction. Attempts to locate the anticipated [6 + 4] transition structure for the reaction using both B3LYP/6-31G* and B3LYP/6-311+G** were unsuccessful. Instead, all attempts lead to a transition structure for the [2 + 4] cycloaddition and no structure was located that would directly lead to **1** on the minimum energy path. An alternative route to the [6 + 4] product would involve the initial formation of **4** followed by a [1,5]-sigmatropic rearrangement to **1** which would then go on to product **2**.

Upon closer examination, one can recognize a trend similar to that observed in the dimerization of cyclopentadiene, this transition structure is able to lead to the [6 + 4] product, Figure 4-5. This apparent merger of the [2 + 4] and [6 + 4] transition structures is however more interesting as the products should be readily distinguishable.

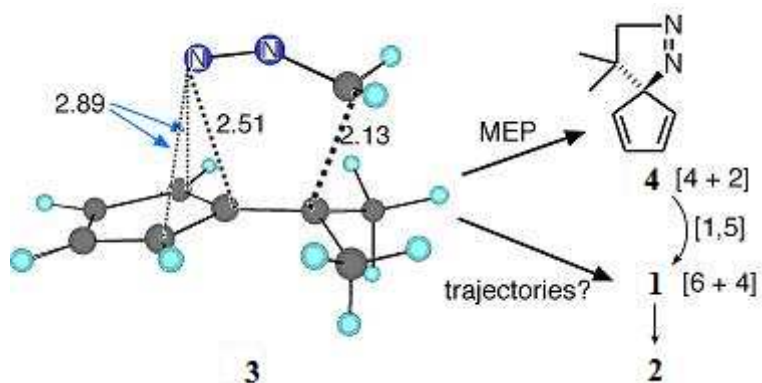


Figure 4-5. Scheme showing possible pathways from the [2 + 4] transition state to product both a [2 + 4] product and a [6 + 4] product.

Dynamics

Trajectories were set up in the usual manner starting from **3** giving each mode its zero point energy (zpe) plus a Boltzmann sampling of vibrational levels, with a random sign for its initial velocity. A Verlet algorithm with all atomic motions freely variable was utilized taking 1-fs steps until either **1** or **2** was formed. To our surprise, all 44 trajectories initiated at **3** ended with the formation of product **1**.

Discussion

The choice between the [2 + 4] and [6 + 4] products is dynamically determined after the rate limiting transition state. For the reaction of dimethylfulvene with diazomethane, contrary to the FMO expectation, a [6 + 4] transition structure leading to **1** on the MEP does not exist by either B3LYP/6-31G* or B3LYP/6-311+G** calculations. All attempts to locate the [6 + 4] transition structure end up at **3**, which is on the MEP leading to the [2 + 4] cycloadduct **4**. This computational result does not explain Houk's observation of a [6 + 4] product. However, it could then be rationalized that an initial formation of **4** followed by a [1,5] sigmatropic shift to **1** which could then rearrange to afford **2**. The likelihood for Houk to miss the formation of **2** is not impossible as the reaction lasted a week at 0 °C.

Another possibility is the direct formation of **2** from **3**, this would involve the twisting of diazomethane relative to dimethylfulvene after the rate limiting transition state. The twisting of diazomethane could be accomplished as a trajectory crosses the potential energy surface and the associated low-energy mode at 53 cm^{-1} is excited.

Conclusion

The reaction of dimethylfulvene with diazomethane is yet another case where the products from a reaction cannot be explained through transition state theory. In this case, the periselectivity of the reaction does not follow the prescribed FMO predictions in which the HOMO of diazomethane would react with the LUMO of dimethylfulvene to give a single [6 + 4] product, **2**. However, the formation of a [2 + 4] product, observable by low temperature ^1H NMR is confirmation of a form of dynamic effect, dynamic determined periselectivity.

CHAPTER V

KINETIC ISOTOPE EFFECT STUDY ON THE RATE ACCELERATION

OBSERVED “ON WATER” REACTIONS

Introduction

Physical and chemical methods can be employed to enhance the rate of difficult to accomplish reactions. Chemical modifications can be as simple as modifying the ratio of reactants, changing a reagent or even changing solvents. There are usually uncomplicated explanations to why these approaches work. However, there are exceptional cases where simple chemical methods result in extraordinary changes in reaction rates. A change in solvent has been recognized as one of the simplest and sometimes most efficient chemical method to affect reaction rates. There have been numerous documented examples of rate accelerations observed in organic reactions by simply switching to a different solvent. Many reactions are straightforwardly sensitive to the solvent polarity. For example, if a reaction of neutral compounds forms charged products, it will normally be accelerated in polar solvents due to stabilization of a partially charged transition state by the polar solvent. More interesting cases have been noted to involve the exploitation of aqueous solvent to afford several fold rate increases with little modification to the target reaction.^{83,84,85,86,87}

For several decades many examples have been documented where water has been utilized successfully as a solvent for synthetic organic chemistry. One class of reactions

which has demonstrated particular success is cycloaddition reactions. Huisman observed the beneficial effects of aqueous solvent on the Diels-Alder reaction of furan with maleic acid in 1973.⁸⁸ However, the concept of aqueous rate acceleration of Diels-Alder reactions did not gain popularity until the 1980s when controversy developed around the topic spearheaded by Breslow followed by Grieco.

In 2005, Sharpless reported a dramatic rate acceleration of the cycloaddition of quadricyclane with dimethyl azodicarboxylate when the reactions were conducted "on water". This process involves vigorous stirring of insoluble organic reactants with water to generate an aqueous suspension. Sharpless noted that the observed rate acceleration does not depend on the amount of water used as long as there is sufficient water present to facilitate clear phase separation.⁸⁹ Since Sharpless's original report, there have been numerous examples in the literature claiming rate acceleration on water. Overall, it must be judged that examples of the phenomenon observed by Sharpless have not been large in number or generally as impressive as the original reaction. The reactions of azodicarboxylates with quadricyclane were the key examples studied by Sharpless. Described here is an experimental and theoretical investigation of the effect of solvents on the cycloaddition reactions of quadricyclane, tables 5-1 a and b. The experimental ¹³C

isotope effects will be determined using NMR methodology developed in our group supported by standard theoretical calculations. The premise of this study is to gain some understanding of what is happening at the rate determining step for the reaction in aqueous versus organic solvent. From this information, we will be able to determine if the mechanism changes with solvent.

Results

The reaction of quadricyclane with diethyl azodicarboxylate (DEAD) was chosen as the target reaction for the study. Of necessity, DEAD was purified to ensure that effects observed in the different solvents were independent of toluene.⁹⁰ The reaction of quadricyclane and DEAD was carried out at 25 °C using water, acetonitrile and toluene as respective solvents. Under these conditions, the reaction is quantitative but at vastly different rates, ranging from a few minutes in water to several days in toluene; paralleling results observed by Sharpless et.al.⁸⁹ More importantly, the results suggest that the kinetics of the reaction of quadricyclane with dimethyl azodicarboxylate and diethyl azodicarboxylate are qualitatively similar.

Table 5-1. Summary of the rate of the cycloaddition of quadricyclane with a) dimethylazodicarboxylate⁸⁹ and b) diethyl azodicarboxylate.

a)	Solvent	Conc [M]	Time to Completion
	toluene	2	>7 d
	CH ₃ CN	2	>120 h
	neat	4.53	72 h
	H ₂ O	4.53	15 h

b)	Solvent	Conc [M]	Time to Completion
	toluene	2	>120 h
	CH ₃ CN	2	84 h
	neat	4.53	48 h
	H ₂ O	4.53	10 min

Reaction of Quadricyclane with Diethyl Azodicarboxylate

The ^{13}C product KIEs for the reaction in each solvent was determined by NMR methodology at natural abundance. For each solvent, two reactions were taken to 15% conversion of quadricyclane and compared to a standard sample which came from a reaction in which 100% of the quadricyclane was converted to product. For standard reactions, the solvent of choice was water because of the reaction rate and ease of purification. The choice of solvent for the reaction is inconsequential as long as the quadricyclane used was from the same stock as the reactions done at low conversion and all the quadricyclane is converted to product. The change in isotopic composition was determined relative to the bridging methylene carbon derived from quadricyclane with the assumption that the isotopic fractionation at that position is negligible. The KIEs were determined from the isotopic composition for the carbons derived from quadricyclane in the product. For the reaction on water, the isotope effects were 1.015 in the olefinic and 1.016 in the aliphatic positions. For the reaction in acetonitrile and in toluene, the isotope effects were quite similar, averaging 1.019 in the olefinic position and 1.020 in the aliphatic position. The isotope effects for the reaction in aqueous versus organic solvent does show a small but significant difference.

Lithium perchlorate solution in ether was also used as a solvent for the reaction. This resulted in the reaction being completed in mere seconds. The KIEs observed in 1 M lithium perchlorate solution was 1.017 and 1.013 at the olefinic and aliphatic positions respectively. These KIEs are distinctly lower than those measured for the

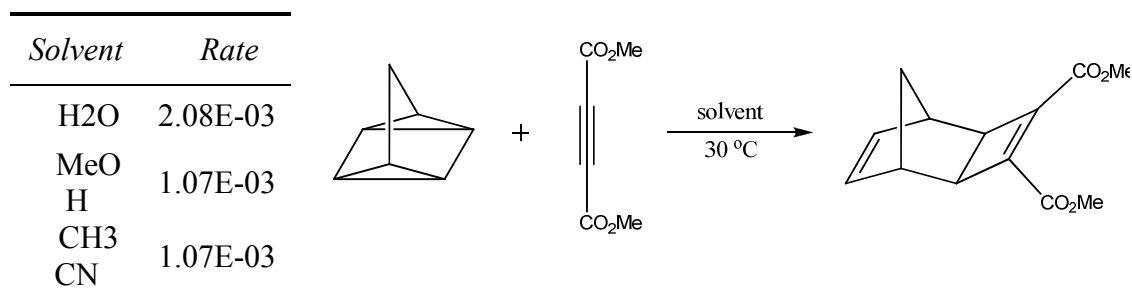
reaction carried out in other organic solvents but much closer to the isotope effect measured for the reaction on water.

Reaction of Quadricyclane with Dimethyl Acetylenedicarboxylate and 1,4-Benzoquinone

The results from the reaction in lithium perchlorate prompted us to investigate the combined effect of solvent with dimethyl acetylenedicarboxylate a similar dienophile with less capability to facilitate an electron transfer process. As a contrast, the reaction with benzoquinone was also studied since, benzoquinone is easily reduced ($E^I_{1/2} = -0.81$ V and $E^{II}_{1/2} = -1.48$ V, both reversible),⁹¹ providing a reasonable possibility for an electron-transfer mediated mechanism. For comparison, dimethyl acetylenedicarboxylate is not so easily reduced ($E_{1/2} = -1.49$, irreversible)⁹² and an electron-transfer mechanism would not be viable.

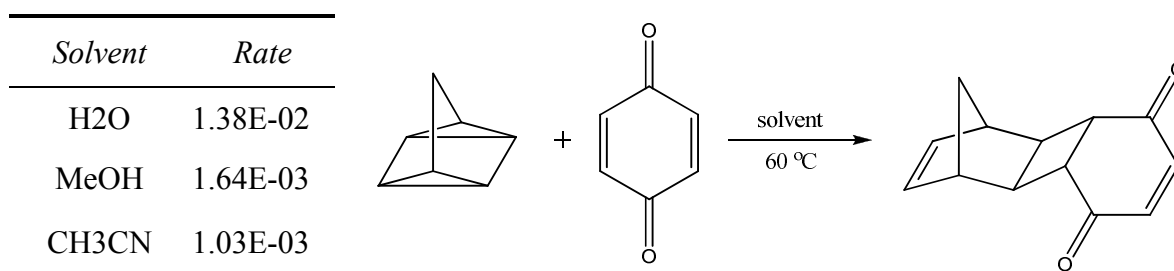
The reaction of quadricyclane with dimethyl acetylenedicarboxylate was explored in water, acetonitrile and methanol. The effect of water on the reaction with dimethyl acetylenedicarboxylate is not nearly as impressive. The reaction in methanol and acetonitrile occur at the same rate while the rate is merely doubled in water. Reaction rates were determined by ¹H NMR analysis of crude reaction mixtures over time, Table 5-2. The reactions were set up simultaneously with vigorous stirring of equimolar amounts of quadricyclane and dimethyl acetylenedicarboxylate to which the different solvents were added.

Table 5-2. Rate of reaction of quadricyclane with dimethyl acetylenedicarboxylate in different solvents determined by ^1H NMR.



Interestingly enough the reaction of quadricyclane with 1,4-benzoquinone, a recognized electron acceptor, had very different results. The rate of reaction in methanol is over 1.5 times faster than in acetonitrile and more than 13 times faster in water. The reactions were set up similarly to those above at 60 °C and analyzed similarly by ^1H NMR, results are summarized below in Table 5-3.

Table 5-3. Rate of reaction of quadricyclane with 1,4-benzoquinone in different solvents determined by ^1H NMR.



Based on the similarity in the trends observed for the reaction of quadricyclane with diethyl azodicarboxylate ($E_{1/2} = -0.497 \text{ V}$)⁹³ and with 1,4-benzoquinone, KIE experiments were carried out similarly to those done with diethyl azodicarboxylate with different results. On water the KIEs are 1.016 in the olefinic position and 1.029 in the aliphatic position while in acetonitrile, the KIEs are 1.014 in the olefinic position and 1.039 in the aliphatic position.

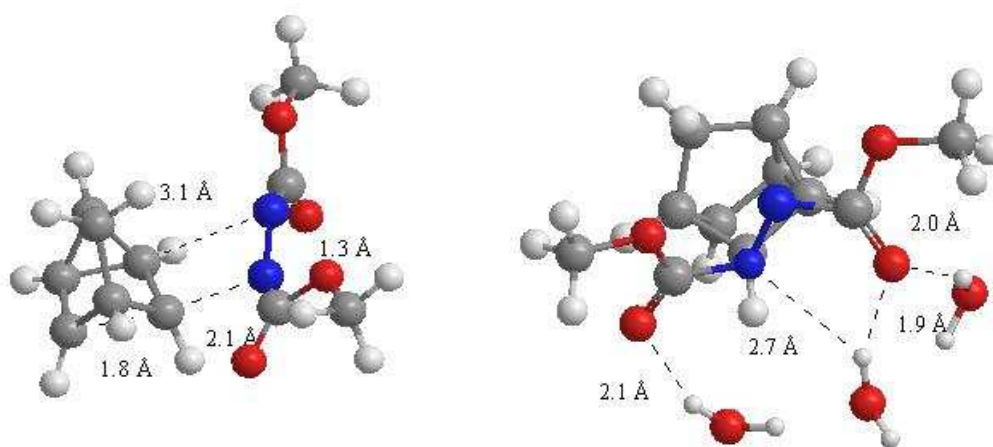


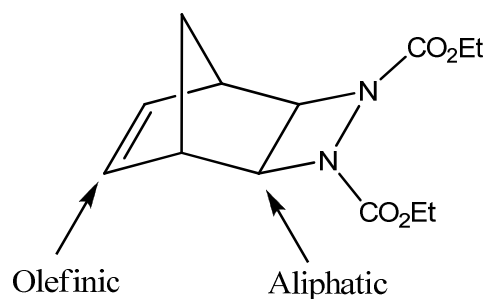
Figure 5-1. $2\sigma+2\sigma+2\pi$ transition structures proposed by Marcus for the cycloaddition of quadricyclane with dimethyl azodicarboxylate a) in organic solvent b) ‘on water’.

Theoretical Models

Standard theoretical calculations have been used to model the transition state for the reaction of quadricyclane with DEAD. The transition state reported in the literature involves a $2\sigma+2\sigma+2\pi$ interaction between quadricyclane and DEAD for organic solvents, Figure 5-1.⁹⁴ The picture of the transition state for the reaction is only slightly modified, involving a series of three water molecules connecting the carbonyl groups of DEAD via

a series of hydrogen bonds.⁶⁰ The KIE for the reaction was predicted from these transition structures proposed by Marcus using UB3LYP functional, Table 5-4, resulted in KIEs within range for the olefinic position at 1.021 but are largely overpredicted for the aliphatic position at 1.036. The transition structure proposed to the reaction on water was also used to predict KIEs for the reaction and resulted in a large inverse isotope effect of 0.977 at the olefinic position and an inflated normal isotope effect of 1.032 at the aliphatic position. The $2\sigma+2\sigma+2\pi$ transition structure for the reaction was also investigated using B1B95 and MPW1K functionals which also predicted excessively small olefinic isotope effects of 1.004 and 0.999 respectively and too large 1.032 and 1.029 respectively isotope effects at the aliphatic positions.

Table 5-4. Predicted KIEs for the generally accepted $2\sigma+2\sigma+2\pi$ theoretical model proposed by Marcus.



	<i>UB3LYP</i>	<i>UB3LYP</i> 3 <i>H₂O</i>	<i>B1B95</i>	<i>MPW1K</i>	<i>H₂O</i>	<i>CH₃CN</i>
Olefinic ¹³ C	1.021	0.977	1.004	0.999	1.015(3) ^a	1.019(3) ^a
Aliphatic ¹³ C	1.036	1.032	1.032	1.029	1.016(3) ^a	1.020(3) ^a

^a Experimental KIEs (k_{12C}/k_{13C}) for the cycloaddition of quadricyclane with DEAD. Standard deviations (n=6) are shown in parentheses.

The failure of the accepted $2\sigma+2\sigma+2\pi$ mechanism to predict the observed isotope effects along with results from experiments with benzoquinone and dimethylacetylene dicarboxylate encouraged us to explore the possibility of an electron transfer mechanism. The isotope effect predicted for the cation radical using UB3LYP is 1.012, Table 5-5. The magnitude of this predicted isotope effect is very close to the observed isotope effect for the reaction of quadricyclane with DEAD in lithium perchlorate, 1.017 at the olefinic and 1.013 at the aliphatic position.

Table 5-5. Predicted KIEs for a theoretical model involving the formation of a quadricyclane cation radical as the rate limiting step.

	<i>UB3LYP</i>	<i>LiClO₄</i>	<i>H₂O</i>	<i>CH₃CN</i>
Olefinic ¹³ C	1.012	1.017(4) ^a	1.015(4) ^a	1.019(4) ^a
Aliphatic ¹³ C	1.012	1.013(3) ^a	1.016(4) ^a	1.020(3) ^a

^a Experimental KIEs (k_{12C}/k_{13C}) for the cycloaddition of quadricyclane with DEAD. Standard deviations (n=6) are shown in parentheses.

Discussion

It has long been recognized that the choice of solvent can have a considerable effect on the outcome of cycloaddition reactions. Aqueous rate acceleration in these reactions has been attributed to a number of effects over the years including solvent

pressure—a direct effect on the volume of activation. Other hypotheses include the formation of micelles and antihydrophobic effects.

In the 1980's Grieco revealed that some previously unsuccessful Diels-Alder reactions were greatly improved when carried out in 5 M lithium perchlorate solutions.^{84,85,86} Grieco's initial explanation for the success of these reactions lay in the ability of lithium perchlorate to act as "a unique ionic medium" which confines solute movement while retaining solvent ordering. He theorized that the mode of action of the lithium perchlorate in accelerating these reactions involved compressing the reactants in much the same manner as the 'macroscopic' application of external pressure.⁸⁶ These early ideas proposed by Grieco have been popular and extend to antihydrophobic effects. Antihydrophobic salts such as lithium perchlorate disrupt the structure of water, reducing the surface tension to make cavitation easier. Alternatively, Breslow has done extensive work on reactivity in aqueous solution. Breslow culminated over a decade of research on the subject with his publication of *Hydrophobic and Antihydrophobic Effects on Organic Reactions*,⁹⁵ in this series he summarized 16 of his own publications cataloguing the effects of different salts on the rate and mechanism of aqueous reactions. Breslow's theory of antihydrophobic effects is essentially a more complex look at micellar interactions. In a 1990 paper, Breslow demonstrated that both guanidinium chloride and lithium perchlorate (two common *antihydrophobic* salts) increase the surface tension of water, thereby dispelling the idea that the mode of action these salts was to reduce the surface tension by disrupting the structure of water to make cavitation

easier. Breslow concluded that the antihydrophobic effect of these salts was to act as a bridge between water and non-polar reactants to directly assist with solvation.⁹⁶

It is unclear why, in the absence of an antihydrophobic reagent, the reaction of quadricyclane with azodicarboxylates should proceed with such vigor in water. A likely possibility is that water is in fact stabilizing polar intermediates formed during the reaction. Forman and Dailey demonstrated that increasing the solvent pressure by the addition of lithium perchlorate does not always increase the rate of all Diels-Alder reactions. Instead an alternative explanation to the argument for increased solvent pressure was presented for rate accelerations observed in lithium perchlorate solution; lithium ion catalysis.⁸⁷

The cycloaddition reaction of quadricyclane appears to be that of a loaded die where, the molecule is highly strained and predisposed to the formation of a cation radical intermediate ($E_{1/2} = +0.91$ V). In addition to this, both the 1,4-benzoquinone reactant and azodicarboxylates have the potential to facilitate electron transfer mechanisms in their reactions. The theoretical predictions for a cation radical intermediate also point in the direction of such a mechanism however, it has been established that traditional theoretical methods have difficulty with predictions involving charged radicals.

Conclusion

The cycloaddition of quadricyclane appears to be a special case with regards to aqueous rate acceleration. The small difference in the observed KIEs suggest that there is a difference in the cycloaddition reaction of quadricyclane with azodicarboxylates and

1,4-benzoquinone in aqueous versus organic solvents. The similarity in the reactivity of azodicarboxylates and 1,4-benzoquinone suggest the possibility that the reaction goes by electron transfer mechanism. Further support came from the absence of significant rate acceleration for the cycloaddition reaction with dimethylacetylene dicarboxylate, which is very similar to the azodicarboxylates that produce significant rate acceleration, with the exception for the ability to facilitate electron transfer under the reaction conditions.

The predicted isotope effects for the reaction proceeding via a $2\sigma+2\sigma+2\pi$ mechanism are well out of the range of the experimentally determined isotope effects. The isotope effects predicted for the reaction involving a cation radical are closer to the observed isotope effects. It should be noted that DFT calculations have difficulty dealing with charged radical species a fact that might account for the difference between experiment and prediction. While, the difference in isotope effects for aqueous versus organic solvents might be attributed to the difference in solvent electronics.

CHAPTER VI

EXPERIMENTAL SECTION

General Procedures

All measurements for ^1H NMR spectra were recorded on Varian XL-300 or Mercury 300 spectrometer while, low temperature ^1H NMR spectra were recorded on a Varian-400 spectrometer. KIEs were determined from ^{13}C and ^2H spectra recorded on Unity 500, or Inova 500 spectrometer. For all experiments, T1 values were determined for each sample using inversion-recovery method thereby reducing errors caused by paramagnetic impurities. ^{13}C integrations were determined numerically using a constant region for each peak that was about 5 times the peak width at half height on either side of the peak. A zero-order baseline was generally applied but in no case was a first order correction employed. Equations 6-1 to 6-3 were used to calculate the experimental KIEs and errors were based on the isotopic enrichment and reaction conversion.

$$\text{KIE}_{\text{calcd}} = \frac{\ln(1 - F)}{\ln[(1 - F)R/R_0]} \quad (6-1)$$

$$\Delta\text{KIE}_F = \frac{\partial\text{KIE}}{\partial F} \Delta F = \frac{-\ln(R/R_0)}{(1 - F)\ln^2[(1 - F)R/R_0]} \Delta F \quad (6-2)$$

$$\Delta KIE_R = \frac{\partial KIE}{\partial (R/R_0)} \Delta (R/R_0) = \frac{-\ln(1-F)}{(R/R_0) \ln^2 [(1-F)R/R_0]} \Delta (R/R_0) \quad (6-3)$$

$$\Delta KIE = KIE * ((\Delta KIE_R/KIE)^2 + (\Delta KIE_F/KIE)^2)^{1/2} \quad (6-4)$$

Theoretical structures and energies were computed using standard procedures in Gaussian98⁹⁷ or Gaussian03.⁶³ Vibrational frequency analyses were carried out on all stationary points. Becke3LYP method implemented in Gaussian with 6-31G* basis set was the standard approach taken for initial optimization of structures. Larger basis sets, CCSD(T) single point energy calculations a variety of other DFT methods were implemented when appropriate. Semiclassical trajectory calculations were also carried out as described previously.⁹⁸⁻¹⁰¹

The structures were all first located by density functional theory calculations employed Becke3LYP⁸² method implemented in Gaussian with 6-31G* basis set. B3LYP calculations with larger basis sets, mPW1K calculations,³² CCSD(T) single point energy calculations, and MP2 calculations were carried out when necessary, starting with B3LYP/6-31G* calculated structures. Semiclassical trajectory calculations were carried out according previously described method.

Singlet Oxygen Ene Reaction of **1**¹

Synthesis of 1-d₆.

3-Methyl-2-(methyl-d₃)-2-butene-1,1,1-d₃ (1,1,1-trideuterio-2-trideuteriomethyl-3-methyl-2-butene, **1**) was prepared by the method of Greene.¹⁰² The deuterium

¹ Experiment performed by N. Rebecca Wiekell with NMR analysis done by Kelmara Kelly.

incorporation in **1** at the labeled methyl groups was 99%, based on the ^1H NMR spectrum of the precursor 3,3-dimethyl-4,4-bis(trideuteriomethyl)oxetane-2-one. Methanol was distilled from 4 Å molecular sieves prior to use. All other reagents were commercially available and used as received. Reaction temperatures were monitored continuously and maintained within 4 °C of the target temperature.

Example Procedure

A mixture of 20 mL of dry methanol, 108 mg (1.20 mmol) of **1**, 10 mg (0.01 mmol) of Rose Bengal, and 4 drops of 1,2-dichloroethane was continually stirred under an oxygen atmosphere at 193 K while being irradiated with a 300-W sunlamp. The reaction was monitored by GC analysis of aliquots, and the irradiation was discontinued after 30% conversion of **1**. The mixture was then warmed to 225 K and 40 mg (1.1 mmol) of NaBH_4 was added. After stirring at 225 K for 6 h, the bulk of the volatiles were removed on a water aspirator, and the mixture was partitioned between 50 mL of dichloromethane and 50 mL of water. The organic phase was then rinsed three times with water, dried with MgSO_4 , and filtered through a small silica plug. The solvent was removed on a rotary evaporator aided by rinsing the product three times with 5-mL portions of benzene- d_6 , affording a sample containing a mixture of **4** and **5** contaminated with benzene- d_6 .

Analogous reactions at 193 K and higher were conducted in methanol as in the example procedure. Analogous reactions at 158 K and 163 K were conducted in 19:1 CHClF_2 :methanol. Analogous reactions at 118 K and 138 K were conducted in 12:6:1 CHClF_2 : CHF_3 :methanol. The reaction at 77 K was liquid nitrogen with the reagents and

5% methanol suspended heterogeneously.

NMR Measurements

Each sample of **4/5** was prepared in 5-mm NMR tubes filled with benzene-d₆ to a constant height of 5.0 cm. The ¹H spectra was recorded on a 400 MHz NMR, using 8-s delays between 45° pulses, a 3.7496-s acquisition time, and collecting 44,932 points. The ratio of **4** and **5** from the integration of the vinylic hydrogens (δ 4.92 and 4.92) and vinylic methyl-group hydrogens (δ 1.71) versus the geminal methyl group hydrogens (δ 1.21), relative to a nondeuterated standard that was generated from the same reaction conditions. The results from six measurements were averaged. Integrations were determined numerically using a constant integration region for each peak in both the sample and standard.

Energy Distributions

The thermal distribution of energy of **6** was determined using a modified PROGDYN program.

RRKM Calculations

Details of calculations can be found in the Appendix.

Tables 6-1 and 6-2 show the relative rates obtained for the abstraction of hydrogen and deuterium from geminal d₆-tetramethylethylene respectively.

Table 6-1. Rates of reaction for hydrogen abstraction in geminal d₆-tetramethylethylene.

bin E	mid bin	50K	100K	150K	200K	263K	298K	350K	
0	6.801	2.18E+11	1.77E+14	4.96E+13	1.18E+13	2.83E+12	0.00E+00	2.18E+11	0.00E+00
175	7.301	2.17E+11	3.31E+13	3.42E+13	1.08E+13	2.17E+12	8.67E+11	4.33E+11	0.00E+00
350	7.801	2.16E+11	2.72E+13	8.74E+13	4.86E+13	1.79E+13	4.53E+12	2.16E+12	6.47E+11
525	8.301	2.15E+11	1.96E+12	4.15E+13	5.25E+13	2.64E+13	8.82E+12	3.66E+12	1.29E+12
700	8.801	2.14E+11	0.00E+00	1.50E+13	3.96E+13	3.51E+13	1.16E+13	4.07E+12	1.71E+12
875	9.301	2.14E+11	0.00E+00	6.41E+12	3.31E+13	3.35E+13	1.75E+13	1.00E+13	3.84E+12
1050	9.801	2.13E+11	0.00E+00	2.98E+12	1.87E+13	3.07E+13	2.02E+13	1.58E+13	4.68E+12
1225	10.301	2.12E+11	0.00E+00	2.12E+11	1.02E+13	2.51E+13	2.34E+13	1.63E+13	9.13E+12
1400	10.801	2.12E+11	0.00E+00	2.12E+11	7.20E+12	1.97E+13	2.35E+13	1.99E+13	9.10E+12
1575	11.301	2.11E+11	0.00E+00	0.00E+00	2.75E+12	1.67E+13	2.20E+13	1.90E+13	1.14E+13
1750	11.801	2.11E+11	0.00E+00	0.00E+00	2.11E+11	1.14E+13	1.81E+13	2.34E+13	1.33E+13
1925	12.301	2.10E+11	0.00E+00	0.00E+00	4.20E+11	6.94E+12	1.79E+13	1.62E+13	1.72E+13
2100	12.801	2.10E+11	0.00E+00	0.00E+00	2.10E+11	2.10E+12	1.78E+13	1.49E+13	1.51E+13
2275	13.301	2.09E+11	0.00E+00	0.00E+00	0.00E+00	2.09E+12	1.44E+13	1.67E+13	1.57E+13
2450	13.801	2.09E+11	0.00E+00	0.00E+00	0.00E+00	1.04E+12	1.11E+13	1.57E+13	1.36E+13
2625	14.301	2.09E+11	0.00E+00	0.00E+00	0.00E+00	2.09E+11	7.09E+12	1.21E+13	1.69E+13
2800	14.801	2.08E+11	0.00E+00	0.00E+00	0.00E+00	0.00E+00	4.99E+12	1.08E+13	1.42E+13
2975	15.301	2.08E+11	0.00E+00	0.00E+00	0.00E+00	2.08E+11	2.49E+12	7.48E+12	1.25E+13
3150	15.801	2.07E+11	0.00E+00	0.00E+00	0.00E+00	2.07E+11	2.28E+12	5.19E+12	1.14E+13
3325	16.301	2.07E+11	0.00E+00	0.00E+00	0.00E+00	2.07E+11	1.24E+12	5.80E+12	1.08E+13
3500	16.801	2.07E+11	0.00E+00	0.00E+00	0.00E+00	0.00E+00	1.03E+12	3.51E+12	8.47E+12
3675	17.301	2.06E+11	0.00E+00	0.00E+00	0.00E+00	0.00E+00	4.13E+11	1.86E+12	9.91E+12
3850	17.801	2.06E+11	0.00E+00	0.00E+00	0.00E+00	0.00E+00	6.18E+11	3.09E+12	6.39E+12
4025	18.301	2.06E+11	0.00E+00	0.00E+00	0.00E+00	0.00E+00	2.06E+11	0.00E+00	4.94E+12
4200	18.801	2.06E+11	0.00E+00	0.00E+00	0.00E+00	0.00E+00	0.00E+00	1.03E+12	3.49E+12
4375	19.301	2.05E+11	0.00E+00	0.00E+00	0.00E+00	0.00E+00	4.11E+11	8.21E+11	4.11E+12
4550	19.801	2.05E+11	0.00E+00	0.00E+00	0.00E+00	0.00E+00	0.00E+00	4.10E+11	2.26E+12
4725	20.301	2.05E+11	0.00E+00	0.00E+00	0.00E+00	0.00E+00	0.00E+00	6.14E+11	1.43E+12
4900	20.801	2.05E+11	0.00E+00	0.00E+00	0.00E+00	0.00E+00	0.00E+00	0.00E+00	1.23E+12
5075	21.301	2.04E+11	0.00E+00	0.00E+00	0.00E+00	0.00E+00	0.00E+00	0.00E+00	2.04E+12
5250	21.801	2.04E+11	0.00E+00	0.00E+00	0.00E+00	0.00E+00	0.00E+00	0.00E+00	0.00E+00
5425	22.301	2.04E+11	0.00E+00	0.00E+00	0.00E+00	0.00E+00	0.00E+00	2.04E+11	6.11E+11
5600	22.801	2.04E+11	0.00E+00	0.00E+00	0.00E+00	0.00E+00	0.00E+00	0.00E+00	1.02E+12
5775	23.301	2.03E+11	0.00E+00	0.00E+00	0.00E+00	0.00E+00	0.00E+00	0.00E+00	6.10E+11
5950	23.801	2.03E+11	0.00E+00	0.00E+00	0.00E+00	0.00E+00	0.00E+00	0.00E+00	0.00E+00
6125	24.301	2.03E+11	0.00E+00	0.00E+00	0.00E+00	0.00E+00	0.00E+00	0.00E+00	2.03E+11
6300	24.801	2.03E+11	0.00E+00	0.00E+00	0.00E+00	0.00E+00	0.00E+00	0.00E+00	4.06E+11
6475	25.301	2.03E+11	0.00E+00	0.00E+00	0.00E+00	0.00E+00	0.00E+00	0.00E+00	0.00E+00
6650	25.801	2.02E+11	0.00E+00	0.00E+00	0.00E+00	0.00E+00	0.00E+00	0.00E+00	0.00E+00
6825	26.301	2.02E+11	0.00E+00	0.00E+00	0.00E+00	0.00E+00	0.00E+00	0.00E+00	2.02E+11
		2.18E+11	2.16E+11	2.15E+11	2.13E+11	2.11E+11	2.10E+11	2.06E+11	

Table 6-2. Rates of reaction for deuterium abstraction in geminal d₆-tetramethylethylene.

bin E	mid bin	50K	100K	150K	200K	263K	298K	350K	
0	6.801	1.80E+11	1.46E+14	4.10E+13	9.71E+12	2.34E+12	0.00E+00	1.80E+11	0.00E+00
175	7.301	1.80E+11	2.73E+13	2.84E+13	8.99E+12	1.80E+12	7.19E+11	3.60E+11	0.00E+00
350	7.801	1.80E+11	2.25E+13	7.28E+13	4.04E+13	1.49E+13	3.77E+12	1.80E+12	5.39E+11
525	8.301	1.80E+11	1.62E+12	3.47E+13	4.38E+13	2.21E+13	7.37E+12	3.05E+12	1.08E+12
700	8.801	1.80E+11	0.00E+00	1.26E+13	3.32E+13	2.95E+13	9.70E+12	3.41E+12	1.44E+12
875	9.301	1.80E+11	0.00E+00	5.39E+12	2.78E+13	2.82E+13	1.47E+13	8.44E+12	3.23E+12
1050	9.801	1.80E+11	0.00E+00	2.51E+12	1.58E+13	2.58E+13	1.71E+13	1.33E+13	3.95E+12
1225	10.301	1.79E+11	0.00E+00	1.79E+11	8.61E+12	2.12E+13	1.97E+13	1.38E+13	7.71E+12
1400	10.801	1.79E+11	0.00E+00	1.79E+11	6.10E+12	1.67E+13	1.99E+13	1.69E+13	7.71E+12
1575	11.301	1.79E+11	0.00E+00	0.00E+00	2.33E+12	1.42E+13	1.86E+13	1.61E+13	9.68E+12
1750	11.801	1.79E+11	0.00E+00	0.00E+00	1.79E+11	9.68E+12	1.54E+13	1.99E+13	1.13E+13
1925	12.301	1.79E+11	0.00E+00	0.00E+00	3.58E+11	5.91E+12	1.52E+13	1.38E+13	1.47E+13
2100	12.801	1.79E+11	0.00E+00	0.00E+00	1.79E+11	1.79E+12	1.52E+13	1.27E+13	1.29E+13
2275	13.301	1.79E+11	0.00E+00	0.00E+00	0.00E+00	1.79E+12	1.24E+13	1.43E+13	1.34E+13
2450	13.801	1.79E+11	0.00E+00	0.00E+00	0.00E+00	8.95E+11	9.48E+12	1.34E+13	1.16E+13
2625	14.301	1.79E+11	0.00E+00	0.00E+00	0.00E+00	1.79E+11	6.08E+12	1.04E+13	1.45E+13
2800	14.801	1.79E+11	0.00E+00	0.00E+00	0.00E+00	0.00E+00	4.29E+12	9.30E+12	1.22E+13
2975	15.301	1.79E+11	0.00E+00	0.00E+00	0.00E+00	1.79E+11	2.15E+12	6.44E+12	1.07E+13
3150	15.801	1.79E+11	0.00E+00	0.00E+00	0.00E+00	1.79E+11	1.97E+12	4.47E+12	9.83E+12
3325	16.301	1.79E+11	0.00E+00	0.00E+00	0.00E+00	1.79E+11	1.07E+12	5.00E+12	9.29E+12
3500	16.801	1.79E+11	0.00E+00	0.00E+00	0.00E+00	0.00E+00	8.93E+11	3.04E+12	7.32E+12
3675	17.301	1.79E+11	0.00E+00	0.00E+00	0.00E+00	0.00E+00	3.57E+11	1.61E+12	8.57E+12
3850	17.801	1.79E+11	0.00E+00	0.00E+00	0.00E+00	0.00E+00	5.36E+11	2.68E+12	5.53E+12
4025	18.301	1.79E+11	0.00E+00	0.00E+00	0.00E+00	0.00E+00	1.79E+11	0.00E+00	4.28E+12
4200	18.801	1.78E+11	0.00E+00	0.00E+00	0.00E+00	0.00E+00	0.00E+00	8.92E+11	3.03E+12
4375	19.301	1.78E+11	0.00E+00	0.00E+00	0.00E+00	0.00E+00	3.57E+11	7.14E+11	3.57E+12
4550	19.801	1.78E+11	0.00E+00	0.00E+00	0.00E+00	0.00E+00	0.00E+00	3.57E+11	1.96E+12
4725	20.301	1.78E+11	0.00E+00	0.00E+00	0.00E+00	0.00E+00	0.00E+00	5.35E+11	1.25E+12
4900	20.801	1.78E+11	0.00E+00	0.00E+00	0.00E+00	0.00E+00	0.00E+00	0.00E+00	1.07E+12
5075	21.301	1.78E+11	0.00E+00	0.00E+00	0.00E+00	0.00E+00	0.00E+00	0.00E+00	1.78E+12
5250	21.801	1.78E+11	0.00E+00	0.00E+00	0.00E+00	0.00E+00	0.00E+00	0.00E+00	0.00E+00
5425	22.301	1.78E+11	0.00E+00	0.00E+00	0.00E+00	0.00E+00	0.00E+00	1.78E+11	5.35E+11
5600	22.801	1.78E+11	0.00E+00	0.00E+00	0.00E+00	0.00E+00	0.00E+00	0.00E+00	8.91E+11
5775	23.301	1.78E+11	0.00E+00	0.00E+00	0.00E+00	0.00E+00	0.00E+00	0.00E+00	5.34E+11
5950	23.801	1.78E+11	0.00E+00	0.00E+00	0.00E+00	0.00E+00	0.00E+00	0.00E+00	0.00E+00
6125	24.301	1.78E+11	0.00E+00	0.00E+00	0.00E+00	0.00E+00	0.00E+00	0.00E+00	1.78E+11
6300	24.801	1.78E+11	0.00E+00	0.00E+00	0.00E+00	0.00E+00	0.00E+00	0.00E+00	3.56E+11
6475	25.301	1.78E+11	0.00E+00	0.00E+00	0.00E+00	0.00E+00	0.00E+00	0.00E+00	0.00E+00
6650	25.801	1.78E+11	0.00E+00	0.00E+00	0.00E+00	0.00E+00	0.00E+00	0.00E+00	0.00E+00
6825	26.301	1.78E+11	0.00E+00	0.00E+00	0.00E+00	0.00E+00	0.00E+00	0.00E+00	1.78E+11
		1.80E+11	1.80E+11	1.80E+11	1.79E+11	1.79E+11	1.79E+11	1.79E+11	1.79E+11

Tables 6-1 and 6-2 show the relative rates obtained for the abstraction of hydrogen and deuterium from trans d₆-tetramethylethylene respectively.

Table 6-3. Rates of reaction for hydrogen abstraction in trans d₆-tetramethylethylene.

bin E	mid bin	50K	100K	150K	200K	263K	298K	350K	
0	6.801	2.05E+11	1.67E+14	4.67E+13	1.11E+13	2.67E+12	0.00E+00	2.05E+11	0.00E+00
175	7.301	2.05E+11	3.12E+13	3.23E+13	1.02E+13	2.05E+12	8.18E+11	4.09E+11	0.00E+00
350	7.801	2.04E+11	2.56E+13	8.26E+13	4.59E+13	1.69E+13	4.28E+12	2.04E+12	6.12E+11
525	8.301	2.04E+11	1.85E+12	3.93E+13	4.97E+13	2.50E+13	8.35E+12	3.46E+12	1.22E+12
700	8.801	2.03E+11	0.00E+00	1.42E+13	3.76E+13	3.33E+13	1.10E+13	3.86E+12	1.62E+12
875	9.301	2.03E+11	0.00E+00	6.08E+12	3.14E+13	3.18E+13	1.66E+13	9.53E+12	3.65E+12
1050	9.801	2.02E+11	0.00E+00	2.83E+12	1.78E+13	2.91E+13	1.92E+13	1.50E+13	4.45E+12
1225	10.301	2.02E+11	0.00E+00	2.02E+11	9.70E+12	2.38E+13	2.22E+13	1.56E+13	8.69E+12
1400	10.801	2.02E+11	0.00E+00	2.02E+11	6.85E+12	1.87E+13	2.24E+13	1.90E+13	8.67E+12
1575	11.301	2.01E+11	0.00E+00	0.00E+00	2.62E+12	1.59E+13	2.09E+13	1.81E+13	1.09E+13
1750	11.801	2.01E+11	0.00E+00	0.00E+00	2.01E+11	1.09E+13	1.73E+13	2.23E+13	1.27E+13
1925	12.301	2.01E+11	0.00E+00	0.00E+00	4.01E+11	6.62E+12	1.71E+13	1.55E+13	1.65E+13
2100	12.801	2.00E+11	0.00E+00	0.00E+00	2.00E+11	2.00E+12	1.70E+13	1.42E+13	1.44E+13
2275	13.301	2.00E+11	0.00E+00	0.00E+00	0.00E+00	2.00E+12	1.38E+13	1.60E+13	1.50E+13
2450	13.801	2.00E+11	0.00E+00	0.00E+00	0.00E+00	1.00E+12	1.06E+13	1.50E+13	1.30E+13
2625	14.301	2.00E+11	0.00E+00	0.00E+00	0.00E+00	2.00E+11	6.79E+12	1.16E+13	1.62E+13
2800	14.801	1.99E+11	0.00E+00	0.00E+00	0.00E+00	0.00E+00	4.79E+12	1.04E+13	1.36E+13
2975	15.301	1.99E+11	0.00E+00	0.00E+00	0.00E+00	1.99E+11	2.39E+12	7.17E+12	1.19E+13
3150	15.801	1.99E+11	0.00E+00	0.00E+00	0.00E+00	1.99E+11	2.19E+12	4.97E+12	1.09E+13
3325	16.301	1.99E+11	0.00E+00	0.00E+00	0.00E+00	1.99E+11	1.19E+12	5.56E+12	1.03E+13
3500	16.801	1.99E+11	0.00E+00	0.00E+00	0.00E+00	0.00E+00	9.93E+11	3.37E+12	8.14E+12
3675	17.301	1.98E+11	0.00E+00	0.00E+00	0.00E+00	0.00E+00	3.97E+11	1.78E+12	9.52E+12
3850	17.801	1.98E+11	0.00E+00	0.00E+00	0.00E+00	0.00E+00	5.94E+11	2.97E+12	6.14E+12
4025	18.301	1.98E+11	0.00E+00	0.00E+00	0.00E+00	0.00E+00	1.98E+11	0.00E+00	4.75E+12
4200	18.801	1.98E+11	0.00E+00	0.00E+00	0.00E+00	0.00E+00	0.00E+00	9.89E+11	3.36E+12
4375	19.301	1.98E+11	0.00E+00	0.00E+00	0.00E+00	0.00E+00	3.95E+11	7.90E+11	3.95E+12
4550	19.801	1.97E+11	0.00E+00	0.00E+00	0.00E+00	0.00E+00	0.00E+00	3.95E+11	2.17E+12
4725	20.301	1.97E+11	0.00E+00	0.00E+00	0.00E+00	0.00E+00	0.00E+00	5.92E+11	1.38E+12
4900	20.801	1.97E+11	0.00E+00	0.00E+00	0.00E+00	0.00E+00	0.00E+00	0.00E+00	1.18E+12
5075	21.301	1.97E+11	0.00E+00	0.00E+00	0.00E+00	0.00E+00	0.00E+00	0.00E+00	1.97E+12
5250	21.801	1.97E+11	0.00E+00	0.00E+00	0.00E+00	0.00E+00	0.00E+00	0.00E+00	0.00E+00
5425	22.301	1.97E+11	0.00E+00	0.00E+00	0.00E+00	0.00E+00	0.00E+00	1.97E+11	5.90E+11
5600	22.801	1.96E+11	0.00E+00	0.00E+00	0.00E+00	0.00E+00	0.00E+00	0.00E+00	9.82E+11
5775	23.301	1.96E+11	0.00E+00	0.00E+00	0.00E+00	0.00E+00	0.00E+00	0.00E+00	5.89E+11
5950	23.801	1.96E+11	0.00E+00	0.00E+00	0.00E+00	0.00E+00	0.00E+00	0.00E+00	0.00E+00
6125	24.301	1.96E+11	0.00E+00	0.00E+00	0.00E+00	0.00E+00	0.00E+00	0.00E+00	1.96E+11
6300	24.801	1.96E+11	0.00E+00	0.00E+00	0.00E+00	0.00E+00	0.00E+00	0.00E+00	3.92E+11
6475	25.301	1.96E+11	0.00E+00	0.00E+00	0.00E+00	0.00E+00	0.00E+00	0.00E+00	0.00E+00
6650	25.801	1.96E+11	0.00E+00	0.00E+00	0.00E+00	0.00E+00	0.00E+00	0.00E+00	0.00E+00
6825	26.301	1.96E+11	0.00E+00	0.00E+00	0.00E+00	0.00E+00	0.00E+00	0.00E+00	1.96E+11
		2.05E+11	2.04E+11	2.03E+11	2.02E+11	2.01E+11	2.01E+11	1.98E+11	

Table 6-4. Rates of reaction for deuterium abstraction in geminal d₆-tetramethylethylene.

bin E	mid bin	50K	100K	150K	200K	263K	298K	350K	
0	6.801	1.98E+11	1.61E+14	4.52E+13	1.07E+13	2.58E+12	0.00E+00	1.98E+11	0.00E+00
175	7.301	1.98E+11	3.01E+13	3.13E+13	9.90E+12	1.98E+12	7.92E+11	3.96E+11	0.00E+00
350	7.801	1.98E+11	2.48E+13	8.00E+13	4.44E+13	1.64E+13	4.15E+12	1.98E+12	5.93E+11
525	8.301	1.97E+11	1.78E+12	3.81E+13	4.81E+13	2.43E+13	8.09E+12	3.35E+12	1.18E+12
700	8.801	1.97E+11	0.00E+00	1.38E+13	3.64E+13	3.23E+13	1.06E+13	3.74E+12	1.58E+12
875	9.301	1.97E+11	0.00E+00	5.90E+12	3.05E+13	3.09E+13	1.61E+13	9.24E+12	3.54E+12
1050	9.801	1.97E+11	0.00E+00	2.75E+12	1.73E+13	2.83E+13	1.87E+13	1.45E+13	4.32E+12
1225	10.301	1.96E+11	0.00E+00	1.96E+11	9.42E+12	2.32E+13	2.16E+13	1.51E+13	8.44E+12
1400	10.801	1.96E+11	0.00E+00	1.96E+11	6.66E+12	1.82E+13	2.18E+13	1.84E+13	8.43E+12
1575	11.301	1.96E+11	0.00E+00	0.00E+00	2.55E+12	1.55E+13	2.04E+13	1.76E+13	1.06E+13
1750	11.801	1.96E+11	0.00E+00	0.00E+00	1.96E+11	1.06E+13	1.68E+13	2.17E+13	1.23E+13
1925	12.301	1.96E+11	0.00E+00	0.00E+00	3.91E+11	6.45E+12	1.66E+13	1.51E+13	1.60E+13
2100	12.801	1.95E+11	0.00E+00	0.00E+00	1.95E+11	1.95E+12	1.66E+13	1.39E+13	1.41E+13
2275	13.301	1.95E+11	0.00E+00	0.00E+00	0.00E+00	1.95E+12	1.35E+13	1.56E+13	1.46E+13
2450	13.801	1.95E+11	0.00E+00	0.00E+00	0.00E+00	9.75E+11	1.03E+13	1.46E+13	1.27E+13
2625	14.301	1.95E+11	0.00E+00	0.00E+00	0.00E+00	1.95E+11	6.62E+12	1.13E+13	1.58E+13
2800	14.801	1.95E+11	0.00E+00	0.00E+00	0.00E+00	0.00E+00	4.67E+12	1.01E+13	1.32E+13
2975	15.301	1.95E+11	0.00E+00	0.00E+00	0.00E+00	1.95E+11	2.33E+12	7.00E+12	1.17E+13
3150	15.801	1.94E+11	0.00E+00	0.00E+00	0.00E+00	1.94E+11	2.14E+12	4.86E+12	1.07E+13
3325	16.301	1.94E+11	0.00E+00	0.00E+00	0.00E+00	1.94E+11	1.17E+12	5.44E+12	1.01E+13
3500	16.801	1.94E+11	0.00E+00	0.00E+00	0.00E+00	0.00E+00	9.71E+11	3.30E+12	7.96E+12
3675	17.301	1.94E+11	0.00E+00	0.00E+00	0.00E+00	0.00E+00	3.88E+11	1.75E+12	9.32E+12
3850	17.801	1.94E+11	0.00E+00	0.00E+00	0.00E+00	0.00E+00	5.82E+11	2.91E+12	6.01E+12
4025	18.301	1.94E+11	0.00E+00	0.00E+00	0.00E+00	0.00E+00	1.94E+11	0.00E+00	4.65E+12
4200	18.801	1.94E+11	0.00E+00	0.00E+00	0.00E+00	0.00E+00	0.00E+00	9.69E+11	3.29E+12
4375	19.301	1.94E+11	0.00E+00	0.00E+00	0.00E+00	0.00E+00	3.87E+11	7.74E+11	3.87E+12
4550	19.801	1.94E+11	0.00E+00	0.00E+00	0.00E+00	0.00E+00	0.00E+00	3.87E+11	2.13E+12
4725	20.301	1.94E+11	0.00E+00	0.00E+00	0.00E+00	0.00E+00	0.00E+00	5.81E+11	1.35E+12
4900	20.801	1.93E+11	0.00E+00	0.00E+00	0.00E+00	0.00E+00	0.00E+00	0.00E+00	1.16E+12
5075	21.301	1.93E+11	0.00E+00	0.00E+00	0.00E+00	0.00E+00	0.00E+00	0.00E+00	1.93E+12
5250	21.801	1.93E+11	0.00E+00	0.00E+00	0.00E+00	0.00E+00	0.00E+00	0.00E+00	0.00E+00
5425	22.301	1.93E+11	0.00E+00	0.00E+00	0.00E+00	0.00E+00	0.00E+00	1.93E+11	5.79E+11
5600	22.801	1.93E+11	0.00E+00	0.00E+00	0.00E+00	0.00E+00	0.00E+00	0.00E+00	9.65E+11
5775	23.301	1.93E+11	0.00E+00	0.00E+00	0.00E+00	0.00E+00	0.00E+00	0.00E+00	5.79E+11
5950	23.801	1.93E+11	0.00E+00	0.00E+00	0.00E+00	0.00E+00	0.00E+00	0.00E+00	0.00E+00
6125	24.301	1.93E+11	0.00E+00	0.00E+00	0.00E+00	0.00E+00	0.00E+00	0.00E+00	1.93E+11
6300	24.801	1.93E+11	0.00E+00	0.00E+00	0.00E+00	0.00E+00	0.00E+00	0.00E+00	3.86E+11
6475	25.301	1.93E+11	0.00E+00	0.00E+00	0.00E+00	0.00E+00	0.00E+00	0.00E+00	0.00E+00
6650	25.801	1.93E+11	0.00E+00	0.00E+00	0.00E+00	0.00E+00	0.00E+00	0.00E+00	0.00E+00
6825	26.301	1.93E+11	0.00E+00	0.00E+00	0.00E+00	0.00E+00	0.00E+00	0.00E+00	1.93E+11
			1.98E+11	1.98E+11	1.97E+11	1.97E+11	1.96E+11	1.95E+11	1.94E+11

From the relative rates obtained in Tables 6-1—6-4 we calculated the RRKM isotope effects for the $^1\text{O}_2$ ene reaction of both geminal and trans d_6 -tetramethylethylene at different temperatures, Tables 6-5 and 6-6.

Table 6-5. Calculated RRKM isotope effects for the $^1\text{O}_2$ ene reaction with geminal d_6 -tetramethylethylene.

Pt 4601		Pt 2251	
Hexact	Dexact	Temp	KIE
2.18E+11	1.8E+11	50	1.210
2.16E+11	1.8E+11	100	1.202
2.15E+11	1.8E+11	150	1.195
2.13E+11	1.79E+11	200	1.188
2.11E+11	1.79E+11	263	1.179
2.1E+11	1.79E+11	298	1.172
2.06E+11	1.79E+11	350	1.154

Table 6-6. Calculated RRKM isotope effects for the $^1\text{O}_2$ ene reaction with trans d₆-tetramethylethylene.

Pt 2641		Pt 2441	
transH	transD	Temp	KIE
2.05E+11	1.98E+11	50	1.034
2.04E+11	1.98E+11	100	1.033
2.03E+11	1.97E+11	150	1.031
2.02E+11	1.97E+11	200	1.030
2.01E+11	1.96E+11	263	1.028
2.01E+11	1.95E+11	298	1.026
1.98E+11	1.94E+11	350	1.021

Equilibration of Dicyclopentadiene

Example Procedure

Dicyclopentadiene was cracked according to literature procedures and allowed to dimerize at room temperature for 36 hours. The dimer was then purified by a series of vacuum distillations resulting in a colorless solid with a melting point of 32 °C which was stored in the freezer as the kinetic sample.

2.00 g of freshly purified dicyclopentadiene was placed in 5 mm x 100 mm sealed tubes and heated in an oil bath for 6 h at 140 °C. The now equilibrated dicyclopentadiene was then purified by vacuum distillation. By analogous procedure, six other equilibrated samples were made from independent dimerization reactions.

NMR Measurements

All samples were made using a constant 500 mg of dicyclopentadiene in 5 mm NMR tubes filled to a constant height of 5 cm with CDCl₃ or acetone-d₆. The ¹³C spectra were recorded at 125.81 MHz using inverse gated decoupling, 100 s delays between calibrated $\pi/2$ pulses, and a 6 s acquisition time to collect 200 084 points for samples in CDCl₃. Samples in acetone-d₆ were recorded at 125.81 MHz using inverse gated decoupling, 100 s delays between calibrated $\pi/2$ pulses, and a 6 s acquisition time to collect 200 084 points. Integrations were numerically determined using a constant integration region for each peak. A zero-order baseline correction was generally applied, but no first-order correction was applied. Six spectra were recorded for each sample of equilibrated dicyclopentadiene and kinetic dicyclopentadiene respectively.

¹³C Results

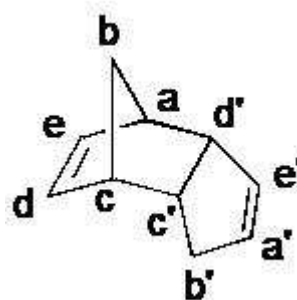
For the ¹³C spectra of dicyclopentadiene the average integrations and standard deviations for each peak in the molecule was determined. The ratios of the average integrations within each sample (k_{12C}/k_{13C} a/a', k_{12C}/k_{13C} b/b', etc.) are shown in Table 6-7 along with the number of spectra in parentheses. The ¹³C KIEs for equilibrated versus kinetic dicyclopentadiene were then calculated (Table 6-8).

Table 6-7. Relative ^{13}C integrations for dicyclopentadiene, with standard deviations.

Position	S1 (6)	S2 (6)	S3 (6)	S4 (6)	S5 (6)	S6 (6)	S7 (6)	average	stdev
a/a'	0.980	0.990	0.975	0.983	0.986	0.978	0.973	0.981	0.006
b/b'	0.996	0.998	0.999	0.996	0.996	1.002	1.001	0.998	0.002
c/c'	1.009	1.005	1.009	1.004	1.004	1.009	1.013	1.008	0.003
d/d'	1.019	1.011	1.022	1.016	1.013	1.021	1.019	1.017	0.004
e/e'	1.004	0.996	1.003	1.001	0.999	0.996	0.996	0.999	0.003

Table 6-8. Intramolecular ^{13}C KIEs in the dimerization of cyclopentadiene. The intramolecular KIEs are defined as $k_{12\text{C}}/k_{13\text{C}}(\text{a})/k_{12\text{C}}/k_{13\text{C}}(\text{a}')$, $k_{12\text{C}}/k_{13\text{C}}(\text{b})/k_{12\text{C}}/k_{13\text{C}}(\text{b}')$, etc.

Position	Intramolecular KIE	stdev
a/a'	1.020	6
b/b'	1.002	2
c/c'	0.992	3
d/d'	0.983	4
e/e'	1.001	3



Reaction of Dimethylfulvene with Diazomethane²

Example Procedure for the Reaction of Dimethylfulvene with Diazomethane

5 g of diazald was dissolved in 20 ml carbitol™ in a 250 ml scratch-free Erlenmeyer flask fitted with a rubber stopper with two fire-polished pipettes. One pipette is connected to a positive nitrogen flow and the other fitted with a rubber tubing connected to another fire polished pipette connected to a rubber septum fitted to the receiving vial containing 2.5 g dimethylfulvene in 2.5 g CDCl₃ kept at -78° C. 10 ml of 30% KOH solution was then added to the stirred diazald solution using syringe. The reaction was stirred until the evolution of yellow gas ceased. The receiving vial was then capped and transferred to the freezer. After 24 h, the reaction vial now contained a bright red-orange solution which was checked by NMR. Special care was taken using fire polished pipettes for all transfers. More diazomethane was generated into the reaction vial in the same manner as above until the reaction was judged to be 80% complete by NMR at which point, the entire reaction mixture was chromatographed using pentane as the eluent. The recovered dimethylfulvene was collected and compared to unreacted dimethylfulvene.

Table 6-9 shows the average ¹³C integrations for the recovered dimethylfulvene. The relative ¹³C integrations and calculated ¹³C KIEs for the cycloaddition of diazomethane with dimethylfulvene are shown in Tables 6-10 and 6-11 respectively.

² Care was taken to ensure that all glassware used for reactions of diazomethane were clean, dry and scratch free. Sure-seal joints were used in place of ground glass joints. All other glassware including pipets and NMR tubes were fire polished and scratch free.

Table 6-9. Average ^{13}C integrations (n = 6) for recovered dimethylfulvene.

	C1	C2	C3	C4	C5
dimethylfulvene 1 (80 \pm 3%)	1010.16	974.44	2079.19	2043.56	2000.00
	(7.7)	(5.5)	(13.7)	(7.5)	(0.0)
dimethylfulvene 1 (80 \pm 3%)	1006.33	977.46	2086.43	2045.48	2000.00
	(6.0)	(6.8)	(14.0)	(8.9)	(0.0)
standard	999.65	969.67	2086.00	2039.10	2000.00
	(6.2)	(7.8)	(11.4)	(7.0)	(0.0)

Table 6-10. Relative ^{13}C integrations for the cycloaddition of diazomethane with dimethylfulvene.

	C1	C2	C3	C4	C5
Dimethylfulvene1	0.990	0.995	1.003	0.998	1.000
Std dev	0.010	0.010	0.009	0.005	0.000
Dimethylfulvene2	0.993	0.992	1.000	0.997	1.000
Std dev	0.009	0.011	0.009	0.006	0.000

Table 6-11. ^{13}C KIEs for the cycloaddition of diazomethane with dimethylfulvene.

	C1	C2	C3	C4	C5
Dimethylfulvene1	1.011	1.005	0.997	1.002	1.000
Std dev	0.010	0.010	0.009	0.005	0.000
Dimethylfulvene2	1.007	1.008	1.000	1.003	1.000
Std dev	0.009	0.011	0.009	0.006	0.000

On Water Reactions of Quadricyclane

Synthesis of Quadricyclane

A solution of 5 g (w mmol) acetophenone in 100 g (x mmol) norbornadiene was divided among 8 10mm x 30mm reaction tubes. The tubes were sealed with rubber septa and placed in Rayonett and allowed to react for 3 days. The reaction was determined to be 98% conversion by ^1H NMR analysis. The resulting pale yellow liquid was then distilled under vacuum to yield 90g of >99.9% pure quadricyclane.

Preparation of Neat Diethyl Azodicarboxylate (DEAD)

DEAD was purchased from Sigma Aldrich as a 40% solution in toluene which was purified by flash chromatography on a 5 cm x 15 cm silica gel packed column using 50:50 pentane: dichloromethane as the eluting solvent. DEAD was collected as the second, bright yellow fraction. Solvent was removed by distillation using a vacuum

aspirator and no heat to afford a DEAD as a deep orange-red liquid confirmed by ^1H NMR.

Example 'On Water' Procedure

A mixture of 5 g of quadricyclane and 1.42 g of DEAD was stirred vigorously and 25 ml of distilled water was added. When all the orange color disappeared, it was judged that all the DEAD had been consumed and an aliquot was analyzed by ^1H NMR which confirmed that all the DEAD was consumed along with 15% of the quadricyclane to form 15% product. The product was then isolated by partitioning into diethyl ether (5 ml was sufficient to create phase separation since both product and quadricyclane are immiscible with water) and the volatiles removed by vacuum transfer. The product, a pale yellow oil, was then distilled under reduced pressure (0.05 mm Hg) to afford 1.5 g of product.

Example Procedure in Acetonitrile

A mixture of 5 g of quadricyclane and 1.42g of DEAD was stirred vigorously and 25 ml of acetonitrile was added. When all the orange color disappeared, it was judged that all the DEAD had been consumed and an aliquot was analyzed by ^1H NMR which confirmed that all the DEAD was consumed along with 15% of the quadricyclane to form 15% product. The volatiles were removed by vacuum transfer and the pale yellow oil, was then distilled under reduced pressure (0.05 mm Hg) to afford 1.8 g of product.

Example Procedure for Preparation of Standard

A mixture of 0.75 g of quadricyclane and 1.5 g of DEAD was stirred vigorously and 5 ml of distilled water was added. When all the orange color disappeared, it was judged that all the DEAD had been consumed and an aliquot was analyzed by ^1H NMR which confirmed that all the quadricyclane was consumed to form product. The product was then isolated by partitioning into diethyl ether (5 ml) and the volatiles removed by vacuum transfer. The product, a pale yellow oil, was then distilled under reduced pressure (0.05 mm Hg) to afford 1.9 g of product.

Tables 6-12 and 6-13 show the relative rate of the cycloaddition reaction of quadricyclane with dimethyl acetylenedicarboxylate and 1,4-benzoquinone respectively in water, methanol and acetonitrile. These rates were determined experimentally by ^1H NMR analysis of each reaction in the different solvents.

Table 6-12. Rate of cycloaddition of quadricyclane with dimethyl acetylenedicarboxylate

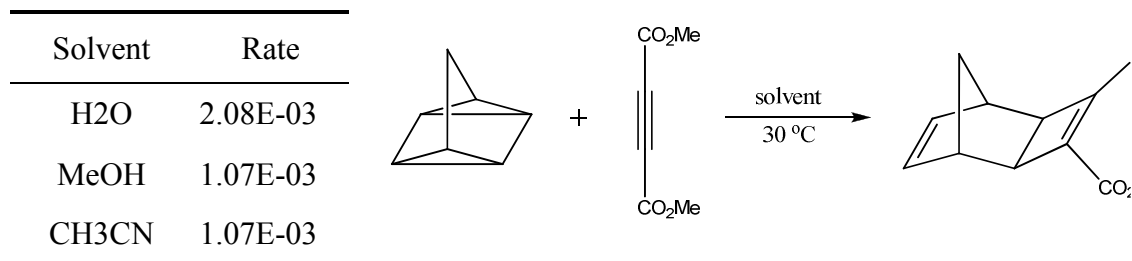
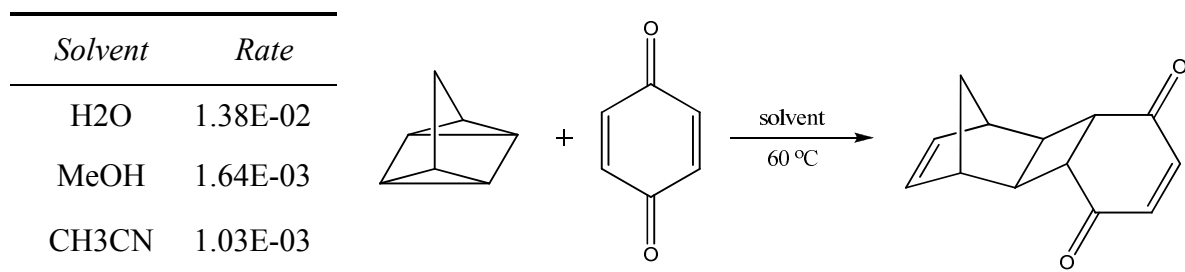


Table 6-13. Rate of cycloaddition of quadricyclane with 1,4-benzoquinone



The average ^{13}C integrations for the product resulting from the cycloaddition of quadricyclane with DEAD in water, acetonitrile and toluene are shown in Table 6-14.

Table 6-15 shows the resulting ^{13}C KIEs for the cycloaddition reaction in each solvent.

Table 6-14. Average ^{13}C integrations (n = 6) for DEAD on water product

% conversion	carbonyl	olefinic	alifatic	quat	OCH ₂	methylene	CH ₃
						assumed	
Standard 1a	2104.54 (5.3)	2140.37 (4.4)	2126.28 (4.0)	2204.27 (3.5)	2044.68 (3.8)	1000.00 (0.0)	2355.28 (2.3)
H ₂ O. 1 (15 ± 3%)	2103.19 (3.0)	2106.28 (4.6)	2092.81 (4.0)	2200.52 (3.2)	2045.28 (4.4)	1000.00 (0.0)	2187.87 (5.9)
Standard 1b	2104.54 (5.3)	2140.37 (4.4)	2126.28 (4.0)	2204.27 (3.5)	2044.68 (3.8)	1000.00 (0.0)	2355.28 (2.3)
Acetonitrile1 (15 ± 3%)	2104.90 (4.9)	2099.28 (5.5)	2082.68 (4.0)	2196.55 (5.1)	2046.20 (5.4)	1000.00 (0.0)	2161.54 (4.2)
Standard 1c	2104.18 (4.4)	2117.18 (3.7)	2112.53 (4.5)	2189.21 (2.8)	2014.56 (2.1)	1000.00 (0.0)	2327.82 (5.0)
Toluene (15 ± 3%)	2090.55 (4.3)	2080.55 (5.0)	2072.95 (4.1)	2191.15 (5.8)	2013.33 (4.2)	1000.00 (0.0)	2167.50 (6.1)
Standard 2a	2037.50 (4.2)	2092.13 (5.6)	2088.68 (4.8)	2150.57 (4.9)	2026.99 (4.6)	1000.00 (0.0)	2324.24 (4.4)
H ₂ O 2. (15 ± 3%)	2047.62 (2.4)	2063.46 (3.9)	2055.41 (2.4)	2147.27 (3.3)	2028.83 (3.5)	1000.00 (0.0)	2155.33 (3.6)
Standard 2b	2064.85 (5.1)	2092.76 (2.9)	2084.43 (6.4)	2137.01 (4.8)	1987.03 (4.2)	1000.00 (0.0)	2303.25 (5.4)
Acetonitrile2 (15 ± 3%)	2063.42 (3.3)	2052.09 (5.4)	2040.18 (3.2)	2132.57 (4.9)	1992.28 (5.2)	1000.00 (0.0)	2116.01 (4.4)
Standard 2c	2080.98 (3.3)	2099.48 (4.2)	2102.73 (3.5)	2162.92 (4.8)	2004.25 (4.2)	1000.00 (0.0)	2344.15 (4.5)
Toluene 2. (15 ± 3%)	2077.76 (4.5)	2063.85 (5.3)	2063.66 (4.2)	2186.34 (3.1)	2010.59 (5.2)	1000.00 (0.0)	2154.23 (3.2)
LiClO ₄ 1 (15 ± 3%)	2049.47 (6.2)	2045.83 (4.4)	2048.08 (4.4)	2090.51 (6.3)	1995.30 (4.2)	1000.00 (0.0)	2050.67 (4.4)
Standard 3	2052.60 (6.6)	2080.11 (6.4)	2073.70 (5.3)	2105.14 (6.2)	1998.06 (4.7)	1000.00 (0.0)	2501.09 (9.3)
LiClO ₄ 2 (15 ± 3%)	2046.66 (4.2)	2044.90 (4.9)	2048.01 (3.0)	2091.56 (4.2)	1993.93 (3.4)	1000.00 (0.0)	2044.07 (6.9)

Table 6-15. ^{13}C KIEs for DEAD on water, with standard deviations.

	carbonyl	olefinic	alifatic	quat	OCH ₂	methylene	CH ₃
						assumed	
H ₂ O 1	1.001	1.016	1.016	1.002	1.000	1.000	1.077
Std dev	0.003	0.003	0.003	0.002	0.003	0.000	0.003
Acetonitrile1	1.000	1.020	1.021	1.004	0.999	1.000	1.090
Std dev	0.003	0.003	0.003	0.003	0.003	0.000	0.002
Toluene1	1.007	1.018	1.019	0.999	1.001	1.000	1.074
Std dev	0.003	0.003	0.003	0.003	0.002	0.000	0.004
H ₂ O 2	0.995	1.014	1.016	1.002	0.999	1.000	1.078
Std dev	0.002	0.003	0.003	0.003	0.003	0.000	0.003
Acetonitrile2	1.001	1.020	1.022	1.002	0.997	1.000	1.088
Std dev	0.003	0.003	0.004	0.003	0.003	0.000	0.003
Toluene2	1.002	1.017	1.019	0.989	0.997	1.000	1.088
Std dev	0.003	0.003	0.003	0.003	0.003	0.000	0.003
LiClO ₄ 1	1.002	1.017	1.013	1.007	1.001	1.000	1.220
Std dev	0.004	0.004	0.003	0.004	0.003	0.000	0.005
LiClO ₄ 2	1.003	1.017	1.013	1.006	1.002	1.000	1.224
Std dev	0.004	0.004	0.003	0.004	0.003	0.000	0.006

The average ^{13}C integrations for the product resulting from the cycloaddition of quadricyclane with 1,4-benzoquinone in water and acetonitrile toluene are shown in Table 6-14. Table 6-15 shows the resulting ^{13}C KIEs for the cycloaddition reaction in each solvent.

Table 6-16. Average ^{13}C integrations (n = 6) for 1,4-benzoquinone on water product

% conversion	C=C (bqz)	olefinic	alifatic	quat(quad)	quat (1,4-benzoquinone)	methylene assumed
Standard 1a	2295.81 (7.3)	2260.13 (7.1)	2061.70 (4.9)	2103.94 (5.7)	2101.60 (6.6)	1000.00 (0.0)
H ₂ O (15 ± 3%)	2554.08 (23.8)	2473.64 (19.2)	2277.68 (13.4)	2368.02 (12.8)	2380.21 (13.9)	1000.00 (0.0)
Standard 1b	2316.65 (7.2)	2273.45 (4.9)	2073.89 (4.9)	2126.27 (5.5)	2120.40 (3.7)	1000.00 (0.0)
Acetonitrile (15 ± 3%)	2291.72 (3.9)	2429.69 (1.4)	2044.44 (2.5)	2115.53 (2.7)	2040.68 (1.7)	1000.00 (0.0)

Table 6-17. ^{13}C KIEs for 1,4-benzoquinone on water, with standard deviations.

	C=C (bqz)	olefinic	alifatic	quat(quad)	quat (1,4-benzoquinone)	methylene assumed
H ₂ O	1.004	1.018	1.016	1.010	1.029	1.000
Std dev	0.009	0.008	0.006	0.005	0.006	0.000
Acetonitrile	1.011	0.936	1.014	1.005	1.039	1.000
Std dev	0.004	0.002	0.003	0.003	0.002	0.000

CHAPTER VII

CONCLUSIONS

In this dissertation I have demonstrated that the methodology developed in the Singleton group for the combinatorial determination of KIEs at every atomic position can be used as a mechanistic probe of reaction mechanisms. It has been demonstrated that the method, with the support of DFT calculations can be used to gain a better but not always complete understanding of the detailed mechanistic path of a reaction. As is the case with the cycloaddition reactions of quadricyclane, a limitation in the ability of conventional DFT calculations has been a hindrance.

For the dimerization of cyclopentadiene, the Singleton methodology had to be expanded to be able to deal with unconventional KIEs. In this case, not only did we have to improve our method for determining the KIEs but we also had to develop a new way in which to interpret them. The mechanism of this deceptively unassuming reaction has actually proven to be an exception to transition state theory, occurring by a new form of dynamic effects, heavy atom dynamic effects.

The mechanism of the $^1\text{O}_2$ en reaction with tetramethylethylene can finally be put

to rest as we have provided a mountain of evidence against the possibility of the mechanism occurring by any form of statistical rate theory. Instead, the temperature insensitivity of the reaction can be explained in terms of dynamic effects. We demonstrated that in order to understand the experimental observations in the reaction, a more complete understanding of phase space needs to be considered.

The cycloaddition of diazomethane with dimethylfulvene proved to be a tricky reaction and as such, it was no surprise that the mechanism was similarly challenging. The experimental observations in this reaction proved to be in direct conflict with theories I have learnt and accepted as infallible rules.

Overall, this dissertation has attempted to answer mechanistic questions of interesting organic reactions as well as brought to light the fact that many ordinary organic reactions are directly influenced by dynamic effects.

REFERENCES

- 1 Melander, L.; Saunders, W. H. *Reaction Rates of Isotopic Molecules*, John Wiley & Sons, New York, 1980.
- 2 (a) Bigeleisen, J.; Mayer, M. G. *J. Am. Chem. Soc.* **1947**, *15*, 261-267. (b) Wolfsberg, M. *Acc. Chem. Res.* **1972**, *5*, 225-233. (c) Bigeleisen, J. *J. Chem. Phys.* **1949**, *17*, 675-678.
- 3 Bell, R. P. *The Tunnel Effect in Chemistry*, Chapman & Hall, London, 1980; pp 60-63.
- 4 Singleton, D. A.; Thomas, A. A. *J. Am. Chem. Soc.* **1995**, *117*, 9357-9358.
- 5 Pascal, R. A., Jr.; Baum, M. W.; Wagner, C. K.; Rodgers, L. R.; Huang, D. S. *J. Am. Chem. Soc.* **1986**, *108*, 6477-6482.
- 6 Carpenter, B. K. *J. Am. Chem. Soc.* **1985**, *107*, 5730-5732.
- 7 Newman-Evans, R. H., Simon, R. J., Carpenter, B. K. *J. Org. Chem.* **1990**, *55*, 695-711.
- 8 Doubleday, C. J. *Phys. Chem. A* **2001**, *105*, 6333-6341.
- 9 Doubleday, C., Li, G., Hase, W. L. *Phys. Chem. Chem. Phys.*, **2002**, *4*, 304-312.
- 10 Singleton, D. A., Hang, C., Szymanski, M. J., Greenwald, E. J., *J. Am. Chem. Soc.* **2003**, *125*, 1176-1177.
- 11 Bekele, T., Lipton, M. A., Singleton, D. A., Christian, C. F. *J. Am. Chem. Soc.* **2005**, *127*, 9216-9223.
- 12 Ussing, B. R., Singleton, D. A. *J. Am. Chem. Soc.* **2005**, *127*, 2888-2899.
- 13 Neureiter, N. P. *J. Org. Chem.* **1959**, *24*, 2044-2048.
- 14 Woodward, R. B., Hoffmann, R. *Angew. Chem. Int. Ed. Engl.* **1969**, *8*, 781-853.

- 15 Doering, W. von E., Sachdev, K. *J. Am. Chem. Soc.* **1974**, *96*, 1168-1187.
- 16 Doering, W. von E., Sachdev, K. *J. Am. Chem. Soc.* **1975**, *97*, 5512-5520.
- 17 For a discussion, see: Carpenter, B. K. *J. Phys. Org. Chem.* **2003**, *16*, 858-868.
- 18 Carpenter, B. K. *Angew. Chem. Int. Ed.* **1998**, *37*, 3340-3350.
- 19 (a) Doubleday, C., Jr.; Bolton, K.; Hase, W. L. *J. Am. Chem. Soc.* **1997**, *119*, 5251-5252. (b) Doubleday, C., Jr.; Bolton, K.; Hase, W. L. *J. Phys. Chem. A* **1998**, *102*, 3648-3658. (c) Doubleday, C.; Nendel, M.; Houk, K. N.; Thweatt, D.; Page, M. *J. Am. Chem. Soc.* **1999**, *121*, 4720-4721. (d) Doubleday, C. *J. Phys. Chem. A* **2001**, *105*, 6333-6341. (e) Doubleday, C.; Li, G.; Hase, W. L. *Phys. Chem. Chem. Phys.* **2002**, *4*, 304-312. (f) Doubleday, C.; Suhrada, C. P.; Houk, K. N. *J. Am. Chem. Soc.* **2006**, *128*, 90-94.
- 20 Hrovat, D. A.; Fang, S.; Borden, W. T.; Carpenter, B. K. *J. Am. Chem. Soc.* **1997**, *119*, 5253-5254.
- 21 (a) Jarzecki, A. A.; Gajewski, J.; Davidson, E. R. *J. Am. Chem. Soc.* **1999**, *121*, 6928-6935. (b) Kless, A.; Nendel, M.; Wilsey, S.; Houk, K. N. *J. Am. Chem. Soc.* **1999**, *121*, 4524-4525.
- 22 (a) Carpenter, B. K. *J. Am. Chem. Soc.* **1996**, *118*, 10329-10330. (b) Sun, L.; Song, K.; Hase, W. L. *Science* **2002**, *296*, 875-878.
- 23 Debbert, S. L.; Carpenter, B. K.; Hrovat, D. A.; Borden, W. T. *J. Am. Chem. Soc.* **2002**, *124*, 7896-7897.
- 24 (a) Vande Linde, S. R.; Hase, W. L. *J. Chem. Phys.* **1990**, *93*, 7962-7980. (b) Cho, Y. J.; Vande Linde, S. R.; Zhu, L.; Hase, W. L. *J. Chem. Phys.* **1992**, *96*, 8275-8287. (c) Hase, W. L. *Science* **1994**, *266*, 998-1002. (d) Wang, H.; Hase, W. L. *J. Am. Chem. Soc.* **1995**, *117*, 9347-9356. (e) Sun, L.; Hase, W. L.; Song, K. *J. Am. Chem. Soc.* **2001**, *123*, 5753-5756.
- 25 (a) Vande Linde, S. R.; Hase, W. L. *J. Phys. Chem.* **1990**, *94*, 6148-6150. (b) Li, G.; Hase, W. L. *J. Am. Chem. Soc.* **1999**, *121*, 7124-7129. (c) Wang, Y.; Hase, W. L.; Wang, H. *J. Chem. Phys.* **2003**, *118*, 2688-2695. (d) Sun, L.; Chang, E.; Song, K.; Hase, W. L. *Can. J. Chem.* **2004**, *82*, 891-899.
- 26 Murrell, J. N.; Laidler, K. J. *Trans. Faraday Soc.* **1968**, *64*, 371-377.

- 27 Metiu, H.; Ross, J.; Silbey, R.; George, T. F. *J. Chem. Phys.* **1974**, *61*, 3200-3209.
- 28 (a) Bosch, E.; Moreno, M.; Lluch, J. M.; Bertran, J. *Chem. Phys. Lett.* **1989**, *160*, 543-548. (b) Quapp, W.; Hirsch, M.; Heidrich, D. *Theor. Chem. Accounts* **1998**, *100*, 285-299. (c) Ramquet, M. -N.; Dive, G.; Dehareng, D. *J. Chem. Phys.* **2000**, *112*, 4923-4934. (d) Quapp, W. *J. Mol. Struct.* **2004**, *695-696*, 95-101. (e) Quapp, W.; Hirsch, M.; Heidrich, D. *Theor. Chem. Accounts* **2004**, *112*, 40-51.
- 29 Valtazanos, P.; Ruedenberg, K. *Theor. Chim. Acta* **1986**, *69*, 281-307.
- 30 Caldin, E. F. *Chem. Rev.* **1969** *69*, 135-158.
- 31 Stern, M. J. ; Weston Jr, R. E. *J. Chem. Phys.* **1974**, *60*, 2803-2807.
- 32 Brunton, G.; Griller, D.; Barclay, L. R. C.; Ingold, K. U. *J. Am. Chem. Soc.* **1976**, *98*, 6803-6811.
- 33 Hudson, R. L.; Shiotani, M.; Williams, F. *Chem. Phys. Lett.* **1977**, *48*, 193-196.
- 34 Zuev, P. S.; Sheridan, R. S. *J. Am. Chem. Soc.* **1994**, *116*, 4123-4124.
- 35 Garcia-Garibay, M. A.; Gamarnik, A.; Bise, R.; Pang, L.; Jenks, W. S. *J. Am. Chem. Soc.* **1995**, *117*, 10264-10275.
- 36 Jonsson, T.; Glickman, M. H.; Sun, S.; Klinman, J. P. *J. Am. Chem. Soc.* **1996**, *118*, 10319-10320.
- 37 Campos, L. M.; Warrior, M. V.; Peterfy, K.; Houk, K. N.; Garcia-Garibay, M. A. *J. Am. Chem. Soc.* **2005**, *127*, 10178-10179.
- 38 Metiu, H.; Ross, J.; Silbey, R.; George, T. F. *J. Chem. Phys.* **1974**, *61*, 3200-3209.
- 39 Valtazanos, P.; Ruedenberg, K. *Theor. Chim. Acta* **1986**, *69*, 281-307.
- 40 Kraus, W. A.; DePristo, A. E. *Theor. Chim. Acta* **1986**, *69*, 309-322.
- 41 Yanai, T.; Taketsugu, T.; Hirao, K. *J. Chem. Phys.* **1997**, *107*, 1137-1146.
- 42 Caramella, P.; Quadrelli, P.; Toma, L. *J. Am. Chem. Soc.* **2002**, *124*, 1130-1131.

- 43 Zhou, C.; Birney, D. M. *Org. Lett.* **2002**, *4*, 3279-3282.
- 44 Yamataka, H.; Aida, M.; Dupuis, M. *Chem. Phys. Lett.* **1999**, *300*, 583-587.
- 45 Bakken, V.; Danovich, D.; Shaik, S.; Schlegel, H. B. *J. Am. Chem. Soc.* **2001**, *123*, 130-134.
- 46 Mann, D. J.; Hase, W. L. *J. Am. Chem. Soc.* **2002**, *124*, 3208-3209.
- 47 Singleton, D. A.; Hang, C.; Szymanski, M. J.; Meyer, M. P.; Leach, A. G.; Kuwata, K. T.; Chen, J. S.; Greer, A.; Foote, C. S.; Houk, K. N. *J. Am. Chem. Soc.* **2003**, *125*, 1319-1328.
- 48 Ussing, B. R.; Singleton, D. A. *J. Am. Chem. Soc.* **2005**, *127*, 2888-2899.
- 49 Bekele, T.; Lipton, M. A.; Singleton, D. A.; Christian, C. F. *J. Am. Chem. Soc.* **2005**, *127*, 9216-9223.
- 50 Singleton, D. A.; Hang, C.; Szymanski, M. J.; Greenwald, E. E. *J. Am. Chem. Soc.* **2003**, *125*, 1176-1177.
- 51 Grdina, B.; Orfanopoulos, M.; Stephenson, L. M. *J. Am. Chem. Soc.* **1979**, *101*, 3111-3112.
- 52 Orfanopoulos, M.; Smonou, I.; Foote, C. S. *J. Am. Chem. Soc.* **1990**, *112*, 3607-3614.
- 53 Gonzalez-Lafont, A.; Moreno, M.; Lluch, J. M. *J. Am. Chem. Soc.* **2004**, *126*, 13089-13094.
- 54 Singleton, D. A.; Thomas, A. A. *J. Am. Chem. Soc.* **1995**, *117*, 9357-9358.
- 55 Jonsson, T.; Glickman, M. H.; Sun, S.; Klinman, J. P. *J. Am. Chem. Soc.* **1996**, *118*, 10319-10320.
- 56 Hammes-Schiffer, S. *Acc. Chem. Res.* **2006**, *39*, 93-100.
- 57 Klinman, J. P. *Pure Appl. Chem.* **2003**, *75*, 601-608.
- 58 Pu, J.; Ma, S.; Gao, J.; Truhlar, D. G. *J. Phys. Chem. B* **2005**, *109*, 8551-8556.

- 59 Marcus, R. A. *J. Chem. Phys.* **1952**, *20*, 355-359.
- 60 Marcus, R. A. *J. Chem. Phys.* **1965**, *43*, 2658-2661.
- 61 Zhu, L.; Hase, W. L. *A General RRKM Program*. Quantum Chemistry Program Exchange, Indiana University: Bloomington, IN, 1994, Program No. QCPE 644.
- 62 Beyer, T.; Swinehart, D. F. *Commun. Assoc. Comput. Machin.* **1973**, *16*, 379.
- 63 Frisch, M. J.; Trucks, G. W.; Schlegel, G. E. Scuseria, M. A. Robb et al., *Gaussian 03*, Revision B.04, Gaussian, Inc., Pittsburgh PA, 2003.
- 64 The VTST isotope effects predicted here do not exactly match those in ref 53 due to the use of a more finely calculated minimum-energy path (see supporting online text).
- 65 A symmetrical intermediate has often been proposed for these reactions, with the isotope effect arising from transition states following the intermediate. The VTST analysis may be viewed as treating the area of the energy surface near the VRI as an intermediate. The failure of conventional or variational transition state theory to predict the temperature trend in the KIE effect weighs strongly against an intermediate with a lifetime long enough for thermal equilibration with solvent.
- 66 Hase, W. L. *Acc. Chem. Res.* **1983**, *16*, 258-264.
- 67 The calculations here apply the general process described in ref 53 but use microcanonical variational RRKM theory to calculate the rate constant for a distribution of energies derived from a thermal distribution calculated for 6 plus the difference in energies (CCSD(T)/aug-cc-pvdz//B3LYP/6-31G* +zpe) between 6 and points in question along the reaction path.
- 68 Elles, C. G.; Cox, M. J.; Crim, F. F. *J. Chem. Phys.* **2004**, *120*, 6973-6979.
- 69 The trajectories in methanol spend relatively little time in an area describable as a peroxide (27% defined by O1-C1 / O1-C2 distances < 1.9 Å) and a majority of the time in an area describable as a diradical / zwitterion (59% defined by having one O1-C distance < 1.7 Å and the other > 1.9 Å).
- 70 As a familiar example, the Diels-Alder reaction of symmetrical addends usually occurs by a Cs-symmetric transition state but affords asymmetric twist-boat or half-chair products.

- 71 Quadrelli, P.; Romano, S.; Toma, L.; Caramella, P. *J. Org. Chem.* **2003**, *68*, 6035-6038.
- 72 Caramella, P.; Quadrelli, P.; Toma, L. *J. Am. Chem. Soc.* **2002**, *124*, 1130-1131.
- 73 See the Appendix for a complete list of methods employed, including a CCSD(T)/6-31+G** exploration along the lowest-energy desymmetrizing normal mode.
- 74 (a) Singleton, D. A.; Szymanski, M. J. *J. Am. Chem. Soc.* **1999**, *121*, 9455-9456. (b) Singleton, D. A.; Schulmeier, B. E. *J. Am. Chem. Soc.* **1999**, *121*, 9313-9317.
- 75 Woodward, R. B.; Katz, T. J. *Tetrahedron* **1959**, *5*, 70-89.
- 76 Singleton, D. A.; Thomas, A. A. *J. Am. Chem. Soc.* **1995**, *117*, 9357-9358.
- 77 Gonzalez-Lafont, A.; Moreno, M.; Lluch, J. M. *J. Am. Chem. Soc.* **2004**, *126*, 13089-13094.
- 78 Singleton, D. A.; Hang, C.; Szymanski, M. J.; Greenwald, E. E. *J. Am. Chem. Soc.* **2003**, *125*, 1176-1177.
- 79 a) K. Fukui, H. Fujimoto, *Bull. Chem. Soc. Jpn.* **1967**, *40*, 2018; b) K. Fukui, H. Fujimoto, *Bull. Chem. Soc. Jpn.* **1969**, *42*, 3399; c) K. Fukui, *Fortschr. Chem. Forsch.* **1970**, *15*, 1; d) K. Fukui, *Acc. Chem. Res.* **1971**, *4*, 57; e) K. N. Houk, *Acc. Chem. Res.* **1975**, *8*, 361; for reviews, see: f) K. N. Houk, in: *Pericyclic Reactions*, Vol. 2, (Eds.: A. P. Marchand; R. E. Lehr), Academic Press, New York, 1977, pp. 181; g) K. Fukui, *Angew. Chem. Int. Ed. Engl.* **1982**, *21*, 801.
- 80 Alder, K., Braden, R., Flock, F. H. *Chem. Ber.* **1961**, *94*, 456-467.
- 81 Houk, K. N., Luskus, L. J. *Tetrahedron Lett.* **1970**, *46*, 4029-4031.
- 82 Marchand, A. P., Lehr, R. E., *Pericyclic Reactions: Organic Chemistry Series 35-II*, Academic Press, New York. pp. 238
- 83 Aggarwal, V. K.; Dean, D. K.; Mereu, A.; Williams, R. J. *Org. Chem.* **2002**, *67*, 510-514.
- 84 Rivera, M.; Lamy-Schalkens, H.; Sainte, F.; Mbiya, K.; Ghosez, L. *Tetrahedron Lett.* **1988**, *29*, 4573-4576.

- 85 Dauben, W. G.; Kessal, C. R.; Takemura, K. H. *J. Am. Chem. Soc.* **1980**, *102*, 6893-6894.
- 86 Grieco, P. A.; Nunes, J. J.; Gaul, M. D. *J. Am. Chem. Soc.* **1990**, *112*, 4595-4596.
- 87 Forman, M. A.; Dailey, W. P. *J. Am. Chem. Soc.* **1991**, *113*, 2761-2762.
- 88 Eggelte, T. A.; De Koning, H.; Huismann, H. O. *Tetrahedron*, **1973**, *29*, 2491-2493.
- 89 Narayan, S.; Muldoon, J.; Finn, M. G.; Fokin, V. V.; Kolb, H. C.; Sharpless, K. B. *Angew. Chem. Int. Ed.* **2005**, *44*, 3275–3279.
- 90 Diethyl azodicarboxylate is commercially available as a 40% solution in toluene.
- 91 Tsutsui, S.; Sakamoto, K.; Yoshida, H.; Kunai, A. *J. Organomet. Chem.* **2005**, *690*, 1324–1331.
- 92 Selmecky, A.D.; Jones, W.D. *Inorg. Chim. Acta.* **2000**, *300–30*, 138–150.
- 93 Zweig, A.; Hoffmann, K. *J. Am. Chem. Soc.* **1963**, *85*, 2736-2739.
- 94 Jung, Y.; Marcus, R. A. *J. Am. Chem. Soc.* **2007**, *129*, 5492-5502.
- 95 Breslow, R. *ACS Sym. Ser.*, **1994**, *568*, 291-302.
- 96 Breslow, R.; Guo, T. *Proc. Natl. Acad. Sci. USA* **1990**, *87*, 167-169.
- 97 Frisch, M. J.; Trucks, G. W.; Schlegel, G. E. Scuseria, M. A. Robb et al., *Gaussian 98*, Revision A.11.2, Gaussian, Inc., Pittsburgh PA, 2001.
- 98 Singleton, D. A.; Hang, C.; Szymanski, M. J.; Greenwald, E. E. *J. Am. Chem. Soc.* **2003**, *125*, 1176-1177.
- 99 Bekele, T.; Christian, C. F.; Lipton, M. A.; Singleton, D. A. *J. Am. Chem. Soc.* **2005**, *127*, 9216-9223.
- 100 Singleton, D. A.; Hang, C.; Szymanski, M. J.; Meyer, M. P.; Leach, A. G.; Kuwata, K. T.; Chen, J. S.; Greer, A.; Foote, C. S.; Houk, K. N. *J. Am. Chem. Soc.* **2003**, *125*, 1319-1328.

- 101 Ussing, B. R.; Singleton, D. A. *J. Am. Chem. Soc.* **2005**, *127*, 2888-2899.
102. Cheng, C.; Seymour, C. A.; Petti, M. A.; Greene, F. D. *J. Org. Chem.* **1984**, *49*, 2910-2916.

APPENDIX

GEOMETRIES AND ENERGIES OF CALCULATED STRUCTURES.....	100
Terms	100
¹ O ₂ Ene Reaction	100
PtA	100
PtB.....	102
Energy Distributions.	103
DRP path for singlet O ₂ + tme Lluch D-side	118
DRP path for singlet O ₂ + tme Lluch H-side	120
DRP path for singlet O ₂ + tme trans3D D-side	122
DRP path for singlet O ₂ + tme trans3D H-side	124
Dimerization of Cyclopentadiene.....	126
DCPD Cope ts.....	126
CpTSmpw1b95	128
CpTSb3pw91	131
CpTSmpw3lyp.....	133
CpTSmpwb1k	136
CpTSmpwpw91	138
Positive DRP Path for dimerization of Cyclopentadiene.....	141
Negative DRP Path for dimerization of Cyclopentadiene	143
Cycloaddition of Dimethylfulvene with Diazomethane.....	145
Dmfulv2+4PD.....	145
Dmfulv2+4ts	147
dmfulv2+4tsBB.....	150
Dmfulv6+4PD.....	151
DmfulvAlkRearTS.....	153

DmfulvRearTS	155
Quadricyclane Cycloaddition	158
QuaddmadB3P	158
Quaddmad3wB3P	160
QuadricyclaneB3P	163
QuadricyclaneCationRadB3P	165
Quadtsb1b95	167
QuadtsRmPWPW91	170
Listing of Dynamics Programs	172
1. Program progdynstarterHP	172
2. Program proggenHP	184
3. Program prog1stpoint.....	198
4. Program prog2ndpoint	202
5. Program progdynb	208
6. Program randgen.....	216
7. Program proganal.....	217
8. progdyn.conf.....	221
RRKM Calculations	226

GEOMETRIES AND ENERGIES OF CALCULATED STRUCTURES

All structures and energies were obtained using standard procedures in Gaussian98 and Gaussian03.

Terms

B3: Becke 3-parameter exchange model

RB: Restricted Becke

HF: Hartree-Fock

LYP: Lee-Yang-Parr gradient-corrected functionals

mPW1K: modified Perdew-Wang 1-parameter model for kinetics

RmPW: Restricted modified Perdew-Wang model

PW91: Perdew-Wang 1991 gradient-corrected functionals

MP2: Möller-Plesset second-order perturbation

RHF: Restricted Hartree-Fock

¹O₂ Ene Reaction

PtA

CCSD(T)= -0.38518359926D+03

Standard orientation:

 Center Atomic Atomic Coordinates (Angstroms)

Number	Number	Type	X	Y	Z
1	6	0	-0.613707	-1.433337	1.546100
2	6	0	-0.613707	-0.195354	0.691324
3	6	0	-0.613707	-0.195354	-0.691324
4	6	0	-0.620052	1.105421	1.438487
5	6	0	-0.620052	1.105421	-1.438487
6	6	0	-0.613707	-1.433337	-1.546100
7	1	0	0.199849	-1.373151	2.278785
8	1	0	-0.493749	-2.361377	0.985711
9	1	0	-1.551665	-1.500446	2.115216
10	1	0	-0.720862	0.951507	2.516569
11	1	0	-1.419590	1.779670	1.110376
12	1	0	0.336797	1.631674	1.257276
13	1	0	0.336797	1.631674	-1.257276
14	1	0	-1.419590	1.779670	-1.110376
15	1	0	-0.720862	0.951507	-2.516569
16	1	0	0.199849	-1.373151	-2.278785
17	1	0	-1.551665	-1.500446	-2.115216
18	1	0	-0.493749	-2.361377	-0.985711
19	8	0	1.661713	-0.100847	0.000000
20	8	0	2.021792	1.103782	0.000000

 Rotational constants (GHZ): 1.9748706 1.8081888 1.4848564

PtB

CCSD(T)= -0.38519404537D+03

Standard orientation:

 Center Atomic Atomic Coordinates (Angstroms)
 Number Number Type X Y Z

 1 6 0 -1.602312 1.437999 -0.154244
 2 6 0 -0.759799 0.271404 0.283332
 3 6 0 0.708967 0.330196 0.267702
 4 6 0 -1.438663 -0.871597 0.949191
 5 6 0 1.498816 -0.712443 0.989453
 6 6 0 1.436766 1.582696 -0.147483
 7 1 0 -1.144431 2.014539 -0.959721
 8 1 0 -1.773352 2.117604 0.692797
 9 1 0 -2.580005 1.086510 -0.498300
 10 1 0 -2.522542 -0.737403 0.984096
 11 1 0 -1.068647 -1.067913 1.960093

12	1	0	-1.185669	-1.755235	0.319700
13	1	0	1.358143	-1.641550	0.401501
14	1	0	1.139290	-0.895631	2.006521
15	1	0	2.560698	-0.457750	1.029520
16	1	0	0.934558	2.115873	-0.957040
17	1	0	2.448695	1.332758	-0.480066
18	1	0	1.525082	2.267161	0.707357
19	8	0	0.049531	-0.364377	-1.120101
20	8	0	0.106160	-1.711685	-1.171670

 Rotational constants (GHZ): 2.1862557 2.1129537 1.6218129

Energy Distributions.

The thermal distribution of energy of **6** was determined using a modified PROGDYN program.

Energy distribution at 50 °C

<i>Bin</i>	<i>Frequency</i>
0	814
0.285714	152

0.785714 125

1.285714 9

Energy distribution at 100 °C

<i>Bin</i>	<i>Frequency</i>
0	228
0.285714	158
0.785714	405
1.285714	193
1.785714	70
2.285714	30
2.785714	14
3.285714	1
3.785714	1

Energy distribution at 150 °C

<i>Bin</i>	<i>Frequency</i>
0	54
0.285714	50
0.785714	225
1.285714	244
1.785714	185
2.285714	155
2.785714	88

3.285714	48
3.785714	34
4.285714	13
4.785714	1
5.285714	2
5.785714	1

Energy distribution at 200 °C

<i>Bin</i>	<i>Frequency</i>
0	13
0.285714	10
0.785714	83
1.285714	123
1.785714	164
2.285714	157
2.785714	144
3.285714	118
3.785714	93
4.285714	79
4.785714	54
5.285714	33

5.785714	10
6.285714	10
6.785714	5
7.285714	1
7.785714	0
8.285714	1
8.785714	1
9.285714	1

Energy distribution at 263 °C

<i>Bin</i>	<i>Frequency</i>
0	0
0.285714	4
0.785714	21
1.285714	41
1.785714	54
2.285714	82
2.785714	95
3.285714	110
3.785714	111
4.285714	104

4.785714	86
5.285714	85
5.785714	85
6.285714	69
6.785714	53
7.285714	34
7.785714	24
8.285714	12
8.785714	11
9.285714	6
9.785714	5
10.28571	2
10.78571	3
11.28571	1
11.78571	0
12.28571	2

Energy distribution at 298 °C

<hr/>		energy
<i>Bin</i>	<i>Frequency</i>	(cm-1)
<hr/>		
0	1	0

0.5	5	175
1	10	350
1.5	20	525
2	24	700
2.5	65	875
3	78	1050
3.5	83	1225
4	96	1400
4.5	99	1575
5	94	1750
5.5	74	1925
6	80	2100
6.5	77	2275
7	69	2450
7.5	52	2625
8	44	2800
8.5	30	2975
9	27	3150
9.5	23	3325
10	14	3500
10.5	11	3675
11	9	3850

11.5	0	4025
12	8	4200
12.5	2	4375
13	3	4550
13.5	1	4725
14	0	4900
14.5	0	5075
15	1	5250

Energy distribution at 300 °C

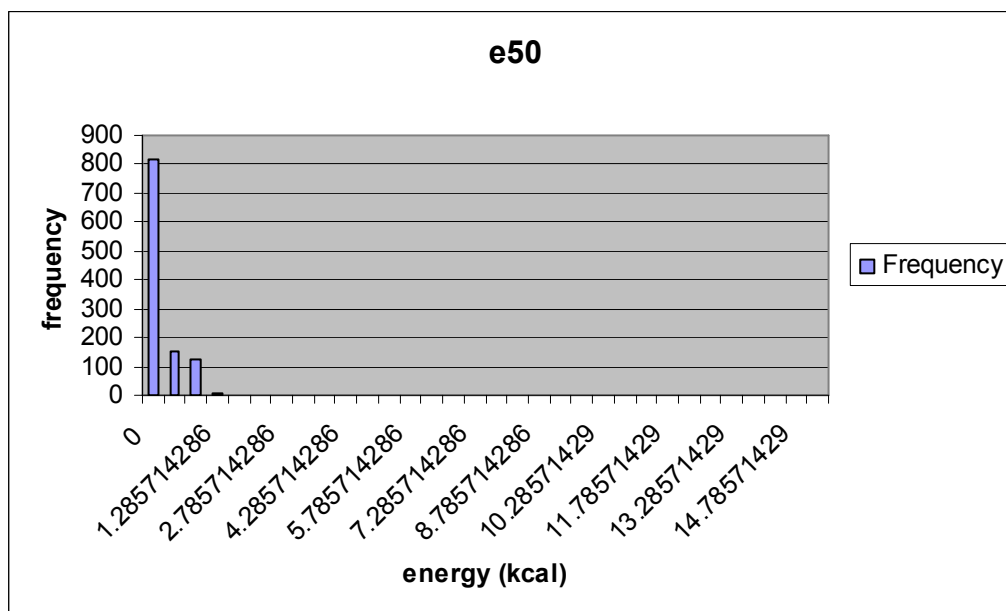
<i>Bin</i>	<i>Frequency</i>
0	1
0.5	3
1	6
1.5	15
2	26
2.5	39
3	50
3.5	85
4	79
4.5	82

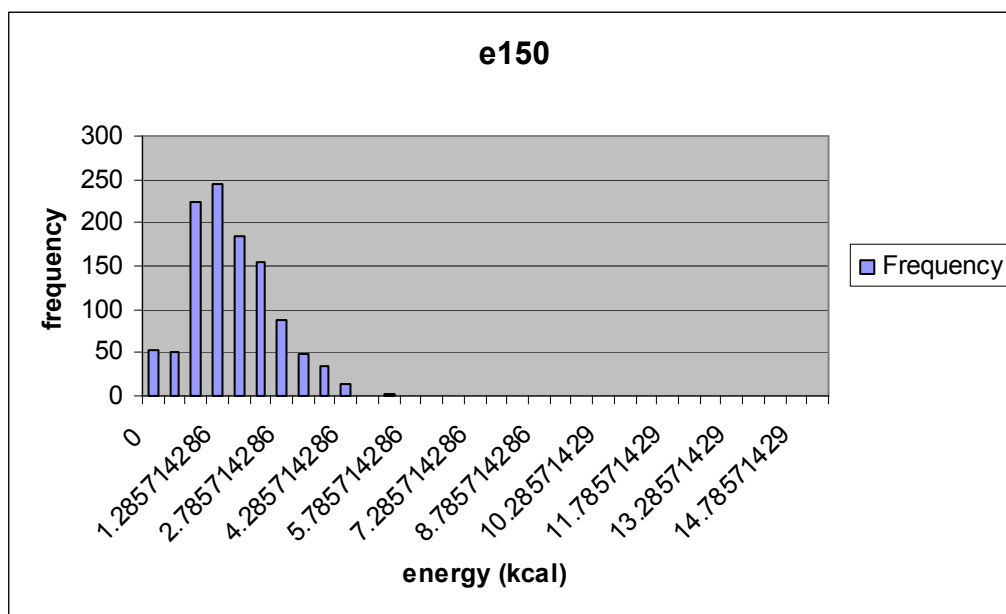
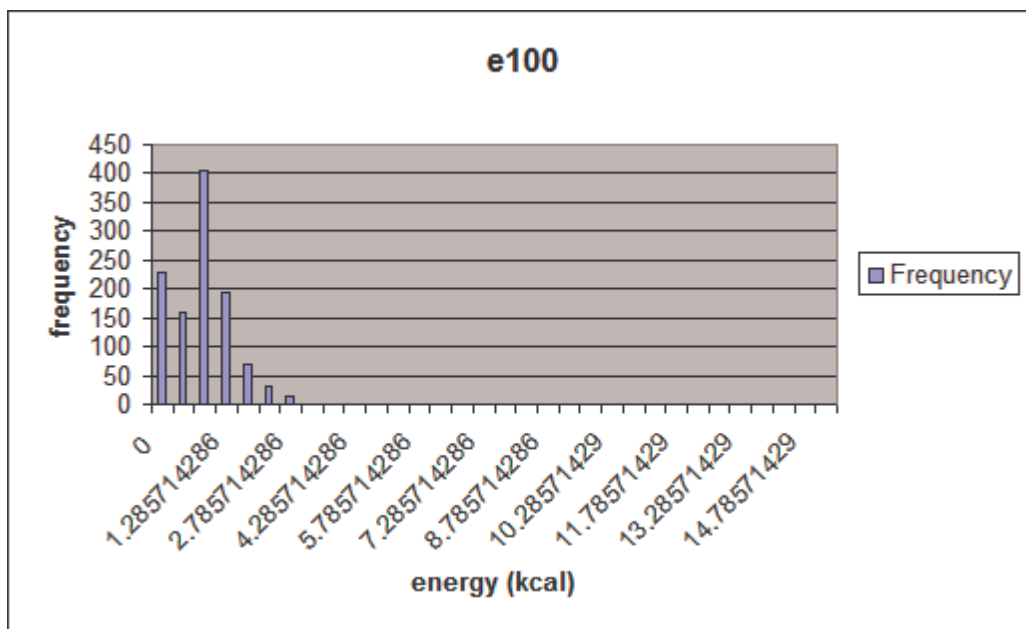
5	79
5.5	73
6	75
6.5	79
7	64
7.5	46
8	34
8.5	35
9	22
9.5	29
10	11
10.5	11
11	8
11.5	3
12	8
12.5	2
13	5
13.5	1
14	1

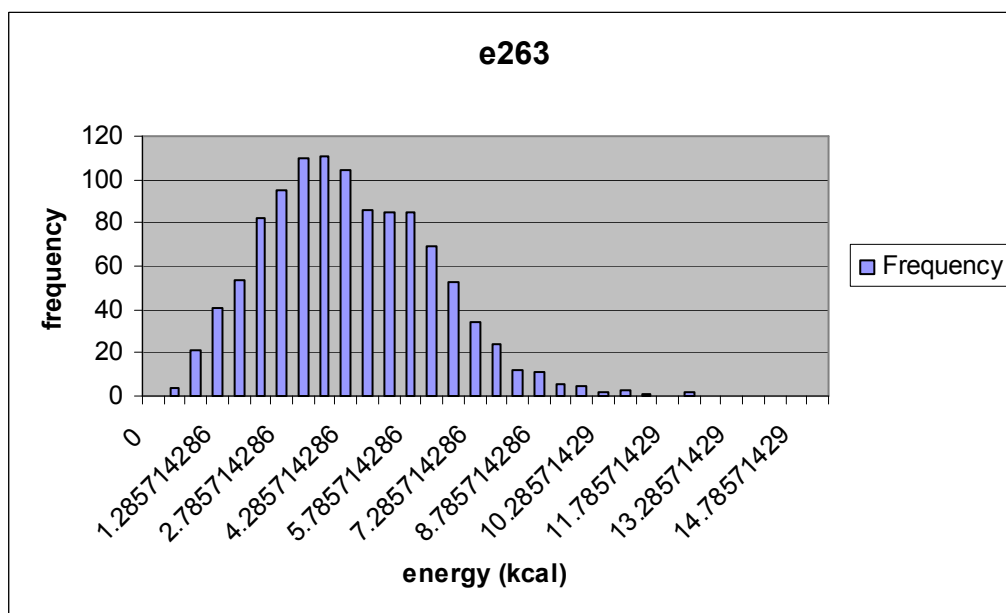
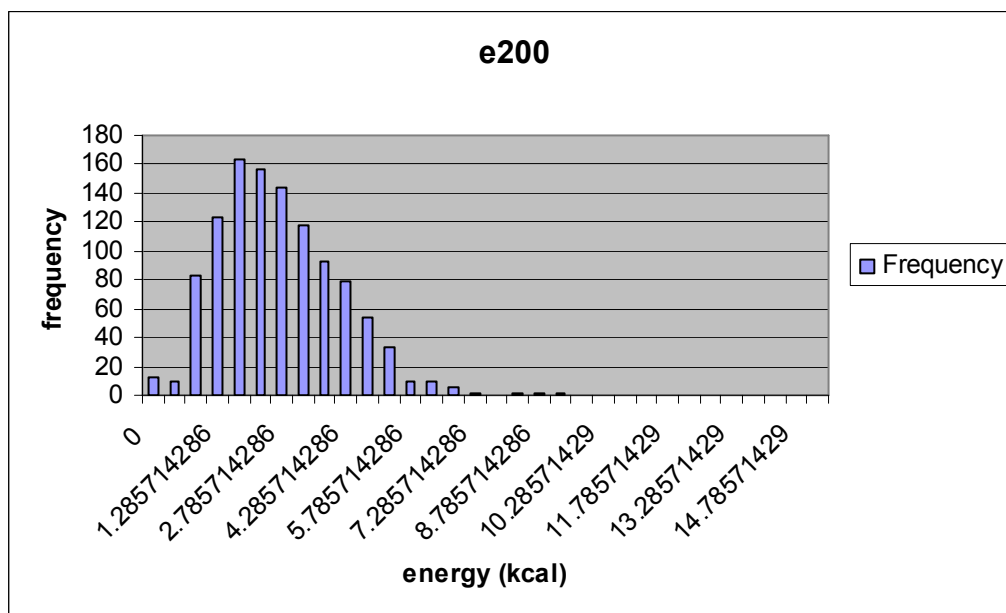
Energy distribution at 350 °C

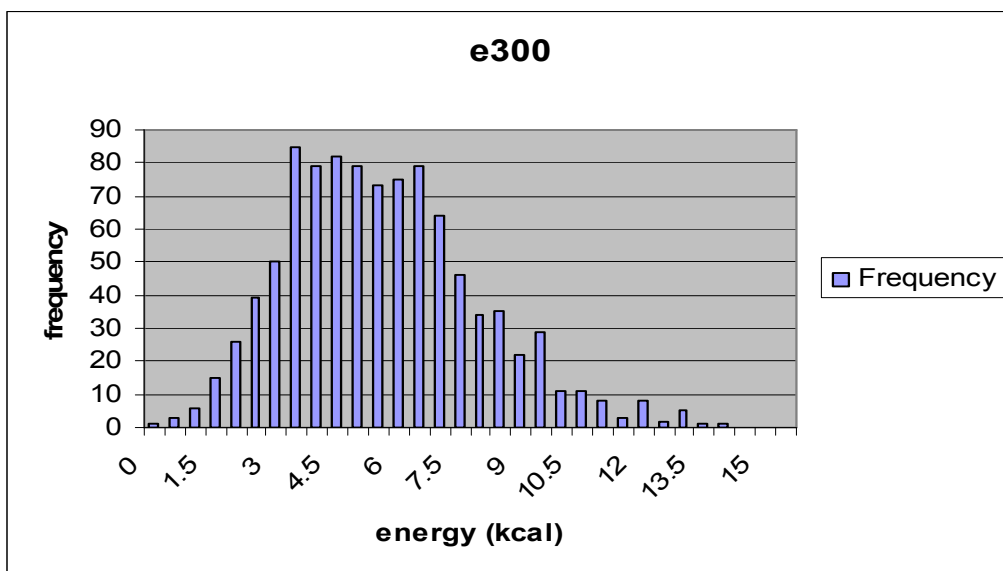
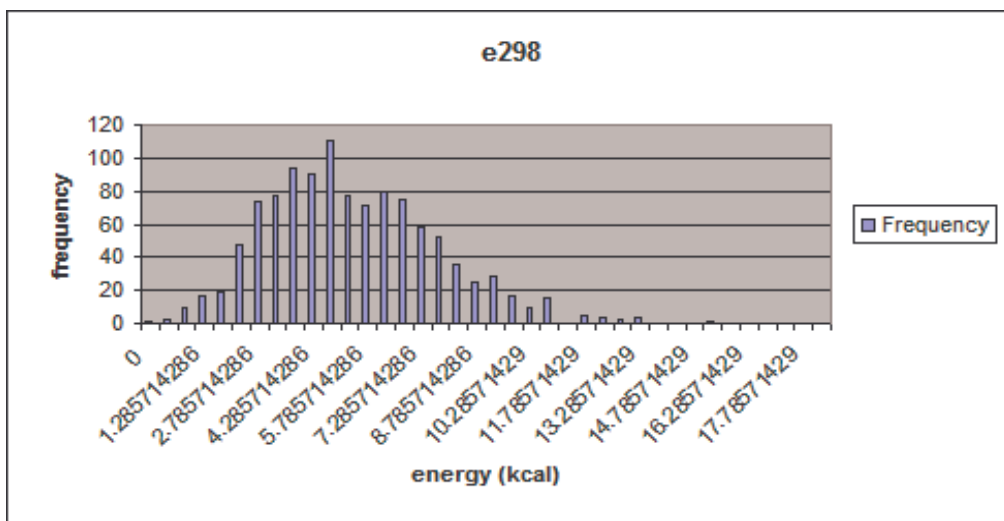
<i>Bin</i>	<i>Frequency</i>
0	0
0.5	1
1	3
1.5	8
2	10
2.5	20
3	35
3.5	33
4	53
4.5	60
5	75
5.5	75
6	77
6.5	70
7	56
7.5	85
8	74
8.5	50
9	60
9.5	38
10	51

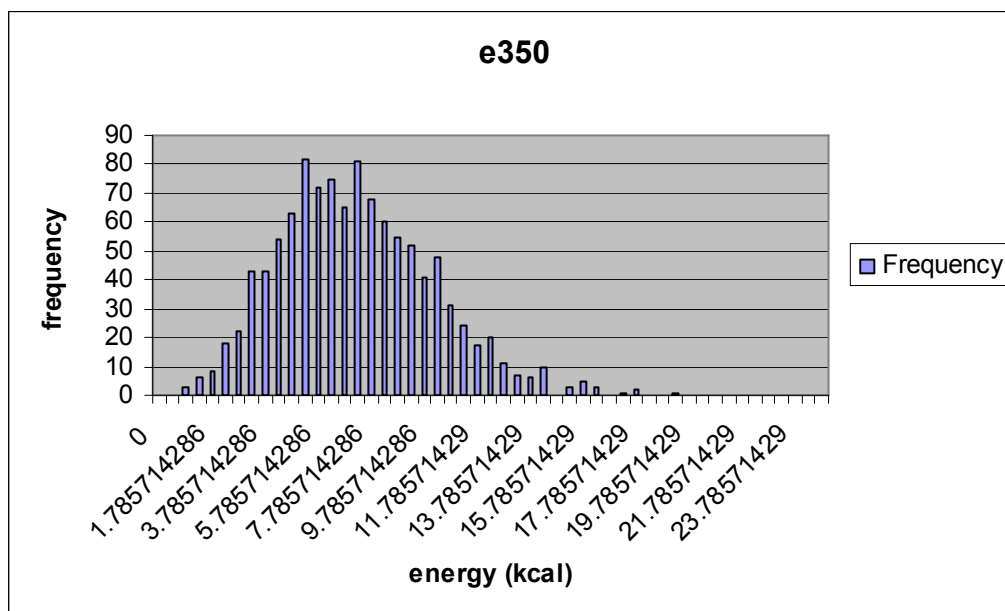
10.5	39
11	23
11.5	28
12	16
12.5	15
13	9
13.5	8
14	8
14.5	5
15	1
15.5	2
16	7
16.5	1
17	0
17.5	2
18	1
18.5	0
19	0
19.5	1











DRP path for singlet O₂ + tme Lluch D-side

pt 1

$E(\text{RB}+\text{HF-LYP}) = -386.136633419$

Standard orientation:

```

-----
Center  Atomic  Atomic      Coordinates (Angstroms)
Number  Number  Type        X          Y          Z
-----
1       6       0      -1.501409  1.530011  -0.221690
2       6       0      -0.714249  0.367961  0.316180
3       6       0       0.725231  0.353280  0.317210
  
```

4	6	0	-1.459050	-0.703339	1.029200
5	6	0	1.445920	-0.738340	1.022570
6	6	0	1.537861	1.496570	-0.222500
7	1	0	-2.485919	1.192532	-0.559230
8	1	0	-1.008178	2.029581	-1.058170
9	1	0	-1.662928	2.279552	0.567160
10	1	0	-2.533900	-0.508058	1.053880
11	1	0	-1.104700	-0.875319	2.050690
12	1	0	-1.269591	-1.638339	0.453090
13	1	0	1.234499	-1.664750	0.438980
14	1	0	1.087670	-0.911380	2.042530
15	1	0	2.524900	-0.567741	1.048330
16	1	0	2.512571	1.135779	-0.564380
17	1	0	1.721252	2.241159	0.566430
18	1	0	1.053542	2.009400	-1.056090
19	8	0	-0.011290	-0.508820	-1.206080
20	8	0	-0.023091	-1.811090	-1.097550

Rotational constants (GHZ): 1.9390821 1.8578548 1.4559198

Zero-point correction= 0.150380 (Hartree/Particle)

Thermal correction to Energy= 0.161128

Thermal correction to Enthalpy= 0.162073

Thermal correction to Gibbs Free Energy=	0.113811
Sum of electronic and zero-point Energies=	-385.986253
Sum of electronic and thermal Energies=	-385.975505
Sum of electronic and thermal Enthalpies=	-385.974561
Sum of electronic and thermal Free Energies=	-386.022822

	E (Thermal)	CV	S
	KCal/Mol	Cal/Mol-Kelvin	Cal/Mol-Kelvin
Total	101.110	38.761	101.574

DRP path for singlet O2 + tme Lluch H-side

pt 1

E(RB+HF-LYP) = -386.136632152

Standard orientation:

Center	Atomic	Atomic	Coordinates (Angstroms)		
Number	Number	Type	X	Y	Z
1	6	0	-1.536853	1.497539	-0.222581
2	6	0	-0.724984	0.353735	0.317149
3	6	0	0.714476	0.367606	0.316289

4	6	0	-1.446396	-0.737331	1.022639
5	6	0	1.458594	-0.704209	1.029219
6	6	0	1.502397	1.529081	-0.221751
7	1	0	-2.512150	1.137821	-0.563981
8	1	0	-1.052467	2.009822	-1.056491
9	1	0	-1.718858	2.242157	0.566579
10	1	0	-2.525307	-0.566109	1.048309
11	1	0	-1.088215	-0.910038	2.042639
12	1	0	-1.235659	-1.664169	0.439449
13	1	0	1.268471	-1.638840	0.452739
14	1	0	1.104185	-0.876522	2.050669
15	1	0	2.533522	-0.509531	1.053979
16	1	0	2.486449	1.190539	-0.559491
17	1	0	1.665051	2.278893	0.566679
18	1	0	1.009303	2.028888	-1.058151
19	8	0	0.010912	-0.508970	-1.206131
20	8	0	0.021872	-1.811210	-1.097461

Rotational constants (GHZ): 1.9371952 1.8592864 1.4562635

Zero-point correction= 0.150375 (Hartree/Particle)

Thermal correction to Energy= 0.161127

Thermal correction to Enthalpy= 0.162071

Thermal correction to Gibbs Free Energy=	0.113673
Sum of electronic and zero-point Energies=	-385.986258
Sum of electronic and thermal Energies=	-385.975505
Sum of electronic and thermal Enthalpies=	-385.974561
Sum of electronic and thermal Free Energies=	-386.022959

	E (Thermal)	CV	S
	KCal/Mol	Cal/Mol-Kelvin	Cal/Mol-Kelvin
Total	101.109	38.757	101.861

DRP path for singlet O2 + tme trans3D D-side

pt 1

E(RB+HF-LYP) = -386.136660193

Standard orientation:

```

-----
Center  Atomic  Atomic      Coordinates (Angstroms)
Number  Number  Type        X          Y          Z
-----
  1      6      0    -1.451652  1.573360 -0.213068
  2      6      0    -0.701073  0.384876  0.320002
  3      6      0     0.740087  0.331227  0.321462
  4      6      0    -1.477165 -0.666741  1.029702

```

5	6	0	1.430756	-0.789218	1.009732
6	6	0	1.580099	1.453424	-0.219718
7	1	0	-0.958486	2.037944	-1.069768
8	1	0	-1.557408	2.340619	0.568032
9	1	0	-2.458710	1.276182	-0.520108
10	1	0	-2.545097	-0.437399	1.059932
11	1	0	-1.124393	-0.855868	2.048692
12	1	0	-1.319337	-1.603279	0.446822
13	1	0	1.184363	-1.702500	0.417812
14	1	0	1.073438	-0.962060	2.030072
15	1	0	2.514825	-0.653639	1.029282
16	1	0	1.111024	1.969930	-1.059848
17	1	0	2.550082	1.072011	-0.552398
18	1	0	1.771723	2.199845	0.565522
19	8	0	-0.037156	-0.499659	-1.206448
20	8	0	-0.083886	-1.800760	-1.100138

Rotational constants (GHZ): 1.9969515 1.8123842 1.4506448

Zero-point correction= 0.150466 (Hartree/Particle)

Thermal correction to Energy= 0.161134

Thermal correction to Enthalpy= 0.162078

Thermal correction to Gibbs Free Energy= 0.114928

Sum of electronic and zero-point Energies= -385.986194
 Sum of electronic and thermal Energies= -385.975527
 Sum of electronic and thermal Enthalpies= -385.974582
 Sum of electronic and thermal Free Energies= -386.021732

	E (Thermal)	CV	S
	KCal/Mol	Cal/Mol-Kelvin	Cal/Mol-Kelvin
Total	101.113	38.734	99.234

DRP path for singlet O2 + tme trans3D H-side

pt 1

E(RB+HF-LYP) = -386.136661396

Standard orientation:

```

-----
Center  Atomic  Atomic      Coordinates (Angstroms)
Number  Number  Type        X         Y         Z
-----
  1      6      0    -1.598631  1.434168 -0.221701
  2      6      0    -0.745726  0.321740  0.319679
  3      6      0     0.694683  0.393960  0.321929
  4      6      0    -1.423590 -0.806939  1.007449
  
```


5	6	0	1.482118	-0.648759	1.032079
6	6	0	1.432997	1.590080	-0.210911
7	1	0	-1.135708	1.955314	-1.062371
8	1	0	-1.798121	2.178715	0.563309
9	1	0	-2.564375	1.041725	-0.553811
10	1	0	-2.509692	-0.687794	1.018939
11	1	0	-1.071018	-0.969705	2.031139
12	1	0	-1.159447	-1.719176	0.421879
13	1	0	1.342321	-1.584361	0.442889
14	1	0	1.125271	-0.848614	2.047549
15	1	0	2.546244	-0.403445	1.070689
16	1	0	0.930901	2.055723	-1.061701
17	1	0	2.439831	1.300804	-0.526321
18	1	0	1.539646	2.354021	0.573319
19	8	0	0.046116	-0.498519	-1.206491
20	8	0	0.111764	-1.798818	-1.100591

Rotational constants (GHZ): 2.0038966 1.8042858 1.4510953

Zero-point correction= 0.150458 (Hartree/Particle)

Thermal correction to Energy= 0.161123

Thermal correction to Enthalpy= 0.162067

Thermal correction to Gibbs Free Energy= 0.114881

Sum of electronic and zero-point Energies= -385.986203
 Sum of electronic and thermal Energies= -385.975538
 Sum of electronic and thermal Enthalpies= -385.974594
 Sum of electronic and thermal Free Energies= -386.021780

	E (Thermal)	CV	S
	KCal/Mol	Cal/Mol-Kelvin	Cal/Mol-Kelvin
Total	101.106	38.715	99.311

Dimerization of Cyclopentadiene

DCPD Cope ts

E(RB+HF-LYP) = -388.175945035

Standard orientation:

```

-----
Center  Atomic  Atomic      Coordinates (Angstroms)
Number  Number  Type        X      Y      Z
-----
  1      1      0    -1.780883 -1.297836  1.402392
  2      6      0    -1.858550 -0.801124  0.428826
  
```

3	6	0	-1.820481	0.703610	0.473637
4	6	0	-1.304721	1.163279	-0.727987
5	6	0	-0.605125	0.136354	-1.367105
6	6	0	-0.652866	-1.067188	-0.492845
7	1	0	-2.788866	-1.148449	-0.048642
8	6	0	0.605149	0.136338	1.367130
9	1	0	-2.368248	1.303139	1.193184
10	1	0	-1.329024	2.195978	-1.063772
11	1	0	-0.195592	0.163561	-2.368698
12	6	0	0.652886	-1.067187	0.492845
13	1	0	-0.660300	-2.026008	-1.018850
14	1	0	0.660328	-2.025997	1.018847
15	1	0	0.195612	0.163546	2.368719
16	6	0	1.304719	1.163275	0.728001
17	6	0	1.820449	0.703624	-0.473648
18	1	0	1.329044	2.195984	1.063780
19	6	0	1.858544	-0.801110	-0.428843
20	1	0	2.368203	1.303135	-1.193199
21	1	0	2.788876	-1.148461	0.048581
22	1	0	1.780828	-1.297821	-1.402415

Rotational constants (GHZ): 2.3996665 1.4198925 1.3461843

Zero-point correction=	0.190514 (Hartree/Particle)
Thermal correction to Energy=	0.197694
Thermal correction to Enthalpy=	0.198638
Thermal correction to Gibbs Free Energy=	0.159248
Sum of electronic and zero-point Energies=	-387.985431
Sum of electronic and thermal Energies=	-387.978251
Sum of electronic and thermal Enthalpies=	-387.977307
Sum of electronic and thermal Free Energies=	-388.016697

CpTSmpw1b95

E(RB+HF-LYP) = -388.186859302

Standard orientation:

Center	Atomic	Atomic	Coordinates (Angstroms)		
Number	Number	Type	X	Y	Z
1	6	0	0.758935	0.111237	1.364007
2	6	0	0.807983	-1.053243	0.556463
3	6	0	1.887835	-0.799358	-0.491380

4	6	0	1.942451	0.704860	-0.501085
5	6	0	1.400574	1.172739	0.666215
6	1	0	1.705956	-1.265398	-1.464637
7	1	0	2.844993	-1.199863	-0.114962
8	6	0	-0.807534	-1.052761	-0.557147
9	6	0	-1.887807	-0.800062	0.490574
10	6	0	-1.943156	0.704124	0.501349
11	6	0	-1.400795	1.173184	-0.665186
12	6	0	-0.758464	0.112453	-1.363638
13	1	0	-1.705978	-1.266639	1.463587
14	1	0	-2.844680	-1.200772	0.113655
15	1	0	2.481052	1.290165	-1.237988
16	1	0	1.399970	2.209748	0.988084
17	1	0	0.301885	0.188470	2.342538
18	1	0	0.709865	-2.042655	0.999002
19	1	0	-0.709195	-2.041751	-1.000599
20	1	0	-0.301431	0.190573	-2.342103
21	1	0	-1.400379	2.210465	-0.986180
22	1	0	-2.482190	1.288621	1.238576

Rotational constants (GHZ): 2.3861557 1.2977400 1.2398937

Leave Link 202 at Sun Jul 20 21:07:03 2008, MaxMem= 62914560 cpu: 0.3

(Enter /home/g03/g03_D02/g03/l301.exe)

Standard basis: 6-31+G(d) (6D, 7F)

There are 214 symmetry adapted basis functions of A symmetry.

Integral buffers will be 131072 words long.

Raffenetti 2 integral format.

Two-electron integral symmetry is turned on.

214 basis functions, 368 primitive gaussians, 214 cartesian basis functions

36 alpha electrons 36 beta electrons

Zero-point correction= 0.188422 (Hartree/Particle)

Thermal correction to Energy= 0.196486

Thermal correction to Enthalpy= 0.197430

Thermal correction to Gibbs Free Energy= 0.155752

Sum of electronic and zero-point Energies= -387.998437

Sum of electronic and thermal Energies= -387.990373

Sum of electronic and thermal Enthalpies= -387.989429

Sum of electronic and thermal Free Energies= -388.031107

	E (Thermal)	CV	S
	KCal/Mol	Cal/Mol-Kelvin	Cal/Mol-Kelvin
Total	123.297	33.274	87.719

CpTSb3pw91

E(RB+HF-PW91) = -388.061470244

Standard orientation:

Center	Atomic	Atomic	Coordinates (Angstroms)		
Number	Number	Type	X	Y	Z
1	6	0	0.758935	0.111237	1.364007
2	6	0	0.807983	-1.053243	0.556463
3	6	0	1.887835	-0.799358	-0.491380
4	6	0	1.942451	0.704860	-0.501085
5	6	0	1.400574	1.172739	0.666215
6	1	0	1.705956	-1.265398	-1.464637
7	1	0	2.844993	-1.199863	-0.114962
8	6	0	-0.807534	-1.052761	-0.557147
9	6	0	-1.887807	-0.800062	0.490574
10	6	0	-1.943156	0.704124	0.501349
11	6	0	-1.400795	1.173184	-0.665186

12	6	0	-0.758464	0.112453	-1.363638
13	1	0	-1.705978	-1.266639	1.463587
14	1	0	-2.844680	-1.200772	0.113655
15	1	0	2.481052	1.290165	-1.237988
16	1	0	1.399970	2.209748	0.988084
17	1	0	0.301885	0.188470	2.342538
18	1	0	0.709865	-2.042655	0.999002
19	1	0	-0.709195	-2.041751	-1.000599
20	1	0	-0.301431	0.190573	-2.342103
21	1	0	-1.400379	2.210465	-0.986180
22	1	0	-2.482190	1.288621	1.238576

 Rotational constants (GHZ): 2.3861557 1.2977400 1.2398937

Leave Link 202 at Thu Jul 31 00:10:55 2008, MaxMem= 62914560 cpu: 0.4

(Enter /home/g03/g03_D02/g03/l301.exe)

Standard basis: 6-31+G(d,p) (6D, 7F)

There are 250 symmetry adapted basis functions of A symmetry.

Integral buffers will be 131072 words long.

Raffenetti 2 integral format.

Two-electron integral symmetry is turned on.

250 basis functions, 404 primitive gaussians, 250 cartesian basis functions

36 alpha electrons 36 beta electrons

Zero-point correction=	0.188224 (Hartree/Particle)
Thermal correction to Energy=	0.196319
Thermal correction to Enthalpy=	0.197263
Thermal correction to Gibbs Free Energy=	0.155567
Sum of electronic and zero-point Energies=	-387.873270
Sum of electronic and thermal Energies=	-387.865175
Sum of electronic and thermal Enthalpies=	-387.864231
Sum of electronic and thermal Free Energies=	-387.905927

	E (Thermal)	CV	S
	KCal/Mol	Cal/Mol-Kelvin	Cal/Mol-Kelvin
Total	123.192	33.457	87.756

CpTSmpw3lyp

E(RB+HF-LYP) = -388.186859302

Standard orientation:

Center Number	Atomic Number	Atomic Type	Coordinates (Angstroms)		
			X	Y	Z

1	6	0	0.758935	0.111237	1.364007
2	6	0	0.807983	-1.053243	0.556463
3	6	0	1.887835	-0.799358	-0.491380
4	6	0	1.942451	0.704860	-0.501085
5	6	0	1.400574	1.172739	0.666215
6	1	0	1.705956	-1.265398	-1.464637
7	1	0	2.844993	-1.199863	-0.114962
8	6	0	-0.807534	-1.052761	-0.557147
9	6	0	-1.887807	-0.800062	0.490574
10	6	0	-1.943156	0.704124	0.501349
11	6	0	-1.400795	1.173184	-0.665186
12	6	0	-0.758464	0.112453	-1.363638
13	1	0	-1.705978	-1.266639	1.463587
14	1	0	-2.844680	-1.200772	0.113655
15	1	0	2.481052	1.290165	-1.237988
16	1	0	1.399970	2.209748	0.988084
17	1	0	0.301885	0.188470	2.342538
18	1	0	0.709865	-2.042655	0.999002
19	1	0	-0.709195	-2.041751	-1.000599

20	1	0	-0.301431	0.190573	-2.342103
21	1	0	-1.400379	2.210465	-0.986180
22	1	0	-2.482190	1.288621	1.238576

Rotational constants (GHZ): 2.3861557 1.2977400 1.2398937

Leave Link 202 at Sun Jul 20 21:17:22 2008, MaxMem= 62914560 cpu: 0.3

(Enter /home/g03/g03_D02/g03/l301.exe)

Standard basis: 6-31+G(d) (6D, 7F)

There are 214 symmetry adapted basis functions of A symmetry.

Integral buffers will be 131072 words long.

Raffenetti 2 integral format.

Two-electron integral symmetry is turned on.

214 basis functions, 368 primitive gaussians, 214 cartesian basis functions

36 alpha electrons 36 beta electrons

Zero-point correction= 0.188422 (Hartree/Particle)

Thermal correction to Energy= 0.196486

Thermal correction to Enthalpy= 0.197430

Thermal correction to Gibbs Free Energy= 0.155752

Sum of electronic and zero-point Energies= -387.998437

Sum of electronic and thermal Energies= -387.990373

Sum of electronic and thermal Enthalpies= -387.989429

Sum of electronic and thermal Free Energies= -388.031107

	E (Thermal)	CV	S
	KCal/Mol	Cal/Mol-Kelvin	Cal/Mol-Kelvin
Total	123.297	33.274	87.719

CpTSmpwb1k

E(RB+HF-LYP) = -388.186859302

Standard orientation:

Center	Atomic	Atomic	Coordinates (Angstroms)			
Number	Number	Type	X	Y	Z	

1	6	0	0.758935	0.111237	1.364007	
2	6	0	0.807983	-1.053243	0.556463	
3	6	0	1.887835	-0.799358	-0.491380	
4	6	0	1.942451	0.704860	-0.501085	
5	6	0	1.400574	1.172739	0.666215	
6	1	0	1.705956	-1.265398	-1.464637	

7	1	0	2.844993	-1.199863	-0.114962
8	6	0	-0.807534	-1.052761	-0.557147
9	6	0	-1.887807	-0.800062	0.490574
10	6	0	-1.943156	0.704124	0.501349
11	6	0	-1.400795	1.173184	-0.665186
12	6	0	-0.758464	0.112453	-1.363638
13	1	0	-1.705978	-1.266639	1.463587
14	1	0	-2.844680	-1.200772	0.113655
15	1	0	2.481052	1.290165	-1.237988
16	1	0	1.399970	2.209748	0.988084
17	1	0	0.301885	0.188470	2.342538
18	1	0	0.709865	-2.042655	0.999002
19	1	0	-0.709195	-2.041751	-1.000599
20	1	0	-0.301431	0.190573	-2.342103
21	1	0	-1.400379	2.210465	-0.986180
22	1	0	-2.482190	1.288621	1.238576

Rotational constants (GHZ): 2.3861557 1.2977400 1.2398937

Leave Link 202 at Sun Jul 20 21:01:53 2008, MaxMem= 62914560 cpu: 0.4

(Enter /home/g03/g03_D02/g03/l301.exe)

Standard basis: 6-31+G(d) (6D, 7F)

There are 214 symmetry adapted basis functions of A symmetry.

Integral buffers will be 131072 words long.

Raffenetti 2 integral format.

Two-electron integral symmetry is turned on.

214 basis functions, 368 primitive gaussians, 214 cartesian basis functions

36 alpha electrons 36 beta electrons

Zero-point correction= 0.188422 (Hartree/Particle)

Thermal correction to Energy= 0.196486

Thermal correction to Enthalpy= 0.197430

Thermal correction to Gibbs Free Energy= 0.155752

Sum of electronic and zero-point Energies= -387.998437

Sum of electronic and thermal Energies= -387.990373

Sum of electronic and thermal Enthalpies= -387.989429

Sum of electronic and thermal Free Energies= -388.031107

	E (Thermal)	CV	S
	KCal/Mol	Cal/Mol-Kelvin	Cal/Mol-Kelvin
Total	123.297	33.274	87.719

CpTSmpwpw91

E(RmPW+HF-PW91) = -388.101737516

Standard orientation:

Center	Atomic	Atomic	Coordinates (Angstroms)			
Number	Number	Type	X	Y	Z	

1	6	0	0.758935	0.111237	1.364007	
2	6	0	0.807983	-1.053243	0.556463	
3	6	0	1.887835	-0.799358	-0.491380	
4	6	0	1.942451	0.704860	-0.501085	
5	6	0	1.400574	1.172739	0.666215	
6	1	0	1.705956	-1.265398	-1.464637	
7	1	0	2.844993	-1.199863	-0.114962	
8	6	0	-0.807534	-1.052761	-0.557147	
9	6	0	-1.887807	-0.800062	0.490574	
10	6	0	-1.943156	0.704124	0.501349	
11	6	0	-1.400795	1.173184	-0.665186	
12	6	0	-0.758464	0.112453	-1.363638	
13	1	0	-1.705978	-1.266639	1.463587	
14	1	0	-2.844680	-1.200772	0.113655	
15	1	0	2.481052	1.290165	-1.237988	
16	1	0	1.399970	2.209748	0.988084	

17	1	0	0.301885	0.188470	2.342538
18	1	0	0.709865	-2.042655	0.999002
19	1	0	-0.709195	-2.041751	-1.000599
20	1	0	-0.301431	0.190573	-2.342103
21	1	0	-1.400379	2.210465	-0.986180
22	1	0	-2.482190	1.288621	1.238576

Rotational constants (GHZ): 2.3861557 1.2977400 1.2398937

Leave Link 202 at Fri Jul 18 14:07:24 2008, MaxMem= 62914560 cpu: 0.2

(Enter /home/g03/g03_D02/g03/l301.exe)

Standard basis: 6-31+G(d,p) (6D, 7F)

There are 250 symmetry adapted basis functions of A symmetry.

Integral buffers will be 131072 words long.

Raffenetti 2 integral format.

Two-electron integral symmetry is turned on.

250 basis functions, 404 primitive gaussians, 250 cartesian basis functions

36 alpha electrons 36 beta electrons

Zero-point correction= 0.193766 (Hartree/Particle)

Thermal correction to Energy= 0.201597

Thermal correction to Enthalpy= 0.202542

Thermal correction to Gibbs Free Energy= 0.161267

Sum of electronic and zero-point Energies= -387.909837
 Sum of electronic and thermal Energies= -387.902006
 Sum of electronic and thermal Enthalpies= -387.901062
 Sum of electronic and thermal Free Energies= -387.942336

	E (Thermal)	CV	S
	KCal/Mol	Cal/Mol-Kelvin	Cal/Mol-Kelvin
Total	126.504	32.099	86.870

Positive DRP Path for dimerization of Cyclopentadiene

pt1

E(RB+HF-LYP) = -388.171831798

Standard orientation:

```

-----
Center  Atomic  Atomic      Coordinates (Angstroms)
Number  Number  Type        X      Y      Z
-----
  1      6      0      0.748404  0.089730  1.371580
  2      6      0      0.776623 -1.063170  0.515652
  
```

3	6	0	1.888349	-0.784545	-0.499774
4	6	0	1.920210	0.719998	-0.486156
5	6	0	1.388020	1.159629	0.702855
6	1	0	1.729629	-1.237881	-1.483300
7	1	0	2.840599	-1.180602	-0.107407
8	6	0	-0.757534	-1.041879	-0.549169
9	6	0	-1.883571	-0.817416	0.464509
10	6	0	-1.950850	0.685734	0.499822
11	6	0	-1.400360	1.180031	-0.656037
12	6	0	-0.728646	0.146231	-1.355690
13	1	0	-1.722801	-1.297539	1.435010
14	1	0	-2.823741	-1.222788	0.053046
15	1	0	2.456740	1.325098	-1.208630
16	1	0	1.392311	2.188939	1.048850
17	1	0	0.297101	0.138272	2.354520
18	1	0	0.716958	-2.056620	0.960268
19	1	0	-0.688145	-2.014439	-1.036420
20	1	0	-0.279719	0.235856	-2.336620
21	1	0	-1.415749	2.221811	-0.962231
22	1	0	-2.507050	1.253842	1.237340

Rotational constants (GHZ): 2.3950337 1.3116669 1.2514458

Zero-point correction=	0.188529 (Hartree/Particle)
Thermal correction to Energy=	0.196671
Thermal correction to Enthalpy=	0.197615
Thermal correction to Gibbs Free Energy=	0.153613
Sum of electronic and zero-point Energies=	-387.983303
Sum of electronic and thermal Energies=	-387.975161
Sum of electronic and thermal Enthalpies=	-387.974216
Sum of electronic and thermal Free Energies=	-388.018219

	E (Thermal)	CV	S
	KCal/Mol	Cal/Mol-Kelvin	Cal/Mol-Kelvin
Total	123.413	33.096	92.611

Negative DRP Path for dimerization of Cyclopentadiene

pt1

E(RB+HF-LYP) = -388.171831805

Standard orientation:

Center	Atomic	Atomic	Coordinates (Angstroms)		
Number	Number	Type	X	Y	Z

1	6	0	-0.728646	0.146233	-1.355690
2	6	0	-0.757526	-1.041870	-0.549177
3	6	0	-1.883560	-0.817425	0.464510
4	6	0	-1.950861	0.685725	0.499821
5	6	0	-1.400361	1.180030	-0.656029
6	1	0	-1.722790	-1.297550	1.435010
7	1	0	-2.823730	-1.222800	0.053039
8	6	0	0.776632	-1.063170	0.515644
9	6	0	1.888350	-0.784536	-0.499773
10	6	0	1.920199	0.720008	-0.486157
11	6	0	1.388009	1.159620	0.702862
12	6	0	0.748404	0.089727	1.371580
13	1	0	1.729640	-1.237860	-1.483290
14	1	0	2.840620	-1.180590	-0.107414
15	1	0	-2.507061	1.253820	1.237350
16	1	0	-1.415761	2.221810	-0.962217
17	1	0	-0.279720	0.235869	-2.336610
18	1	0	-0.688131	-2.014440	-1.036440
19	1	0	0.716973	-2.056630	0.960251
20	1	0	0.297102	0.138258	2.354530
21	1	0	1.392299	2.188940	1.048870
22	1	0	2.456719	1.325120	-1.208620

Rotational constants (GHZ): 2.3950391 1.3116695 1.2514495

Zero-point correction= 0.188529 (Hartree/Particle)

Thermal correction to Energy= 0.196671

Thermal correction to Enthalpy= 0.197615

Thermal correction to Gibbs Free Energy= 0.153627

Sum of electronic and zero-point Energies= -387.983302

Sum of electronic and thermal Energies= -387.975161

Sum of electronic and thermal Enthalpies= -387.974216

Sum of electronic and thermal Free Energies= -388.018205

	E (Thermal)	CV	S
	KCal/Mol	Cal/Mol-Kelvin	Cal/Mol-Kelvin
Total	123.413	33.096	92.582

Cycloaddition of Dimethylfulvene with Diazomethane

Dmfulv2+4PD

E(RB+HF-LYP) = -459.483600745

Standard orientation:

Center Number	Atomic Number	Atomic Type	Coordinates (Angstroms)		
			X	Y	Z

1	6	0	-2.483979	0.078621	0.751468
2	6	0	-1.225272	0.431582	1.071310
3	6	0	-0.320425	0.228323	-0.131850
4	6	0	-1.277574	-0.312697	-1.166779
5	6	0	-2.515654	-0.390429	-0.643451
6	6	0	1.018194	-0.538952	0.115197
7	6	0	1.549885	-1.167376	-1.189243
8	6	0	0.933314	-1.612768	1.207428
9	6	0	1.919697	0.655139	0.502387
10	7	0	1.324091	1.837262	-0.169881
11	7	0	0.152156	1.639003	-0.522503
12	1	0	-3.409862	-0.727873	-1.156977
13	1	0	-0.985613	-0.558198	-2.179733
14	1	0	-3.350771	0.132838	1.401881
15	1	0	-0.882563	0.849475	2.010521
16	1	0	2.964467	0.552049	0.190993
17	1	0	1.917024	0.864196	1.581256
18	1	0	1.904260	-2.106301	1.336266
19	1	0	0.637290	-1.192464	2.173704

20	1	0	0.202731	-2.384176	0.939534
21	1	0	2.560902	-1.560079	-1.029057
22	1	0	0.917700	-1.998103	-1.518759
23	1	0	1.601590	-0.433879	-2.001742

Rotational constants (GHZ): 1.7997878 1.0647610 0.9558825

Zero-point correction= 0.194617 (Hartree/Particle)

Thermal correction to Energy= 0.204410

Thermal correction to Enthalpy= 0.205354

Thermal correction to Gibbs Free Energy= 0.160285

Sum of electronic and zero-point Energies= -459.400574

Sum of electronic and thermal Energies= -459.390781

Sum of electronic and thermal Enthalpies= -459.389837

Sum of electronic and thermal Free Energies= -459.434906

	E (Thermal)	CV	S
	KCal/Mol	Cal/Mol-Kelvin	Cal/Mol-Kelvin
Total	128.269	39.466	94.857

Dmfulv2+4ts

E(RB+HF-LYP) = -459.521300446

Standard orientation:

Center	Atomic	Atomic	Coordinates (Angstroms)		
Number	Number	Type	X	Y	Z
1	6	0	1.287057	-0.295065	-1.165342
2	6	0	0.407421	-0.394322	-0.000073
3	6	0	1.287257	-0.295105	1.165117
4	6	0	2.578831	-0.192456	0.723078
5	6	0	2.578691	-0.192323	-0.723494
6	6	0	-0.960927	-0.736305	0.000158
7	6	0	-2.015915	1.162985	-0.001198
8	7	0	-0.952600	1.997757	0.000005
9	7	0	0.191962	2.094307	0.000352
10	1	0	3.461764	-0.109104	1.347596
11	1	0	0.965403	-0.333756	2.198714
12	1	0	3.461496	-0.108769	-1.348169
13	1	0	0.965056	-0.333368	-2.198904
14	6	0	-1.575138	-1.310633	-1.270133
15	6	0	-1.574695	-1.308526	1.271479
16	1	0	-2.603410	1.228891	0.913270
17	1	0	-2.600322	1.228545	-0.917673

18	1	0	-2.670265	-1.281026	-1.235000
19	1	0	-1.247481	-0.782778	-2.169762
20	1	0	-1.283683	-2.363580	-1.381570
21	1	0	-2.669847	-1.280523	1.235999
22	1	0	-1.281713	-2.360741	1.385724
23	1	0	-1.248032	-0.777743	2.169731

Rotational constants (GHZ): 1.5797854 0.9912161 0.8438211

Zero-point correction= 0.189410 (Hartree/Particle)

Thermal correction to Energy= 0.200502

Thermal correction to Enthalpy= 0.201446

Thermal correction to Gibbs Free Energy= 0.153268

Sum of electronic and zero-point Energies= -459.351053

Sum of electronic and thermal Energies= -459.339962

Sum of electronic and thermal Enthalpies= -459.339017

Sum of electronic and thermal Free Energies= -459.387196

	E (Thermal)	CV	S
	KCal/Mol	Cal/Mol-Kelvin	Cal/Mol-Kelvin
Total	125.817	42.270	101.400

dmfulv2+4tsBB

E(RB+HF-LYP) = -459.663091677

Standard orientation:

```

-----
Center  Atomic  Atomic      Coordinates (Angstroms)
Number  Number  Type        X        Y        Z
-----
  1      6      0      1.284843 -0.297264 -1.163500
  2      6      0      0.407704 -0.391455  0.000023
  3      6      0      1.284925 -0.297231  1.163487
  4      6      0      2.577466 -0.194004  0.722101
  5      6      0      2.577411 -0.194006 -0.722218
  6      6      0      -0.966031 -0.722676  0.000058
  7      6      0      -2.004266  1.139585 -0.000335
  8      7      0      -0.954931  1.998940 -0.000042
  9      7      0      0.178504  2.111646  0.000143
 10      1      0      3.457037 -0.113373  1.346743
 11      1      0      0.967767 -0.334071  2.195761
 12      1      0      3.456930 -0.113320 -1.346926
 13      1      0      0.967597 -0.334053 -2.195750
 14      6      0      -1.571179 -1.307608 -1.269275
 15      6      0      -1.571231 -1.307164  1.269571

```

16	1	0	-2.589950	1.201537	0.913625
17	1	0	-2.589373	1.201428	-0.914681
18	1	0	-2.664185	-1.292830	-1.235181
19	1	0	-1.248282	-0.779821	-2.167441
20	1	0	-1.263864	-2.353858	-1.373496
21	1	0	-2.664234	-1.292456	1.235385
22	1	0	-1.263867	-2.353355	1.374228
23	1	0	-1.248441	-0.778996	2.167554

 Rotational constants (GHZ): 1.5818512 0.9945160 0.8458592

Dmfulv6+4PD

E(RB+HF-LYP) = -459.348490621

Standard orientation:

Center	Atomic	Atomic	Coordinates (Angstroms)		
Number	Number	Type	X	Y	Z
1	6	0	-2.497388	0.167526	0.229894
2	6	0	-1.087716	0.599615	0.544748
3	6	0	-0.246521	-0.583787	0.160810

4	6	0	-1.062693	-1.573657	-0.263831
5	6	0	-2.459484	-1.112162	-0.193378
6	6	0	1.231057	-0.359994	0.077620
7	6	0	1.981661	-1.543076	-0.550085
8	6	0	1.833989	-0.038885	1.465959
9	6	0	1.363993	0.891481	-0.841874
10	7	0	0.402803	2.012900	-0.673278
11	7	0	-0.688160	1.907721	-0.096590
12	1	0	-3.316319	-1.725506	-0.453249
13	1	0	-0.759373	-2.543445	-0.644457
14	1	0	-3.367762	0.789658	0.397047
15	1	0	-1.017858	0.819717	1.622587
16	1	0	1.257193	0.601749	-1.896128
17	1	0	2.357095	1.347460	-0.744831
18	1	0	2.911320	0.147411	1.380376
19	1	0	1.379346	0.851148	1.914403
20	1	0	1.686952	-0.877973	2.154792
21	1	0	3.044936	-1.307174	-0.676078
22	1	0	1.909599	-2.431058	0.088697
23	1	0	1.570982	-1.798691	-1.533257

Rotational constants (GHZ): 1.7025712 1.1395238 0.8441474

Zero-point correction= 0.194966 (Hartree/Particle)
 Thermal correction to Energy= 0.204659
 Thermal correction to Enthalpy= 0.205603
 Thermal correction to Gibbs Free Energy= 0.160752
 Sum of electronic and zero-point Energies= -459.396525
 Sum of electronic and thermal Energies= -459.386832
 Sum of electronic and thermal Enthalpies= -459.385888
 Sum of electronic and thermal Free Energies= -459.430739

	E (Thermal)	CV	S
	KCal/Mol	Cal/Mol-Kelvin	Cal/Mol-Kelvin
Total	128.425	39.058	94.397

DmfulvAlkRearTS

E(RB+HF-LYP) = -459.382747095

Standard orientation:

```

-----
Center  Atomic  Atomic      Coordinates (Angstroms)
Number  Number  Type        X          Y          Z
-----
  1      6      0    -0.533198 -0.936412 -0.188078
  
```

2	6	0	-1.621678	-0.979701	0.704634
3	6	0	-2.470714	0.076556	0.354403
4	6	0	-1.972249	0.755649	-0.787419
5	6	0	-0.775651	0.147480	-1.151483
6	1	0	-1.735301	-1.669120	1.530438
7	1	0	-3.374462	0.346811	0.891997
8	1	0	-2.439653	1.594409	-1.287807
9	1	0	-0.233481	0.257104	-2.079789
10	7	0	0.419315	-1.939048	-0.403825
11	7	0	1.621680	-1.729107	-0.209038
12	6	0	1.959160	-0.369717	0.380764
13	1	0	2.910301	-0.102618	-0.091161
14	1	0	2.168081	-0.595241	1.434423
15	6	0	0.936033	0.727562	0.223278
16	6	0	0.331107	1.299715	1.475536
17	6	0	1.377154	1.806865	-0.760946
18	1	0	0.300204	0.578214	2.295158
19	1	0	0.907807	2.178108	1.799897
20	1	0	-0.695876	1.642391	1.285805
21	1	0	0.579552	2.527520	-0.960093
22	1	0	1.722792	1.394617	-1.714102
23	1	0	2.223287	2.356905	-0.318863

Rotational constants (GHZ): 1.6155871 1.2008486 0.9291577

Zero-point correction= 0.192467 (Hartree/Particle)

Thermal correction to Energy= 0.202069

Thermal correction to Enthalpy= 0.203013

Thermal correction to Gibbs Free Energy= 0.158214

Sum of electronic and zero-point Energies= -459.342945

Sum of electronic and thermal Energies= -459.333343

Sum of electronic and thermal Enthalpies= -459.332399

Sum of electronic and thermal Free Energies= -459.377198

	E (Thermal)	CV	S
	KCal/Mol	Cal/Mol-Kelvin	Cal/Mol-Kelvin
Total	126.800	38.732	94.288

DmfulvRearTS

E(RB+HF-LYP) = -459.425005278

Standard orientation:

Center	Atomic	Atomic	Coordinates (Angstroms)		
Number	Number	Type	X	Y	Z

1	6	0	-2.563631	0.124662	0.628623
2	6	0	-1.243477	0.329822	1.019182
3	6	0	-0.368788	-0.420039	0.095559
4	6	0	-1.207452	-1.038613	-0.837087
5	6	0	-2.542290	-0.709228	-0.507161
6	6	0	1.128009	-0.431791	0.154487
7	6	0	1.723520	-1.774414	-0.325473
8	6	0	1.670435	-0.109857	1.564522
9	6	0	1.661169	0.666879	-0.836300
10	7	0	0.811999	1.866955	-0.790637
11	7	0	-0.273693	1.939617	-0.347479
12	1	0	-3.416599	-1.042488	-1.057955
13	1	0	-0.901079	-1.650274	-1.676999
14	1	0	-3.443688	0.532452	1.109808
15	1	0	-0.911935	0.834530	1.917682
16	1	0	1.600659	0.336500	-1.880094
17	1	0	2.695140	0.964772	-0.633722
18	1	0	2.765483	-0.166116	1.576185
19	1	0	1.385652	0.893828	1.896220
20	1	0	1.287906	-0.826548	2.297650
21	1	0	2.818629	-1.723903	-0.367585

22	1	0	1.448977	-2.575428	0.367146
23	1	0	1.357744	-2.047866	-1.319638

Rotational constants (GHZ): 1.7115893 1.0424683 0.8846037

Zero-point correction= 0.192282 (Hartree/Particle)

Thermal correction to Energy= 0.202134

Thermal correction to Enthalpy= 0.203078

Thermal correction to Gibbs Free Energy= 0.157865

Sum of electronic and zero-point Energies= -459.367237

Sum of electronic and thermal Energies= -459.357385

Sum of electronic and thermal Enthalpies= -459.356441

Sum of electronic and thermal Free Energies= -459.401654

	E (Thermal)	CV	S
	KCal/Mol	Cal/Mol-Kelvin	Cal/Mol-Kelvin
Total	126.841	39.528	95.159

Quadricyclane Cycloaddition**QuaddmadB3P**

E(RB+HF-LYP) = -837.821329555

Standard orientation:

Center	Atomic	Atomic	Coordinates (Angstroms)			
Number	Number	Type	X	Y	Z	

1	8	0	1.889882	-1.342765	-1.448027	
2	8	0	2.390120	-1.790726	0.718937	
3	8	0	-2.805187	-0.123479	-0.684132	
4	8	0	-2.119962	-2.028435	0.332009	
5	6	0	3.699859	-2.195498	0.299770	
6	6	0	1.561321	-1.391964	-0.274756	
7	7	0	0.300362	-1.117497	0.308616	
8	7	0	-0.536908	-0.652817	-0.566199	
9	6	0	-0.506238	3.168327	-0.457359	
10	6	0	-1.100300	2.084443	0.326014	
11	6	0	-0.232080	1.880842	1.573571	

12	6	0	0.969663	3.140888	-0.184644
13	6	0	1.128990	2.140974	0.938745
14	6	0	-3.497939	-2.411892	0.478624
15	6	0	-0.353407	1.372542	-0.821349
16	6	0	-1.910099	-0.851650	-0.286351
17	6	0	1.115966	1.641582	-0.491354
18	1	0	3.637509	-3.027743	-0.407375
19	1	0	4.212941	-2.504130	1.211687
20	1	0	4.228776	-1.363592	-0.175933
21	1	0	1.947441	1.177913	-1.003197
22	1	0	-0.483421	2.608310	2.354262
23	1	0	-1.003341	3.738685	-1.232044
24	1	0	-2.176506	1.946708	0.343607
25	1	0	-0.308910	0.866681	1.976141
26	1	0	-4.039054	-1.677939	1.081984
27	1	0	1.676918	3.913868	-0.459071
28	1	0	-3.976124	-2.498544	-0.500992
29	1	0	2.052851	2.102316	1.505266
30	1	0	-0.736041	1.300661	-1.828199
31	1	0	-3.470457	-3.379305	0.981179

Rotational constants (GHZ): 0.5058786 0.4819191 0.2859342

Zero-point correction=	0.243641 (Hartree/Particle)
Thermal correction to Energy=	0.259776
Thermal correction to Enthalpy=	0.260720
Thermal correction to Gibbs Free Energy=	0.198383
Sum of electronic and zero-point Energies=	-837.577802
Sum of electronic and thermal Energies=	-837.561667
Sum of electronic and thermal Enthalpies=	-837.560723
Sum of electronic and thermal Free Energies=	-837.623060

	E (Thermal)	CV	S
	KCal/Mol	Cal/Mol-Kelvin	Cal/Mol-Kelvin
Total	163.012	59.417	131.199

Quaddmad3wB3P

E(UB+HF-LYP) = -1067.13555055

Standard orientation:

Center	Atomic	Atomic	Coordinates (Angstroms)		
Number	Number	Type	X	Y	Z

1	6	0	-3.625794	-1.967911	-1.365911
2	8	0	-2.216022	-1.738116	-1.516750
3	6	0	-1.547502	-1.382829	-0.406667
4	8	0	-2.100808	-1.251350	0.689652
5	7	0	-0.187089	-1.277780	-0.708303
6	7	0	0.486270	-0.803693	0.301411
7	6	0	1.868608	-1.124379	0.316816
8	8	0	2.651174	-0.597681	1.095703
9	8	0	2.205207	-2.129741	-0.503302
10	6	0	3.561516	-2.600940	-0.391505
11	1	0	4.266370	-1.803880	-0.642175
12	1	0	3.758287	-2.952007	0.624841
13	1	0	3.635401	-3.421253	-1.105853
14	1	0	-3.812541	-2.725331	-0.599905
15	1	0	-3.964484	-2.316041	-2.342117
16	1	0	-4.139818	-1.040796	-1.094393
17	6	0	1.091082	2.921668	-0.540599
18	6	0	1.703643	1.640550	-0.905915
19	6	0	1.183978	1.247546	-2.294144
20	6	0	-0.238343	1.780341	-2.152999
21	6	0	-0.217554	2.993983	-1.256827

22	6	0	-0.689392	1.608432	-0.720066
23	6	0	0.570208	1.327626	0.085921
24	1	0	0.660142	1.427533	1.162379
25	1	0	-1.697960	1.435174	-0.363660
26	1	0	-0.857502	3.864080	-1.328273
27	1	0	-0.969351	1.708304	-2.950577
28	1	0	1.747420	1.751130	-3.088340
29	1	0	1.199398	0.166471	-2.457805
30	1	0	2.711276	1.410698	-0.570958
31	1	0	1.449822	3.604576	0.219224
32	1	0	0.505320	0.694166	3.298131
33	8	0	1.363338	1.146884	3.166137
34	1	0	1.918224	0.498564	2.695603
35	1	0	-1.572604	-0.639867	3.809111
36	8	0	-1.247049	-0.054317	3.109291
37	1	0	-1.287747	-0.578171	2.276740
38	1	0	-2.755829	1.272114	2.202093
39	8	0	-3.348265	1.274974	1.428319
40	1	0	-3.311391	0.345107	1.143165

Rotational constants (GHZ): 0.3327265 0.2711215 0.2523038

Zero-point correction=	0.318685 (Hartree/Particle)
Thermal correction to Energy=	0.343469
Thermal correction to Enthalpy=	0.344414
Thermal correction to Gibbs Free Energy=	0.263230
Sum of electronic and zero-point Energies=	-1066.816921
Sum of electronic and thermal Energies=	-1066.792136
Sum of electronic and thermal Enthalpies=	-1066.791192
Sum of electronic and thermal Free Energies=	-1066.872376

	E (Thermal)	CV	S
	KCal/Mol	Cal/Mol-Kelvin	Cal/Mol-Kelvin
Total	215.530	87.889	170.866

QuadricyclaneB3P

E(RB+HF-LYP) = -271.452918254

Standard orientation:

Center	Atomic	Atomic	Coordinates (Angstroms)		
Number	Number	Type	X	Y	Z

1	6	0	1.153429	0.551569	-0.000026
2	6	0	0.775580	-0.710581	-0.758767
3	6	0	-0.775537	-0.710567	-0.758799
4	6	0	-1.153465	0.551511	0.000025
5	6	0	-0.775541	-0.710621	0.758763
6	6	0	0.775577	-0.710525	0.758804
7	1	0	1.427461	-1.233050	1.450688
8	1	0	-1.427394	-1.233254	1.450593
9	6	0	-0.000041	1.541502	0.000000
10	1	0	-0.000072	2.181038	-0.892532
11	1	0	-0.000044	2.181038	0.892531
12	1	0	-2.189916	0.878344	0.000046
13	1	0	-1.427390	-1.233145	-1.450671
14	1	0	1.427466	-1.233161	-1.450607
15	1	0	2.189862	0.878464	-0.000047

 Rotational constants (GHZ): 4.3932549 4.3414651 3.2397641

Zero-point correction= 0.128321 (Hartree/Particle)

Thermal correction to Energy= 0.132926

Thermal correction to Enthalpy= 0.133870

Thermal correction to Gibbs Free Energy= 0.100435

Sum of electronic and zero-point Energies= -271.324598
 Sum of electronic and thermal Energies= -271.319993
 Sum of electronic and thermal Enthalpies= -271.319048
 Sum of electronic and thermal Free Energies= -271.352484

	E (Thermal)	CV	S
	KCal/Mol	Cal/Mol-Kelvin	Cal/Mol-Kelvin
Total	83.412	20.090	70.370

QuadricyclaneCationRadB3P

E(UB+HF-LYP) = -271.146807536

Standard orientation:

```

-----
Center  Atomic  Atomic      Coordinates (Angstroms)
Number  Number  Type        X      Y      Z
-----
  1      6      0      1.157191  0.514568 -0.000002
  2      6      0      0.741141 -0.660301 -0.841045
  3      6      0     -0.741145 -0.660290 -0.841049
  4      6      0     -1.157188  0.514575  0.000002
  
```

5	6	0	-0.741145	-0.660297	0.841045
6	6	0	0.741141	-0.660293	0.841050
7	1	0	1.388403	-1.339605	1.383222
8	1	0	-1.388409	-1.339612	1.383209
9	6	0	0.000004	1.518827	-0.000001
10	1	0	0.000005	2.150237	-0.893398
11	1	0	0.000006	2.150237	0.893397
12	1	0	-2.202256	0.808617	0.000007
13	1	0	-1.388410	-1.339599	-1.383220
14	1	0	1.388402	-1.339620	-1.383208
15	1	0	2.202260	0.808605	-0.000007

 Rotational constants (GHZ): 4.3526681 4.2352761 3.3944555

Zero-point correction= 0.127764 (Hartree/Particle)

Thermal correction to Energy= 0.132734

Thermal correction to Enthalpy= 0.133678

Thermal correction to Gibbs Free Energy= 0.099049

Sum of electronic and zero-point Energies= -271.050604

Sum of electronic and thermal Energies= -271.045634

Sum of electronic and thermal Enthalpies= -271.044690

Sum of electronic and thermal Free Energies= -271.079320

	E (Thermal)	CV	S
	KCal/Mol	Cal/Mol-Kelvin	Cal/Mol-Kelvin
Total	83.292	21.538	72.884

Quadtsb1b95

E(RB+HF-B95) = -837.507664271

Standard orientation:

Center	Atomic	Atomic	Coordinates (Angstroms)			
Number	Number	Type	X	Y	Z	

1	8	0	2.225951	-0.640013	-1.424155	
2	8	0	2.814887	-1.042461	0.712837	
3	8	0	-2.561395	-0.931091	-0.864687	
4	8	0	-1.426670	-2.403253	0.404356	
5	6	0	4.167686	-1.069550	0.277829	
6	6	0	1.917755	-0.827501	-0.264006	
7	7	0	0.635252	-0.892313	0.305133	
8	7	0	-0.272216	-0.728150	-0.600647	

9	6	0	-1.313743	2.826960	-0.522521
10	6	0	-1.717623	1.605180	0.147387
11	6	0	-1.023560	1.552035	1.495994
12	6	0	0.024612	3.197263	0.004820
13	6	0	0.280639	2.206504	1.097431
14	6	0	-2.636231	-3.144687	0.539672
15	6	0	-0.645342	1.198063	-0.876522
16	6	0	-1.526514	-1.303203	-0.347016
17	6	0	0.617616	1.822154	-0.315429
18	1	0	4.314005	-1.843405	-0.476977
19	1	0	4.758865	-1.284056	1.165113
20	1	0	4.456356	-0.107637	-0.149941
21	1	0	1.606881	1.646279	-0.705154
22	1	0	-1.571282	2.122467	2.249546
23	1	0	-1.818302	3.283465	-1.361478
24	1	0	-2.697171	1.175616	-0.020985
25	1	0	-0.869476	0.528457	1.842077
26	1	0	-3.402845	-2.543657	1.029866
27	1	0	0.524348	4.143510	-0.135490
28	1	0	-3.002966	-3.458831	-0.438031
29	1	0	1.086855	2.370417	1.798294
30	1	0	-0.841152	1.073709	-1.929625

31 1 0 -2.379322 -4.007864 1.148731

 Rotational constants (GHZ): 0.5420095 0.4831241 0.2994825

Zero-point correction= 0.246582 (Hartree/Particle)

Thermal correction to Energy= 0.262279

Thermal correction to Enthalpy= 0.263223

Thermal correction to Gibbs Free Energy= 0.202841

Sum of electronic and zero-point Energies= -837.270336

Sum of electronic and thermal Energies= -837.254639

Sum of electronic and thermal Enthalpies= -837.253695

Sum of electronic and thermal Free Energies= -837.314078

	E (Thermal)	CV	S
	KCal/Mol	Cal/Mol-Kelvin	Cal/Mol-Kelvin
Total	164.583	58.439	127.086

QuadtsRmPWPW91

E(RmPW+HF-PW91) = -837.567287452

Standard orientation:

Center	Atomic	Atomic	Coordinates (Angstroms)			
Number	Number	Type	X	Y	Z	

1	8	0	1.904540	-1.230202	-1.425320	
2	8	0	2.435769	-1.645096	0.706365	
3	8	0	-2.764618	-0.212016	-0.686799	
4	8	0	-2.001669	-2.049649	0.326041	
5	6	0	3.727865	-2.011975	0.271263	
6	6	0	1.594530	-1.279466	-0.260315	
7	7	0	0.349324	-1.025654	0.322717	
8	7	0	-0.497699	-0.626492	-0.549701	
9	6	0	-0.666828	3.027628	-0.427303	
10	6	0	-1.168737	1.949152	0.388588	
11	6	0	-0.244493	1.771427	1.574496	
12	6	0	0.802669	3.114727	-0.193345	
13	6	0	1.056224	2.119993	0.894407	
14	6	0	-3.341884	-2.486758	0.464796	

15	6	0	-0.428250	1.321452	-0.810793
16	6	0	-1.847781	-0.886998	-0.286430
17	6	0	1.023317	1.650102	-0.530052
18	1	0	3.677299	-2.840421	-0.430068
19	1	0	4.268085	-2.305206	1.163820
20	1	0	4.225135	-1.175534	-0.213727
21	1	0	1.853046	1.232319	-1.070663
22	1	0	-0.501191	2.462625	2.375693
23	1	0	-1.232931	3.579779	-1.157284
24	1	0	-2.226110	1.739699	0.431007
25	1	0	-0.240316	0.751035	1.949293
26	1	0	-3.916600	-1.779276	1.055410
27	1	0	1.438755	3.937265	-0.469327
28	1	0	-3.809233	-2.598546	-0.509324
29	1	0	1.997825	2.126167	1.418181
30	1	0	-0.844132	1.238320	-1.798077
31	1	0	-3.282970	-3.443187	0.969779

 Rotational constants (GHZ): 0.5350779 0.4951651 0.2989505

Zero-point correction= 0.252296 (Hartree/Particle)

Thermal correction to Energy= 0.267835

Thermal correction to Enthalpy=	0.268779
Thermal correction to Gibbs Free Energy=	0.207905
Sum of electronic and zero-point Energies=	-837.322616
Sum of electronic and thermal Energies=	-837.307078
Sum of electronic and thermal Enthalpies=	-837.306134
Sum of electronic and thermal Free Energies=	-837.367007

	E (Thermal)	CV	S
	KCal/Mol	Cal/Mol-Kelvin	Cal/Mol-Kelvin
Total	168.069	57.025	128.119

Listing of Dynamics Programs

1. Program progdynstarterHP

```
#!/bin/bash
```

```
# This is the master control program for dynamics, in the form of a Unix Shell Script.
```

```
#
```

```
# Necessary input files:
```


freqinHP - This is the standard output from a Gaussian 98 or 03 frequency calculation using freq=hpmodes.

progdyn.conf - This is a file giving a variety of configuration options, called on by many of the subprograms.

#

Optional input:

isomernumber - A number in file isomernumber provides a start for numbering runs.

detour - A signal file that, by existing, signals the program to do a side calculations

nogo - A signal file that, by existing, signals the program to stop between points

#

Programs called:

proggenHP - An awk program that starts a trajectory, giving each mode its zero point energy (if a quasiclassical calculation) plus random additional excitations depending on the temperature.

prog1stpoint - Awk program that creates the first Gaussian input file for each run

prog2ndpoint - Awk program that creates the second Gaussian input file for each run

progdynb - Creates subsequent Gaussian input files until run is completed, used the awk

proganal - A program to analyze the latest point and see if a run is done. This program must be redone for each new system. Elaborate changes are often programmed into proganal, such as the automatic changing of configuration variables.

```
# randgen – A program that generates random numbers between 0 and 1. These are
generated all at once and stored in a file for use by proggenHP.

#

# Output files

# isomernumber – A running tab of the run number

# geoRecord – A record of all the starting positions and velocities.

# geoPlusVel – Created by proggen, this gives starting position and velocities for current
run.

# g03.com – Created by prog1stpoint, prog2ndpoint, and progdynb, this is the latest
input

#   file for Gaussian03 for current run and latest point.

# olddynrun and olderdynrun – files containing the last two outputs from Gaussian, for
creation

# of the next point

# dyn - A record of all of the Gaussian outputs.

# dynfollowfile – A short record of the runs and their results.

# skipstart - A signal file that, by existing, tells progdynstarterHP that we are in the
middle of a run.

# diagnostics – optional output that follows which subprograms are running and
configuration variables, decided by variable in progdyn.conf

# vellist – optional output that list the velocities of each atom, decided by variable in
progdyn.conf
```

A number of files starting with 'temp' are created then later erased.

#progdynstarterHP, made to use high=precision modes from Gaussian freq output

#updated to create a random number file temp811 that is used by proggenHP

#version September 16, 2005, made for workstations

#version August 2007 to allow periodic copying of g03.log to dyn putting it under control of progdynb

#version Feb 2008 moves variables like the scratch directory and location of randgen to the beginning

#version March 2008 added proganal reporting to points 1 and 2

OUTLINE

A. initialize to perform Gaussian jobs and know where we are

start loop

B. if no file named "skipstart" then generate a new isomer. Get rid of skipstart to start new isomer.

#

AA

#origdir, randdir, scratchdir, g03root, logfile, randdir all may need varied from system to system and assigned here or by program calling this one

export g03root=/usr/local/g03

source \$g03root/g03/bsd/g03.profile

```
origdir=`pwd`
cd $origdir
logfile=docslog
randdir=~/.bin
scratchdir=$TMPDIR

rm -f nogo # assume that if someone is starting a job, they want it to go.
rm -f diagnostics # contains extra info from start of progFS

while (true)
do
#BBBBBBBBBBBBBBBBBBBBBBBBBBBBBBBBBBBBBBBBBBBBBBBBBBBBBBBBBBBB
if (test -f skipstart) then
    echo "skipping start and continuing from previous runs"
else
# change from older versions - freqin and most other files are in origdir. Advantage is
compartmentalization.
# Also allows separate configurations for separate runs, so we can move to using config
files.
# Disadvantage is multiple copies of files.

    cd $origdir

    echo 3 > runpointnumber
```

```

$randdir/randgen > temp811

# lets keep the next 8 lines as the only difference between progdynstarter and
progdynstarterHP

awk '/      1      2      3      4/,/Harmonic frequencies/ {print}' freqinHP >
temp401

awk '/Frequencies --/ {print $3;print $4;print $5;print $6;print $7}' temp401 >
tempfreqs

awk '/Reduced masses/ {print $4;print $5;print $6;print $7;print $8}' temp401 >
tempredmass

awk '/Force constants/ {print $4;print $5;print $6;print $7;print $8}' temp401 >
tempfrc

awk '/0/ && ((length($1) < 2) && ($1 < 4)) {print}' temp401 > tempmodes

awk '/has atomic number/ {print}' freqinHP > tempmasses

awk '/Standard orientation:./,/tional const/ {if ($3==0) print}' freqinHP > tempstangeos

awk -f proggenHP freqinHP > geoPlusVel

if (test -f isomernumber) then

    cp isomernumber temp533

    awk 'BEGIN {getline;i=$1+1;print i}' temp533 > isomernumber

    rm temp533

else

    echo 1 > isomernumber

fi

```

```

rm g03.com

awk -f prog1stpoint geoPlusVel > g03.com

# TO DO - put error checking in prog1stpoint, prog2ndpoint, and progdynb so no
g03.com unless things are ok

if (test -s g03.com) then

    rm tempfreqs tempredmass tempfrc tempmodes tempstangeos tempmasses temp401
temp811

    cat isomernumber >> geoRecord

    cat geoPlusVel >> geoRecord

    cat g03.com

    rm -f goingwell

    cd $scratchdir

    $g03root/g03/g03 $origdir/g03.com > $origdir/g03.log

    cd $origdir

    grep 'Normal termination' g03.log > goingwell

    if (test -s goingwell) then

        cat g03.log >> dyn

        awk -f proganal g03.log >> dynfollowfile

        cp g03.log olderdynrun

    else

        break

    fi

```

```
else
    break
fi
rm g03.com
awk -f prog2ndpoint g03.log > g03.com
if (test -s g03.com) then
    rm -f goingwell
    cd $scratchdir
    $g03root/g03/g03 $origdir/g03.com > $origdir/g03.log
    cd $origdir
    grep 'Normal termination' g03.log > goingwell
    if (test -s goingwell) then
        cp g03.log olddynrun
        cat g03.log >> dyn
        awk -f proganal g03.log >> dynfollowfile
# old program progdyn replaced here with commands from progdyn
    awk '/Input orientation/,/Distance matrix/ {print}' olddynrun > temp101
    awk '/ 0 / {print}' temp101 > old
    awk '/Input orientation/,/Distance matrix/ {print}' olderdynrun > temp102
    awk '/ 0 / {print}' temp102 > older
    awk -f progdynb olddynrun > g03.com
    rm -f temp101 temp102 old older tempchk
```

```
    else
        break
    fi
else
    break
fi

# we've just completed a start, so lets skipstart until instructed otherwise
    echo "skipping start" > skipstart
fi

while (true)
do
#increment runpointnumber
    if (test -f runpointnumber) then
        cp runpointnumber temp533
        awk 'BEGIN {getline;i=$1+1;print i}' temp533 > runpointnumber
        rm temp533
    else
        echo 4 > runpointnumber
    fi
# this loop always starts with a g03.com in place - because of the loss of former program
progdyn, I
```



```

# may have to worry about how each it is to restart from a bad run

rm -f goingwell

cd $scratchdir

$g03root/g03/g03 $origdir/g03.com > $origdir/g03.log

cd $origdir

grep 'Normal termination' g03.log > goingwell

if (test -s goingwell) then

    cp olddynrun olderdynrun

    cp g03.log olddynrun

# old program progdyn replaced here too

    awk '/Input orientation/,/Distance matrix/ {print}' olddynrun > temp101

    awk '/ 0 / {print}' temp101 > old

    awk '/Input orientation/,/Distance matrix/ {print}' olderdynrun > temp102

    awk '/ 0 / {print}' temp102 > older

    awk -f progdynb olddynrun > g03.com

    rm -f temp101 temp102 old older tempchk

# line removed to move the command under control of progdynb    cat g03.log >> dyn

else

    break

fi

# here is a cool link that lets you interrupt the dynamics with a short job, then

```

```
# it automatically goes back to the dynamics just make the file 'detour' and it
```

```
# will delete detour, run run.com, then go back to dynamics
```

```
if (test -f detour) then
```

```
    rm detour
```

```
    date >> $logfile
```

```
    cat run.com >> $logfile
```

```
    cp run.log temp.log
```

```
    cd $scratchdir
```

```
    $g03root/g03/g03 $origdir/run.com > $origdir/run.log
```

```
    cd $origdir
```

```
fi
```

```
#stop it all nicely by creating a nogo file
```

```
if (test -f nogo) then
```

```
    break
```

```
fi
```

```
#figure out if this isomer is done
```

```
awk -f proganal g03.log >> dynfollowfile
```

```
rm -f tempdone
```

```
awk -f proganal g03.log > temp281
```

```
awk '/XXXX/ {print}' temp281 > tempdone
```

```
rm temp281

if (test -s tempdone) then

    rm -f skipstart

    rm -f olddynrun

    rm -f olderdynrun

    rm -f geoPlusVel

    break

fi

done

# We've got to break a second time to get out of this loop

# if we really want to quit. Otherwise, it will start over

# at the top

if (test -f nogo) then

    break

fi

if (test -s goingwell) then

    echo "probably starting a new point"

else

    break

fi

done
```

exit 0

2. Program proggenHP

```
BEGIN {  
# updated June 2008 to incorporate new method for choosing displacements with  
initialdis 2  
# updated Jan 17 2008 - bug fix for > 99 atoms, 300 excitations of low modes possible  
# version August 2007 - incorporates classical trajectory calculation option  
#also allows listing of number of imaginary frequencies  
# version Sept 16, 2005 - incorporates searchdir but not yet rotation  
# now reads random numbers from temp811, starting at a random place  
# The input files are generated before this and are tempfreqs, tempredmass,  
# tempfrfc, tempmodes, and tempstangeos.  
# It will count the number of atoms.  
  
# Gets from progdyn.conf  
# timestep, scaling, temp, and initialdis.  
# default values  
initialDis=0  
timeStep=1E-15  
scaling=1.0
```

```
temp=298.15

#default is quassiclassical

classical=0

#default is starting from transition state

numimag=1

# read progdyn.conf for configuration info

blankLineTester=10

while (blankLineTester>1) {
  getline < "progdyn.conf"
  if ($1=="method") method=$2
  if ($1=="charge") charge=$2
  if ($1=="multiplicity") multiplicity=$2
  if ($1=="memory") memory=$2
  if ($1=="processors") processors=$2
  if ($1=="checkpoint") checkpoint=$2
  if ($1=="diagnostics") diag=$2
  if ($1=="initialdis") initialDis=$2
  if ($1=="timestep") timeStep=$2
  if ($1=="scaling") scaling=$2
  if ($1=="temperature") temp=$2
  if ($1=="searchdir") searchdir=$2
```

```

if ($1=="classical") classical=$2
if ($1=="numimag") numimag=$2
if ($1=="highlevel") highlevel=$2
if ($1=="title") {
    title1=$2
    title2=$3
    title3=$4
    title4=$5
}
blankLineTester=length($0)
}

```

```

if (diag==1) print "***** starting proggen *****" >>
"diagnostics"
if (diag==1) print "method,charge,multiplicity,memory" >> "diagnostics"
if (diag==1) print method,charge,multiplicity,memory >> "diagnostics"
if (diag==1) print "processors,checkpoint,title,initialdis,timestep,scaling,temperature" >>
"diagnostics"
if (diag==1) print
processors,checkpoint,title1,title2,title3,title4,initialDis,timeStep,scaling,temp >>
"diagnostics"

```

```
i=1;j=1;k=1
```

```
c=29980000000
```

```
h=6.626075E-34
```

```
avNum=6.02E23
```

```
numAtoms=0
```

```
# put geometries into array, also figure out number of atoms
```

```
# note that this picks out the last geometry in a file, assuming
```

```
# that if there is an optimization followed by a freq, nothing else follows
```

```
# kludgy - repeats last line twice - must be a better way
```

```
do {
```

```
  getline < "tempstangeos"
```

```
  if (oldline==$0) $0=""
```

```
  oldline=$0
```

```
  atom = $1
```

```
  if (atom>numAtoms) numAtoms=atom
```

```
  atNum[atom]=$2
```

```
  geoArr[atom,1]=$4
```

```
  geoArr[atom,2]=$5
```

```
  geoArr[atom,3]=$6
```

```
  velArr[atom,1]=0
```

```
  velArr[atom,2]=0
```

```
    velArr[atom,3]=0
  }
while (length($0) > 0)

#output the number of atoms - this will help in reading the file later
print numAtoms

# put in atomic symbols and atomic weights - this will have to be edited for isotopic
labeling
for (i=1;i<=numAtoms;i++) {
  getline < "tempmasses"
  if (i<100) atWeight[i]=$9
  if (i>99) atWeight[i]=$8
  if (atNum[i]==1) atSym[i]="H"
  if (atNum[i]==5) atSym[i]="B"
  if (atNum[i]==6) atSym[i]="C"
  if (atNum[i]==7) atSym[i]="N"
  if (atNum[i]==8) atSym[i]="O"
  if (atNum[i]==9) atSym[i]="F"
  if (atNum[i]==13) atSym[i]="Al"
  if (atNum[i]==17) atSym[i]="Cl"
```



```
# print atNum[i],atSym[i],atWeight[i],geoArr[i,1],geoArr[i,2],geoArr[i,3]
}

# read in frequencies, scale them, read in Reduced masses, read in force
#constants, replace negative frequencies by 8 wavenumbers
numFreq=3*numAtoms-6
for (i=1;i<=numFreq;i++) {
  getline < "tempfreqs"
  freq[i]=$0*scaling
  if (freq[i]<0) freq[i]=8
}
for (i=1;i<=numFreq;i++) {
  getline < "tempredmass"
  redMass[i]=$0
}
for (i=1;i<=numFreq;i++) {
  getline < "tempfrfc"
  frc[i]=$0
  if (frc[i]==0) frc[i]=0.0001
# print freq[i],redMass[i],frc[i]
}
```

```
# read in the modes

#the next 10 lines are commented for low precision modes, uncommented for high
precision modes

for (i=1;i<=numFreq;i+=5) {
  for (j=1;j<=(3*numAtoms);j++) {
    getline < "tempmodes"
    mode[i,$2,$1]=$4
    mode[i+1,$2,$1]=$5
    mode[i+2,$2,$1]=$6
    mode[i+3,$2,$1]=$7
    mode[i+4,$2,$1]=$8
  }
}

#the next 14 lines are uncommented for low precision modes, commented for high
precision modes

#for (i=1;i<=numFreq;i+=3) {
# for (j=1;j<=numAtoms;j++) {
#   getline < "tempmodes"
#   mode[i,j,1]=$3
#   mode[i,j,2]=$4
#   mode[i,j,3]=$5
#   mode[i+1,j,1]=$6
```

```

# mode[i+1,j,2]=$7
# mode[i+1,j,3]=$8
# mode[i+2,j,1]=$9
# mode[i+2,j,2]=$10
# mode[i+2,j,3]=$11
# }
# }
for (i=1;i<=numFreq;i++) {
# print mode[i,1,1],mode[i,1,2],mode[i,1,3]
}

#convert freqs to units used in spreadsheat, pick a random number,
#and decide vibrational quantum state and energy
srand()
# want to read from temp811, starting at a random place
tester=rand()*1000
for (i=1;i<=tester;i++) {
  getline < "temp811"
}
for (i=1;i<=numFreq;i++) {
  getline < "temp811"
  randArr[i]=$1
}

```

```

getline < "temp811"

randArrB[i]=$1

getline < "temp811"

randArrC[i]=$1

}

# for a QM distribution for a harmonic oscillator in its ground state, we want to generate
a set of random numbers

#between -2 and 2 weighted such that numbers toward the center are properly more
common

i=1

while (i<=numFreq) {

  getline < "temp811"

  tempNum=2*($1-.5)

  prob=exp(-(tempNum^2))

  getline < "temp811"

  if ($1<prob) {

    randArrD[i]=tempNum

    i++

  }

}

for (i=1;i<=numFreq;i++) {

```

```

zpeJ[i]=0.5*h*c*freq[i]
zpeK[i]=zpeJ[i]*avNum*0.239/1000
#program so that if the temp is too low, it just acts like 0 K
if (temp<10) {
    vibN[i]=0
}
if (temp>=10) {
    zpeRat[i]=exp((-2*zpeK[i])/(0.001987*temp))
#if classical, treat as modes spaced by 10 wavenumbers
if (classical==1) {
    Espace=0.5*h*c*10*avNum*0.239/1000
    zpeRat[i]=exp((-2*Espace)/(0.001987*temp))
}
Q[i]=1/(1-zpeRat[i])
newRand=randArr[i]
# print newRand
vibN[i]=0
tester=1/Q[i]
# 2008 updated line below to get up to 300 excitations of low modes
for (j=1;j<=(300*zpeRat[i]+2);j++) {
    if (newRand>tester) vibN[i]++
    tester=tester+((zpeRat[i]^j)/Q[i])
}

```

```

    }
  }
}

```

figure out mode energies and maximum classical shift and then

actual shift

```
for (i=1;i<=numFreq;i++) {
```

```
  modeEn[i]=(zpeJ[i]*1E18)*(2*vibN[i]+1)
```

```
  if (classical==1) modeEn[i]=(0.5*h*c*10*1E18)*(2*vibN[i])
```

no 1/2 hv for imaginary frequencies

treating modes with frequencies <10 as translations, ignoring their zero point energies

```
  if (freq[i]<10) modeEn[i]=(zpeJ[i]*1E18)*(2*vibN[i])
```

```
  maxShift[i]=(2*modeEn[i]/frc[i])^0.5
```

```
  if (initialDis==2) shift[i]=maxShift[i]*randArrD[i]
```

```
  if (initialDis==1) shift[i]=maxShift[i]*(2*(randArrC[i]-0.5))
```

```
  if (initialDis==0) shift[i]=0
```

no displacements along imaginary frequencies and very low ones - it is better to treat these

as translations - employing a shift can give you initial weird geometries

```
  if (freq[i]<10) shift[i]=0
```

```
  if (numimag==1) shift[1]=0
```

```
  if (numimag==2) shift[2]=0
```

```

    }
for (i=1;i<=numFreq;i++) {
# print zpeJ[i],zpeK[i],zpeRat[i],Q[i],vibN[i],modeEn[i],maxShift[i],shift[i]
    }

# multiply each of the modes by its shift and add them up
for (i=1;i<=numFreq;i++) {
    for (j=1;j<=numAtoms;j++) {
        for (k=1;k<=3;k++) {
            shiftMode[i,j,k]=mode[i,j,k]*shift[i]
            geoArr[j,k]=geoArr[j,k]+shiftMode[i,j,k]
        }
    }
}

#output the new geometry.
for (j=1;j<=numAtoms;j++) {
    print atSym[j],geoArr[j,1],geoArr[j,2],geoArr[j,3],atWeight[j]
}

#now start toward velocities
for (i=1;i<=numFreq;i++) {

```

```

kinEn[i]=100000*(modeEn[i]-0.5*frc[i]*shift[i]^2)

vel[i]=(2*kinEn[i]/(redMass[i]/avNum))^0.5

#it is tricky here to set the velocities for modes along reaction coordinate
#I think I would like to have them all going the same direction, but setting
#the right direction is difficult. I guess the thing to do is pick one direction
#and go with it, and if there is a problem the program will have to be changed here.
#use searchdir in progdyn.conf to change directions
#fixed this with numimag to allow for ground state dynamics and systems with two
imaginary frequencies
#when two, only the lowest one is sent in the searchdir direction, other is sent in random
direction

if (numimag>1) numimag=1

if (i>numimag) {
    if (randArrB[i]<0.5) vel[i]=-vel[i]
}

if (i==numimag) {
    if (searchdir=="negative") vel[i]=-vel[i]
}

# print vel[i]

}

# multiply each of the modes by its velocity and add them up

```



```

for (i=1;i<=numFreq;i++) {
  for (j=1;j<=numAtoms;j++) {
    for (k=1;k<=3;k++) {
      velMode[i,j,k]=mode[i,j,k]*vel[i]*timeStep
      velArr[j,k]=velArr[j,k]+velMode[i,j,k]
    }
  }
}

#output the velocities. The markers let a later program grab these velocities.
for (j=1;j<=numAtoms;j++) {
  print velArr[j,1],velArr[j,2],velArr[j,3]
}

#anything else I add to the file is not going to be read but will be useful
#for error checking
for (i=1;i<=numFreq;i++) {
  if (initialDis<1.5) print randArr[i],vibN[i],vel[i]
  if (initialDis==2) print randArr[i],randArrD[i],vibN[i],vel[i]
}

print "temp ",temp
print "initialDis",initialDis

```

```
print "timeStep",timeStep  
print "numimag",numimag  
  
}
```

3. Program prog1stpoint

```
BEGIN {  
# version Feb 2008 incorporates methodfile, boxon and boxsize, though this point  
unaffected by box  
# version Jan 2008 - allows for ONIOM jobs, fixed atoms  
# version Sept 2005 - incorportates meth3, meth4, meth5, meth6, but not yet rotation  
# this program creates the first input file for g03  
# the title should be changed as appropriate  
# the isomer number comes from a file isomernumber  
  
#initialization  
atomnumber=0  
  
# read progdyn.conf for configuration info  
blankLineTester=10  
while (blankLineTester>1) {
```

```
getline < "progdyn.conf"

if ($1=="method") method=$2

if ($1=="method2") meth2=$2

if ($1=="charge") charge=$2

if ($1=="multiplicity") multiplicity=$2

if ($1=="memory") memory=$2

if ($1=="processors") processors=$2

if ($1=="checkpoint") checkpoint=$2

if ($1=="diagnostics") diag=$2

if ($1=="method3") meth3=$2

if ($1=="method4") meth4=$2

if ($1=="method5") meth5=$2

if ($1=="method6") meth6=$2

if ($1=="highlevel") highlevel=$2

if ($1=="fixedatom1") fixedatom1=$2

if ($1=="fixedatom2") fixedatom2=$2

if ($1=="fixedatom3") fixedatom3=$2

if ($1=="fixedatom4") fixedatom4=$2

if ($1=="methodfile") methodfilelines=$2

if ($1=="title") {

    title1=$2

    title2=$3
```

```

title3=$4

title4=$5

}

blankLineTester=length($0)

}

if (diag==1) print "***** starting prog1stpoint *****" >>
"diagnostics"

if (diag==1) print "method,charge,multiplicity,memory" >> "diagnostics"

if (diag==1) print method,charge,multiplicity,memory >> "diagnostics"

if (diag==1) print "processors,checkpoint,title" >> "diagnostics"

if (diag==1) print processors,checkpoint,title1,title2,title3,title4 >> "diagnostics"

getline < "isomernumber"

isomernum = $1

print "%nproc=" processors

print "%mem=" memory

print "%chk=" checkpoint

print "#p " method " force scf=(tight,nosym) "

#print "IOp(3/76=0572004280)" #for mPW1K in g03

if (meth2=="unrestricted") print "guess=mix" #for unrestricted calculations

if (length(meth3)>2) print meth3

```

```
if (length(meth4)>2) print meth4

print ""

# make the title four words exactly, leaving out spaces if necessary

print title1,title2,title3,title4

print "runpoint 1"

print "runisomer ", isomernum

print ""

print charge,multiplicity

}
```

```
(/C / || /H / || /O / || /N / || /B / || /F / || /Cl / || /Al /) {

  atomnumber++

  printf("%s %.7f %.7f %.7f", $1, $2, $3, $4)

  if (atomnumber>highlevel) printf(" %s", "M")

  print ""

}
```

```
END {

print ""

if (length(meth5)>2) print meth5

if (length(meth6)>2) print meth6

if (methodfilelines>=1) {
```

```
for (i=1;i<=methodfilelines;i++) {  
    getline < "methodfile"  
    print $0  
    }  
}  
print ""  
}
```

4. Program prog2ndpoint

```
BEGIN {  
  
# version Feb 2008 incorporates methodfile, boxon and boxsize, though this point  
unaffected by box  
  
# version Jan 2008 - allows for ONIOM jobs, fixed atoms  
  
# version Sept 9, 2005 - incorporates meth3, meth4, meth5, meth6, but not yet rotation  
  
# read progdyn.conf for configuration info  
  
blankLineTester=10  
  
while (blankLineTester>1) {  
    getline < "progdyn.conf"  
  
    if ($1=="method") method=$2  
  
    if ($1=="method2") meth2=$2  
  
    if ($1=="charge") charge=$2
```

```
if ($1=="multiplicity") multiplicity=$2
if ($1=="memory") memory=$2
if ($1=="processors") processors=$2
if ($1=="checkpoint") checkpoint=$2
if ($1=="diagnostics") diag=$2
if ($1=="method3") meth3=$2
if ($1=="method4") meth4=$2
if ($1=="method5") meth5=$2
if ($1=="method6") meth6=$2
if ($1=="highlevel") highlevel=$2
if ($1=="fixedatom1") fixedatom1=$2
if ($1=="fixedatom2") fixedatom2=$2
if ($1=="fixedatom3") fixedatom3=$2
if ($1=="fixedatom4") fixedatom4=$2
if ($1=="methodfile") methodfilelines=$2
if ($1=="title") {
    title1=$2
    title2=$3
    title3=$4
    title4=$5
}
blankLineTester=length($0)
```

```
}

if (diag==1) print "***** starting prog2ndpoint *****" >>
"diagnostics"

if (diag==1) print "method,charge,multiplicity,memory" >> "diagnostics"

if (diag==1) print method,charge,multiplicity,memory >> "diagnostics"

if (diag==1) print "processors,checkpoint,title" >> "diagnostics"

if (diag==1) print processors,checkpoint,title1,title2,title3,title4 >> "diagnostics"

# TO DO : move timestep to progdyn.conf

i=1;j=1;k=1

timestep=1E-15

avNum=6.02E23

#get the isomer number from file

getline < "isomernumber"

isomernum = $1

print "%nproc=" processors

print "%mem=" memory

print "%chk=" checkpoint

print "#p " method " force scf=(tight,nosym) "
```



```

#print "IOp(3/76=0572004280)" #for mPW1K in g03

if (meth2=="unrestricted") print "guess=mix" #for unrestricted calculations

if (meth2=="read") print "guess=tcheck" #for reading orbitals from check, sometimes
faster, sometimes not

if (length(meth3)>2) print meth3

if (length(meth4)>2) print meth4

print ""

# make the title four words exactly, leaving out spaces if necessary

print title1,title2,title3,title4

print "runpoint 2"

print "runisomer ", isomernum

print ""

print charge,multiplicity

# ok, now we have to figure the second point. this should be

#  $x(t) = x + v*t + 1/2*F*t^2/m$ 

# so we need to set up arrays for position, velocity, and force

getline < "geoPlusVel"

numAtoms=$1

# first the geometry

for (i=1;i<=numAtoms;i++) {

    getline < "geoPlusVel"

```

```

weight[i]=$5

atSym[i]=$1

for (j=1;j<=3;j++) {
    geoArr[i,j]=$ (1+j)
}

}

#now we go ahead and add the velocities

for (i=1;i<=numAtoms;i++) {
    getline < "geoPlusVel"
    for (j=1;j<=3;j++) {
        arr[i,j]=$j+geoArr[i,j]
    }
}

# print arr[i,1],arr[i,2],arr[i,3]

}

# first end the BEGIN

}

# now we go ahead and translate the forces and add them

(/      1  / || /      5  / || /      6  / || /      7  / || /      8  / || /      9  / || /
13  / || /      17  /) && length($3) > 9 {
i=$1
for (j=1;j<=3;j++) {
    forceArr[i,j]=$ (2+j)
}
}

```

```

    }
# print i,weight[i],forceArr[i,1],forceArr[i,2],forceArr[i,3]
}

END {

# turn the forces into motion
for (i=1;i<=numAtoms;i++) {
    for (j=1;j<=3;j++) {

forceArr[i,j]=0.5*1E10*forceArr[i,j]*627.509*(4184/(0.5292*avNum))*1E10*(timestep
^2)/(weight[i]/(avNum*1000))

    arr[i,j]=arr[i,j]+forceArr[i,j]

# if atoms are fixed, replace calcd new position by original position
    if ((i==fixedatom1) || (i==fixedatom2) || (i==fixedatom3) || (i==fixedatom4))
arr[i,j]=geoArr[i,j]
    }

# print forceArr[i,1],forceArr[i,2],forceArr[i,3]
    printf("%s %.7f %.7f %.7f",atSym[i],arr[i,1],arr[i,2],arr[i,3])

    if (i>highlevel) printf(" %s", "M")

    print ""

    }

print ""

```

```

if (length(meth5)>2) print meth5
if (length(meth6)>2) print meth6
if (methodfilelines>=1) {
  for (i=1;i<=methodfilelines;i++) {
    getline < "methodfile"
    print $0
  }
}
print ""
}

```

5. Program progdynb

```

BEGIN { #this is the main routine for generating new .com files by the Verlet
algorithm
# May 2008 added option to put out velocities in vellist - make diag=2
# version Feb 2008 incorporates methodfile, boxon and boxsize
# version Jan 2008 incorporates fixed atoms, oniom, and velocity damping
# version August 2007 incorporates keepevery to decrease size of dyn file
# version Sept 11, 2005 - incorportates meth3, meth4, meth5, meth6, but not yet rotation

OFS=" ";i=1;j=1;k=1

```

```
# TO DO - move timestep to progdyn.conf

timestep=1E-15

avNum=6.02E23

#allow for damping from file named damping, but limit its range

damping=1

getline < "damping"

if (($1>0.05) && ($1<2.1)) damping=$1

# read progdyn.conf for configuration info

blankLineTester=10

while (blankLineTester>1) {

    getline < "progdyn.conf"

    if ($1=="method") method=$2

    if ($1=="method2") meth2=$2

    if ($1=="charge") charge=$2

    if ($1=="multiplicity") multiplicity=$2

    if ($1=="memory") memory=$2

    if ($1=="processors") processors=$2

    if ($1=="checkpoint") checkpoint=$2

    if ($1=="diagnostics") diag=$2

    if ($1=="method3") meth3=$2

    if ($1=="method4") meth4=$2
```

```
if ($1=="method5") meth5=$2
if ($1=="method6") meth6=$2
if ($1=="highlevel") highlevel=$2
if ($1=="keepevery") keepevery=$2
if ($1=="fixedatom1") fixedatom1=$2
if ($1=="fixedatom2") fixedatom2=$2
if ($1=="fixedatom3") fixedatom3=$2
if ($1=="fixedatom4") fixedatom4=$2
if ($1=="boxon") boxon=$2
if ($1=="boxsize") boxsize=$2
if ($1=="methodfile") methodfilelines=$2
if ($1=="title") {
    title1=$2
    title2=$3
    title3=$4
    title4=$5
}
blankLineTester=length($0)
}

if (diag==1) print "***** starting progdynb *****" >>
"diagnostics"
```

```
if (diag==1) print "method,charge,multiplicity,memory" >> "diagnostics"
```

```
if (diag==1) print method,charge,multiplicity,memory >> "diagnostics"
```

```
if (diag==1) print "processors,checkpoint,title" >> "diagnostics"
```

```
if (diag==1) print processors,checkpoint,title1,title2,title3,title4 >> "diagnostics"
```

```
# get number of atoms and weights from geoPlusVel
```

```
getline < "geoPlusVel"
```

```
numAtoms=$1
```

```
for (i=1;i<=numAtoms;i++) {
```

```
    getline < "geoPlusVel"
```

```
    weight[i]=$5
```

```
    atSym[i]=$1
```

```
}
```

```
for (at=1;at<=numAtoms;at++) {
```

```
    getline < "old"
```

```
    oldarr[at,1]=$4
```

```
    oldarr[at,2]=$5
```

```
    oldarr[at,3]=$6
```

```
}
```

```
for (at=1;at<=numAtoms;at++) {
```

```

getline < "older"

olderarr[at,1]=$4

olderarr[at,2]=$5

olderarr[at,3]=$6

}

```

record atom velocities for IVR analysis. This is actually the velocity in the previous run, which is the easiest to calculate.

```

getline < "isomernumber"

isomernum = $1

getline < "runpointnumber"

runpointnum = $1

if (diag==2) print "runpoint ",runpointnum-1,"runisomer ",isomernum >> "vellist"

for (at=1;at<=numAtoms;at++) {

    atomVel=((oldarr[at,1]-olderarr[at,1])^2      +      (oldarr[at,2]-olderarr[at,2])^2

    +(oldarr[at,3]-olderarr[at,3])^2)^.5

if (diag==2) print atomVel >> "vellist"

}

}

```

#must adjust next line for weird atoms


```

(/      1  /||/      5  /||/      6  /||/      7  /||/      8  /||/      9  /||/
13  /||/      17  /) && length($3) > 9 {
i=$1
for (j=1;j<=3;j++) {
    forceArr[i,j]=$i*(2+j)
}
# print i,weight[i],forceArr[i,1],forceArr[i,2],forceArr[i,3]
}

END {
for (i=1;i<=numAtoms;i++) {
    for (j=1;j<=3;j++) {

forceArr[i,j]=1E10*forceArr[i,j]*627.509*(4184/(0.5292*avNum))*1E10*(timestep^2)/
(weight[i]/(avNum*1000))

        arr[i,j]=arr[i,j]+forceArr[i,j]
    }
}

if ((runpointnum % keepevery)==0) system("cat g03.log >> dyn")

print "%nproc=" processors
print "%mem=" memory
print "%chk=" checkpoint

```

```
print "# " method " force scf=(maxcycle=200) "  
#print "IOP(3/76=0572004280)" #for mPW1K in g03  
if (meth2=="unrestricted") print "guess=mix" #for unrestricted calculations  
if (meth2=="read") print "guess=tcheck" #for reading orbitals from check, sometimes  
faster, sometimes not  
print "pop=none "  
if (length(meth3)>2) print meth3  
if (length(meth4)>2) print meth4  
#print "pop=none IOP(2/9=10,6/12=2)" #old IOPs for g98  
print ""  
print title1,title2,title3,title4  
print "runpoint ",runpointnum  
print "runisomer ",isomernum  
print ""  
print charge,multiplicity  
for (i=1;i<=numAtoms;i++) {  
  for (j=1;j<=3;j++) {  
    newarr[i,j]=oldarr[i,j]+damping*(oldarr[i,j]-olderarr[i,j])+forceArr[i,j]  
    if ((i==fixedatom1) || (i==fixedatom2) || (i==fixedatom3) || (i==fixedatom4))  
newarr[i,j]=oldarr[i,j]  
#turn around atoms outside the box  
    if (boxon==1) {
```

```

    if (newarr[i,j]>boxsize) {
        if (oldarr[i,j]>olderarr[i,j])    newarr[i,j]=oldarr[i,j]+damping*(olderarr[i,j]-
oldarr[i,j])+forceArr[i,j]
    }
    if (newarr[i,j]<-1*boxsize) {
        if (oldarr[i,j]<olderarr[i,j])    newarr[i,j]=oldarr[i,j]+damping*(olderarr[i,j]-
oldarr[i,j])+forceArr[i,j]
    }
}
}
}

printf("%s %.7f %.7f %.7f",atSym[i],newarr[i,1],newarr[i,2],newarr[i,3])

if (i>highlevel) printf(" %s", "M")

print ""

}

print ""

if (length(meth5)>2) print meth5

if (length(meth6)>2) print meth6

if (methodfilelines>=1) {

    for (i=1;i<=methodfilelines;i++) {

        getline < "methodfile"

        print $0

    }

}

```

```
    }  
    print ""  
}
```

6. Program randgen

```
# c program  
  
# this can be replaced by a more reliable random number  
# generator when available on a system  
  
#include <stdio.h>  
  
#include <stdlib.h>  
  
  
int a,b,c;  
  
double d;  
  
  
int product(int x, int y);  
  
int main(void)  
{  
    int count=1;  
    srand48(time (0));  
    while (count<=10000)
```

```

{
    d = drand48();
    printf("%.20f\n", d);
    count++;
}
return 0;
}

```

7. Program proganal

```

# pronounced pro-ganal
# this program requires serious rewriting for each new molecule
# or for reordered atoms, in order to pull out distances of interest
# revised from file used late 2005 and early 2006, getting dyns into separate files
# and adding extra functions
BEGIN {
    getline < "isomernumber"
    isomer=$1
}

/ tme reaction/ {
    printf("%s %s %s %s %s %s  ", $1, $2, $3, $4, $6, $8)
}

```

```

runpoint=$6
}
/ 1 C 0.000000/,/ 6 C 0.000000/ {
  if(($1==19)) {
    COd=$4
    COh=$5
  }
}
/ 6 C 0.000000/,/ 11 H 0.000000/ {
  if(($1==20)) {
    OH=$7
  }
}
/ 11 H 0.000000/,/ 16 H 0.000000/ {
  if(($1==20)) {
    if($4<OH) OH=$4
    OD=$5
    if($3<OH) OH=$3
    if($6<OD) OD=$6
    if($7<OD) OD=$7
  }
}
}

```

```

END {
    printf("%s    %.3f    %s    %.3f                %s    %.3f    %s    %.3f
", "COh", COh, "COd", COd, "OD", OD, "OH", OH)
    if (runpoint>400) {
        print "Too many points. XXXX"
        killdyn(isomer)
    }
    if ((COh>2.2) && (COd>2.2)) {
        print "Dead nothing favored XXXX"
        killdyn(isomer)
    }
    if (OD<1.2) {
        print "Deuterium reacted XXXX"
        movedyn(isomer)
    }
    if (OH<1.2) {
        print "Hydrogen has reacted XXXX"
        movedyn(isomer)
    }
    # if ((OD>OH) && (COh<COd)) print "H trans is favored"
    # if ((OD<OH) && (COh>COd)) print "D trans is favored"
    # if ((OD>OH) && (COh>COd)) print "Nothing favored"

```

```
# if ((OD<OH) && (COh<COd)) print "Nothing favored"
```

```
  system("date +%D-%T")
```

```
}
```

```
function movedyn(isomer) {
```

```
  if (isomer==1) system("mv dyn dyn1")
```

```
  if (isomer==2) system("mv dyn dyn2")
```

```
  if (isomer==3) system("mv dyn dyn3")
```

```
  if (isomer==4) system("mv dyn dyn4")
```

```
  if (isomer==5) system("mv dyn dyn5")
```

```
  if (isomer==6) system("mv dyn dyn6")
```

```
  if (isomer==7) system("mv dyn dyn7")
```

```
  if (isomer==8) system("mv dyn dyn8")
```

```
  if (isomer==9) system("mv dyn dyn9")
```

```
  if (isomer==10) system("mv dyn dyn10")
```

```
  if (isomer==11) system("mv dyn dyn11")
```

```
  if (isomer==12) system("mv dyn dyn12")
```

```
  if (isomer==13) system("mv dyn dyn13")
```

```
  if (isomer==14) system("mv dyn dyn14")
```

```
  if (isomer==15) system("mv dyn dyn15")
```

```
  if (isomer==16) system("mv dyn dyn16")
```

```
  if (isomer==17) system("mv dyn dyn17")
```



```
if (isomer==18) system("mv dyn dyn18")
if (isomer==19) system("mv dyn dyn19")
if (isomer==20) system("mv dyn dyn20")
if (isomer==21) system("mv dyn dyn21")
if (isomer==22) system("mv dyn dyn22")
if (isomer==23) system("mv dyn dyn23")
if (isomer==24) system("mv dyn dyn24")
if (isomer==25) system("mv dyn dyn25")
if (isomer==26) system("mv dyn dyn26")
if (isomer==27) system("mv dyn dyn27")
if (isomer==28) system("mv dyn dyn28")
if (isomer==29) system("mv dyn dyn29")
if (isomer==30) system("mv dyn dyn30")
}
```

```
function killdyn(isomer) {
    system("rm -f dyn")
}
```

8. progdyn.conf

#conf file for dynamics. This is read by awk programs prog1stpoint, prog2ndpoint, and progdynb.

```
#The programs won't read anything past the first blank line,  
#and this file must end with a blank line. You can add to these comments but  
#don't use keywords as the first word on a line. Don't delete lines - the program  
#has no built in default values if they aren't here.  
#values here are read repeatedly and can be changed in the middle of runs  
method B3LYP/6-31G*  
method2 read #The options here are restricted, unrestricted, and read.  
#If the method is U..., put unrestricted here and the .com files will have in them  
guess=mix.  
#If you put read here, the .com files will contain guess=tcheck, which sometimes makes  
things faster, sometimes not.  
charge 0  
multiplicity 1  
memory 200000000  
checkpoint dyn6.chk #uses one checkpoint file repeatedly  
processors 1  
diagnostics 2 # 1 prints out extra stuff to a file "diagnostics" 2 prints out velocities to a  
file "vellist"  
title tme reaction gem6Dpos 163disNew # the title must be exactly four words  
#use initialdis 0 for no displacements, forcing all trajectories to start from the same  
point, use initialdis 1 for the displacement method originally used
```

#which picks a linearly random position along each mode, and use initialdis 2 for the newer displacement method which gives a ground-state QM-correct displacement distribution

initialdis 2

timestep 1E-15

scaling 1.0

temperature 163.15

#add extra lines to .com files to implement things like the iop for mPW1k

#Leave the second word blank if you are not going to use them. otherwise any word you put in will end up in the com file

#only a single term with no spaces can be added, one per method line

#method3 IOp(3/76=0572004280)

#add the line below with big structures to get it to put out the distance matrix and the input orientation

method3 iop(2/9=2002)

method4

#method5 and method6 are placed at the end of the file instead of in the keyword section

method5

method6

#for more complicated ends of .com files, it will be necessary to put the ends in a file

#methodfile 6

#searchdir says what direction to follow the mode associated with the imaginary frequency.

#put as values the words "negative" or "positive"

searchdir positive

#for quassiclassical dynamics, the default, use 0. for classical dynamics, use 1 below

classical 0

#line below gives number of negative frequencies - if 0, treats as ground state and direction of all modes is random

#if 1, negative freq will go direction of searchdir

#if 2, only lowest freq will go direction of searchdir and other imag mode will go in random direction

numimag 1

the line below tells progdynb how often to write g03.log to file dyn, after the first two points. Use 1 for most dynamics

until excessive, but use a higher integer if doing long term classical dynamics.

keepevery 10

for ONIOM jobs, the following line states the number of highlevel atoms, which must come before the medium level atoms

make this number 999 if not ONIOM

highlevel 999

#use fixedatom1, fixedatom2, fixedatom3, fixedatom4 to fix atoms in space.

#note that fixing one atom serves no useful purpose and messes things up, while

```
#fixing two atoms fixes one distance, and  
#fixing three has the effect of fixing three distances, not just two  
#in current form fixed atoms only are meant to work with no displacements, that is,  
initialdis=0  
#fixedatom1 3  
#fixedatom2 10  
#fixedatom3 14  
#dynamics with solvent molecules tends to blast molecules away. Because of this,  
#it would be good to have a pressure and periodic boundary conditions, etc, but until  
#I learn how to do this, I can just restrict the molecules to a box  
#atoms outside this box get bounced. Set box size so as to fit the entire initial molecule  
but not have too much extra room  
#the box does not affect anything until progdynb  
boxon 0  
boxsize 7.5  
#to be implemented:  
rotation 0 #use 1 to turn on rotational modes  
#since displacements run into a problem with easy rotation modes such as a methyl  
group,  
#it would be easy to turn off displacements for particular modes. Sometimes this would  
be  
#the right thing to do but it would be awkward to explain it in a paper.
```

numberlimitedmodes 0

limitedmodes 3 5

#updated Aug 9, 2007 to include the possibility of classical dynamics by the keyword
classical

#updated Jan 2008 to include fixed atoms, ONIOM jobs, keepevery, and box size

#updated Feb 2008 to include methodfile parameter

RRKM Calculations

These were carried out on points from the B3LYP/6-31G* DRP using QCPE
PROGRAM NO. 644 (by Zhu and Hase).⁶¹ The input was set up as outlined in the
manual.

1. Two title cards indicating the point of interest from the DRP
2. E_{MIN} set at the difference in energy between pointA and pointB + 0.25 kcal/mol
which is half the bin size. ΔE (upward increment) was set to 0.5 kcal/mol
corresponding to the bin size for the energy distribution described previously.
The number of successive molecular energies for which the calculation was
made, n_E , was set to 40.
3. KROT was set to 0 as is for standard calculations.
4. J_{MIN} , ΔJ , n_J and T_{rot} were set to 1,1,1 and 300 respectively.
5. NANH was set to 0
6. JDEN was set to 0

7. JSUM was set to 0
8. σ_p (the reaction path degeneracy) was set to 1.0
9. The number of molecular frequencies, n_f , was set to 54 ($3n-6$) and n_r , the number of free internal rotors, was set to 0.
10. The molecular frequencies from pointB were included for each structure with 7 frequencies per line in cm^{-1} units.
11. The principal moments of inertia were included for pointB in AMU-Å^2 units.
12. The reduced moments of inertia for internal rotors of the molecule, was set to 0.
13. The symmetry number for each of the internal rotors was set to 0.
14. NCRIT, the critical configuration, was set to 0.
15. E_0 , the threshold energy, was set as the difference in energy between pointB and the point of interest from the DRP in kcal/mol.
16. The number of molecular frequencies of the critical configuration, n_f^\ddagger , was set to 53 ($3n-7$) and n_r^\ddagger , the number of free internal rotors of the critical configuration, was set to 0.
17. The molecular frequencies from the geometry of each point of interest from the DRP were included with 7 frequencies per line in cm^{-1} units.
18. The external moments of inertia for the critical configuration (each structure of interest from the DRP) were included in AMU-Å^2 units.

VITA

Kelmar K. Kelly received her Bachelor of Science degree in chemistry and biology from St. Francis College in Brooklyn, New York in 2003. She entered the Ph.D. program in Chemistry at Texas A&M University in September 2003. She received her Ph.D. in May 2009 working under the direction of Dr. Daniel A. Singleton. Her primary research interests include physical organic chemistry.

Kelmar K. Kelly may be reached at Eastman Chemical Company, P.O. Box 7444, Longview, TX 75607. USA.